Technology Collaboration Programme
by IEA

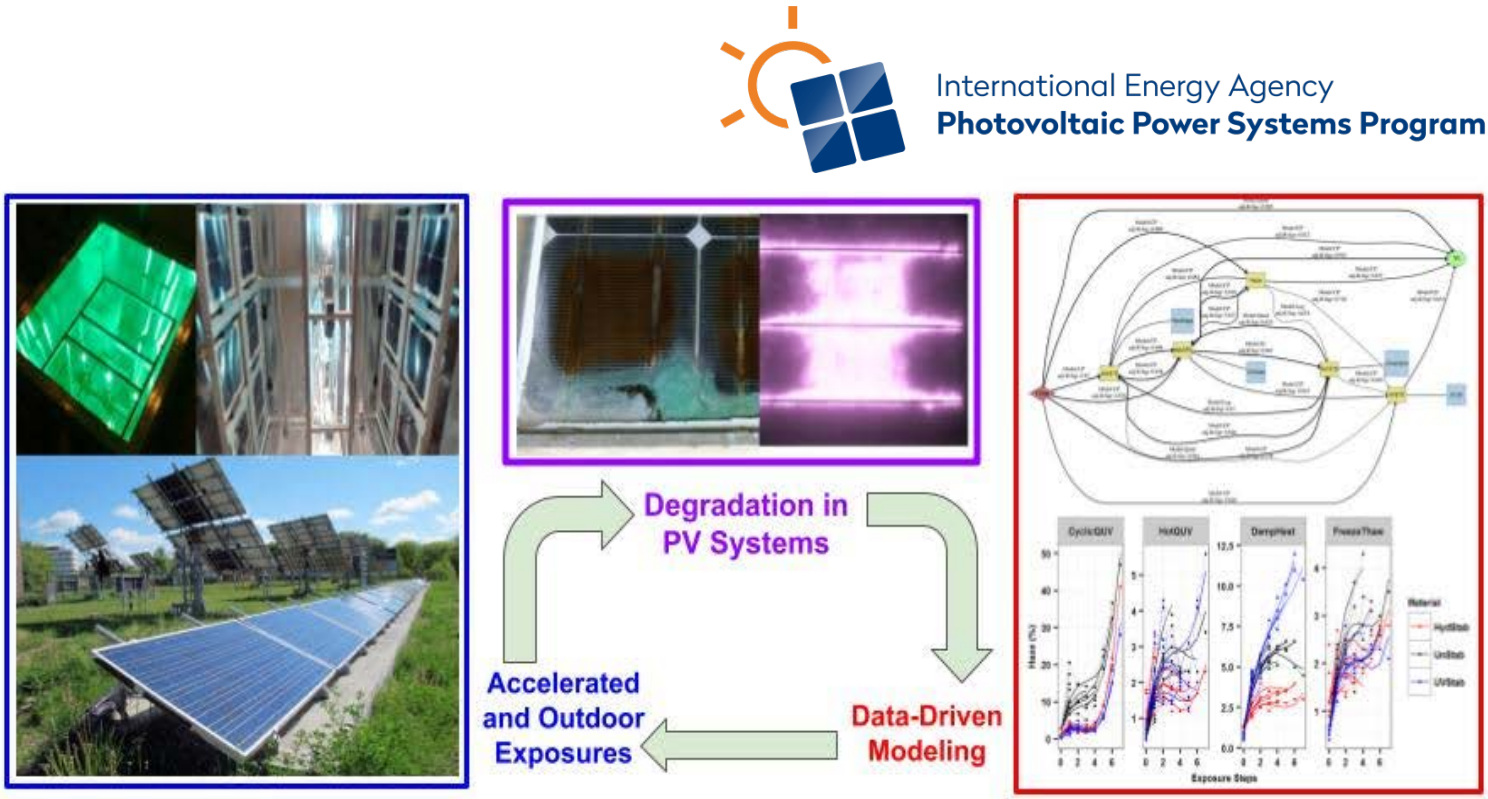

International Energy Agency
Photovoltaic Power Systems Programme

Task 13 Performance, Operation and Reliability of Photovoltaic Systems

PVPS

Service Life Estimation for Photovoltaic Modules

2021

Report IEA-PVPS T13-16:2021

What is IEA PVPS TCP?

The International Energy Agency (IEA), founded in 1974, is an autonomous body within the framework of the Organization for Economic Cooperation and Development (OECD). The Technology Collaboration Programme (TCP) was created with a belief that the future of energy security and sustainability starts with global collaboration. The programme is made up of 6.000 experts across government, academia, and industry dedicated to advancing common research and the application of specific energy technologies.

The IEA Photovoltaic Power Systems Programme (IEA PVPS) is one of the TCP's within the IEA and was established in 1993. The mission of the programme is to "enhance the international collaborative efforts which facilitate the role of photovoltaic solar energy as a cornerstone in the transition to sustainable energy systems." In order to achieve this, the Programme's participants have undertaken a variety of joint research projects in PV power systems applications. The overall programme is headed by an Executive Committee, comprised of one delegate from each country or organisation member, which designates distinct 'Tasks,' that may be research projects or activity areas.

The IEA PVPS participating countries are Australia, Austria, Belgium, Canada, Chile, China, Denmark, Finland, France, Germany, Israel, Italy, Japan, Korea, Malaysia, Mexico, Morocco, the Netherlands, Norway, Portugal, South Africa, Spain, Sweden, Switzerland, Thailand, Turkey, and the United States of America. The European Commission, Solar Power Europe, the Smart Electric Power Alliance (SEPA), the Solar Energy Industries Association and the Cop- per Alliance are also members.

Visit us at: www.iea-pvps.org

What is IEA PVPS Task 13?

Within the framework of IEA PVPS, Task 13 aims to provide support to market actors working to improve the operation, the reliability and the quality of PV components and systems. Operational data from PV systems in different climate zones compiled within the project will help provide the basis for estimates of the current situation regarding PV reliability and performance.

The general setting of Task 13 provides a common platform to summarize and report on technical aspects affecting the quality, performance, reliability and lifetime of PV systems in a wide variety of environments and applications. By working together across national boundaries we can all take advantage of research and experience from each member country and combine and integrate this knowledge into valuable summaries of best practices and methods for ensuring PV systems perform at their optimum and continue to provide competitive return on investment.

Task 13 has so far managed to create the right framework for the calculations of various parameters that can give an indication of the quality of PV components and systems. The framework is now there and can be used by the industry who has expressed appreciation towards the results included in the high-quality reports.

The IEA PVPS countries participating in Task 13 are Australia, Austria, Belgium, Canada, Chile, China, Denmark, Finland, France, Germany, Israel, Italy, Japan, the Netherlands, Norway, Spain, Sweden, Switzerland, Thailand, and the United States of America.

COVER PICTURE

Range of activities involved in service life modelling. Source: CWRU, Cleveland / Roger French.

ISBN 978-3-907281-05-5: Task 13 Report T13-16:2021

INTERNATIONAL ENERGY AGENCY

PHOTOVOLTAIC POWER SYSTEMS PROGRAMME

IEA PVPS Task 13

Performance, Operation and Reliability of Photovoltaic Systems

Service Life Estimation for Photovoltaic Modules

Report IEA-PVPS T13-16:2021

June 2021

ISBN 978-3-907281-05-5

AUTHORS

Main Authors

Karl-Anders Weiß, Fraunhofer ISE, Freiburg, Germany
Laura S. Bruckman, CWRU, Cleveland, USA
Roger H. French, CWRU, Cleveland, USA
Gernot Oreski, PCCL, Leoben, Austria
Tadanori Tanahashi, AIST, Koriyama, Japan

Contributing Authors

Julián Ascéncio-Vásquez, 3E, Brussels, Belgium
Luis F. Castillion-Gandara, PCCL, Leoben, Austria
Gabriele Eder, OFI, Vienna, Austria
Nikola Hrelja, EDF, Moret Loing et Orvanne, France
Mike van Iseghem, EDF, Moret Loing et Orvanne, France
Ismail Kaaya, Fraunhofer ISE, Freiburg, Germany
Sascha Lindig, EURAC Research, Bolzano, Italy
JiQi Liu, CWRU, Cleveland, USA
Stefan Mitterhofer, University of Ljubljana, Ljubljana, Slovenia
Lukas Neumaier, SAL Silicon Austria Labs, Villach, Austria
Kunal Rath, CWRU, Cleveland, USA
Sameera Nalin Venkat, CWRU, Cleveland, USA
Raymond J. Wieser, CWRU, Cleveland, USA

Editors

Ulrike Jahn, VDE Renewables GmbH, Alzenau, Germany
Karl-Anders Weiß, Fraunhofer ISE, Freiburg, Germany

TABLE OF CONTENTS

Acknowledgements 6
List of Abbreviations 7
Executive Summary 11
1 Introduction 13
1.1 Purpose 13
1.2 Overview / State of the Art 13
2 Terms and Definitions 15
2.1 Service Life Prediction 19
2.2 Definition of End-of-Life 19
3 Climatic Stressors 21
3.1 Introduction to Climatic Stressors 21
3.2 Macroclimatic Loads 21
3.3 Conditions in Accelerated Testing 24
3.4 Microclimatic Loads for Modules 27
4 Modelling Approaches 35
4.1 Issues in Empirical Modelling: Bias versus Variance Trade-Off 35
4.2 Degradation Models of PV Module Materials, Components and Specific Degradation Modes 37
4.3 Photovoltaic Performance Models 52
5 Conclusion 65
References 67

ACKNOWLEDGEMENTS

This report received valuable contributions from several IEA-PVPS Task 13 members and other international experts. A special thanks goes to Ms. Bianca Krumm from Fraunhofer ISE for organizing and coordinating all contributors and their contributions as well as for thoroughly editing the report.

The authors would like to thank Laura Bruckman and Werner Herrmann for reviewing this report.

Case Western Reserve University's work on this report was supported by the U.S. Department of Energy's Office of Energy Efficiency and Renewable Energy (EERE) under Solar Energy Technologies Office (SETO) Agreement Number DE-EE-0008550.

This report is supported by the German Federal Ministry for Economic Affairs and Energy (BMWi) under contract no. 0324304A and 0324304B.

This report is supported by the Austrian Federal Government, represented by the Austrian Research Promotion Agency (FFG) under contract no. 876736.

This report is also supported by The New Energy and Industrial Technology Development Organization (NEDO), Japan, under contract #15100576-0.

This report has received funding from the European Union's Horizon 2020 programme under GA. No. 721452 – H2020-MSCA-ITN-2016.

LIST OF ABBREVIATIONS

A	Pre-Exponential Factor of the Arrhenius Equation
AAA	Polymeric Backsheet Consisting of Three Layers of Polyamide
ABC	Approximate Bayesian Computation
AC	Alternating Currents
Ag	Silver
AI-BSF	Cell type
AIC	Akaike Information Criterion
AH	Tropical climate with high irradiation based on Köppen-Geiger-Photovoltaic climate zone scheme
AK	Tropical climate with very high irradiation based on Köppen-Geiger-Photovoltaic climate zone scheme
ARIMA	Autoregressive Integrated Moving Average
ASHRAE	American Society of Heating, Refrigerating, and Air-Conditioning Engineers
ASTM	American Society for Testing and Materials – US Standardization Organization
B	Desert climate based on Köppen-Geiger-Photovoltaic climate zone scheme
BWh	Arid climate, desert climate, hot desert based on the Köppen-Geiger climate zone scheme
β	The Coefficients of Additive Models, e. g. $Y = \beta_o + \beta_1 X_1 + \varepsilon$
BoM	Bill of Materials
C	Concentration
C-AST	Combined-Accelerated Stress Test
CCC	Cross Correlation Coefficient
CCSF	Cross Correlation Scale Factor
CEC	Commission of the European Communities
Cfa	Temperate, Humid-Subtropical Köppen-Geiger Climate Zone
CS	Climatic Stressors
CSD	Classical Seasonal Decomposition
D	Diffusion Coefficient
DH	Damp Heat
DMT	Derjaguim-Muller-Toporov Model
EL	Electroluminescence
ε	The error term of an Additive Model
E_{POA}	Insolation in Plane of Array

ESTI	European Solar Test Installation
ERA5	Copernicus Climate Change Service ERA5 Dataset
EVA	Ethylene-Vinyl Acetate
FEM	Finite Element Method
FF	Fill Factor
FTIR	Fourier Transform Infrared
H_2	Dihydrogen
H_2O	Water
HVAC	Heating, Ventilation, Air Conditioning
HW	Holt-Winters statistical method
HY's Model	Hsueh and Yanaka Model
IEA	International Energy Agency
IEC	International Electrotechnical Commission
IR	Infrared
I_{sc}	Short-Circuit Current
I-V	Current-Voltage
JPL	Jet Propulsion Laboratory
KG	Köppen-Geiger climate zone scheme
K_{Ross}	Ross Coefficient
KGPV	Köppen-Geiger Photovoltaic climate zone scheme
L&DS	Lifetime and Degradation Science
LID	Light-Induced Degradation
LSCM	Laser Scanning Confocal Microscopy
MC	Monte-Carlo
MD	Molecular Dynamics
MS-PL	Multi-Step Performance Losses
Mpp	Maximum Power Point
μ	The mean of a population
N	Nitrogen
Na	Sodium
NaOH	Sodium Hydroxide
Na_2SiO_3	Sodium Metasilicate
nA	Nanoampere
netSEM	Network Structural Equation Modelling
NIR	Near-Infrared
NREL	US National Renewable Energy Laboratory
O	Oxygen
P(t)	Power as function of time

P (Pa)	Partial Water Vapour Pressure
PA	Polyamide
PCA	Principal Component Analysis
$P_{Critical}$	Minimum Required Functional Property Level
PDCZ	Photovoltaic Degradation Climate Zones
PERC	Cell Type
PET	Poly-Ethylene Terephthalate
PID	Potential Induced Degradation
PL	Photoluminescence
PLR	Performance Loss Rate
P_{max}	Maximum Generating Power
P_{mpp}	MPP-Power
PR	Performance Ratio
PR_{tc}	Temperature-Corrected Performance Ratio
PV	Photovoltaic(s)
PVLIB	PVlib, a Python Package of functions for PV calculations
PVM	Photovoltaic Module
R&D	Research and Development
RD	Reaction-Diffusion
RH	Relative Humidity
R_{iso}	Isolation Resistance
RMSE	Root Means Square Error
R_s	Series Resistance
R_{sh}	Shunt Resistance
S	Solubility of Water
Si	Silicon
Si_xN_y	Silicon Nitride
SLP	Service Life Prediction
STC	Standard Test Conditions
STL	Seasonal and Trend Decomposition using LOESS
t	Time
T	Temperature
T_{amb}	Ambient Temperature
TC	Thermal Cycling
TCO	Transparent-Conductive Oxide
TGA	Thermogravimetric Analysis
T_{mod}	Module Temperature
TPO	Thermoplastic Polyolefin

V_{mpp}	MPP-Voltage
UV	Ultraviolet
V	Voltage
VIS	Visual
V_{oc}	Open-Circuit Voltage
WS	Wind Speed
WVP	Water Vapour Pressure
WVTR	Water Vapour Transmission Rate
XCT	X-Ray Computed Tomography
YDS	Yearly Degradation Score
YI	Yellowness Index

EXECUTIVE SUMMARY

The economic success of photovoltaic (PV) power plants depends crucially on their lifetime energy yield. Degradation effects and the total lifetime directly influence the produced electricity and therefore the cash flow, which also impacts the levelized costs of energy (LCOE) and therefore the profitability of the power plant. In most cases, the lifetimes and degradation rates that are used to estimate the system performance are not system-specific but are based on average values from the evaluations of older systems or data sheets. So, these values unfortunately have no direct correlation with the specific components of the specific PV system, nor the operational and climatic conditions at the specific location. Also, the mathematical models used for calculating the expected power output typically expect linear degradation rates which are not in line with real degradation processes found in the field, which are typically non-linear.

This report gives an overview on empirical degradation modelling and service life prediction of PV modules since they are the major components of PV systems that are subject to the effects of degradation. For other components no comparable scientific data is available. The structure of the document addresses different stakeholders with different backgrounds. Chapter 1 begins with a short introduction including a condensed overview of the state of the art.

Chapter 2 follows with the definition of relevant terms and definitions. Since especially in discussions on lifetime and degradation different terms are not used coherently in industry or science, the authors try to improve the situation with this dedicated glossary. In addition, the extremely relevant term “end-of-life” is discussed with different definitions, depending on the point of view and perspective of the user and the typical factors impacting the PV module or PV system. For this “end-of-life” term, no definition which is generally applicable in all situations can be given. Since the definition is crucial for the calculated service life, yield, and all related parameters, through to LCOE it is important to be aware of this when evaluating power plants and PV investments.

Climatic factors play a major role in degradation and are by nature location specific. It is precondition for the creation of meaningful service life prediction or degradation data to know about the relevant (climatic) stressors. Therefore Chapter 3 introduces the different relevant climatic stressors as well as classification schemes and methodologies to handle and analyse them. The chapter also describes differences and relations of the so called macro-climatic stressors, describing the climatic conditions in the ambience of the modules, and the situation at material level, the so called micro-climatic stressors. The latter describes the relevant parameters for degradation processes and so also the mathematical models addressing module degradation and service life prediction. The ambient macro-climatic conditions at specific locations can be estimated using data for the climatic regions or adapted climatic maps and so be classified using climatic classification schemes which exist also specified for PV purpose like e.g. the Köppen-Geiger PV scheme. For the determination of microclimatic loads - which are typically input parameters for degradation models, further calculations are necessary. The report presents possible ways to determine the necessary data for the most important micro-climatic parameters which are temperature and humidity. This data is also very important for the definition of accelerated tests, which can deliver module specific parameters for the service life and degradation prediction. Chapter 3 also describes basic ac-

celerated ageing tests, as described in the respective IEC standards, and how they can support degradation and service life prediction and modelling as well as their limitations.

Chapter 4 addresses general degradation and service-life modelling approaches including related issues. It starts in section 4.1 with general issues of empirical modelling one has to be aware of when working on mathematical modelling solutions for service life and degradation prediction and interpreting results. There are very different approaches for empirical modelling of the lifetime performance prediction and service life of products such as PV modules empirical statistical modelling, and empirical physical modelling. Physical empirical models are those that utilize analytic or numerical forms to represent the fundamental physics and chemistry of the phenomena. Statistical models, often referred to as data driven models, use mathematical forms which are able to fit the (measured) data without direct relation to physical or chemical processes. Both approaches use empirical (measured) data to determinate parameters which can be used for predicting future behaviour.

Section 4.2 introduces on one hand models for specific degradation modes or phenomena of modules (e.g., backsheet or cell cracking or electrochemical corrosion). On the other hand, modelling approaches for degradation effects of components and materials are presented. A special focus is here on degradation of polymeric materials since these materials are known to be sensitive to degradation effects causes by typical climatic stressors like high temperature, humidity and UV radiation. The modelling approaches using predictive models and inferential mechanistic models are presented using polyethyleneterephtalate (PET) degradation as catchable example. It is shown that different modelling approaches are necessary to describe all degradation effects. Weak points of modules can be identified and focussed optimization of products can be supported.

Performance degradation models are addressed in Section 4.3 which are the core models for the prediction of degradation of modules over time for specific types and locations. Combined with defined end-of-life conditions, these models can be used for service life prediction. Different approaches which have been specifically developed for PV modules are presented. Starting with an approach focusing on physical and chemical processes and the specific application. An approach to develop performance loss rate (PLR) models following the statistical methodology is presented as well including the processes to determine the relevant parameters from field data.

The modelling approaches are presented including the methodological approach to the problem the used input data, and parameters related to specific module types or local climatic conditions, down to calculations of degradation rates over time or remaining useful lifetime (RUL) or total expected lifetime.

The latest scientific work shows that service lifetime and degradation models for PV modules are of specific use if they combine different modelling approaches and include know-how and modelling parameters of the most relevant degradation effects. Such models can differentiate between the behaviour of different module types and to include the situation at different service locations. For some modules, it is also necessary to use multi-step modelling approaches to enable meaningful results.

Advanced approaches of data analysis and modelling also enable the determination of degradation signatures which can be related to specific degradation effects. This approach is expected to be very helpful in future work to identify failures based on operational data.

Since uncertainties of input parameters can have significant impact on the results but are often not totally avoidable, these topics are addressed in Chapter 4.3.

1 INTRODUCTION

The economic success and environmental impact of PV power plants depends crucially on the degradation and service life of the PV modules and other components of the PV power plants. The behaviour of PV modules is especially relevant since they typically show gradual degradation effects over time. The useful service lifetime and degradation of PV modules directly influences the lifetime yield of electricity, and therefore, the levelized cost of the electricity (LCOE) produced [1]. Degradation and service life are influenced not only by the materials used and the quality of module manufacturing, but also by local environmental effects that dictate the exposure conditions of the PV modules. Therefore, the lifetime and degradation of PV modules cannot be determined easily and are not valid for all locations and applications. Since both are dependent on local and operational conditions, the prediction of service lifetime from PV module degradation rates must be taken into consideration all of these factors and incorporate them into mathematical models.

1.1 Purpose

The report introduces the influencing factors for service life and degradation of PV modules and components as well as the modelling of degradation effects and service life prediction. It describes relevant stresses and load effects in section 3 and different modelling approaches, as well as models which have shown to fulfil the requirements of PV stakeholders in section 4. The descriptions are written in a way to address the needs of readers from all stakeholder groups, so on one hand people with no background in mathematical modelling who are interested in the influencing factors, potential of service life prediction, and interpretation of given data, as well as experts in reliability and degradation modelling. The chapters therefore briefly describe the approaches and background as well as examples and list relevant literature for further reading.

1.2 Overview / State of the Art

The increasing deployment of PV worldwide is a clear indication that PV will play a big role in the worldwide energy mix. This increasing trend in the inclusion of PV is exciting, but also comes with several challenges. They include the following: reliability issues, reliable integration of PV power in electrical grids, end-of-life issues (how to deal with out of service PV modules or PV components), and many others. To address these issues, two main approaches are being used: 1) experimental investigations and 2) mathematical modelling.

In the experimental approach, usually different testing conditions are applied according to established standards to accelerate the ageing of PV modules. According to the applied conditions, different degradation modes can be induced and through different characterization techniques the physical/chemical kinetics of the induced modes can be understood. This understanding helps the manufacturers to improve the different PV materials and components and hence the reliability of PV modules. The understanding also helps to develop degradation rate models used in lifetime estimations. Although this area is highly studied by different research groups, it is also among the still challenging topics in the field. This is because the current standardized testing procedures are designed to induce specific degradation mechanisms that cannot directly be used to evaluate the reliability of PV modules in real-world operations [2].This challenge is well known, and some research groups are designing

testing procedures that can induce several degradation mechanisms using more combined stress conditions [3]–[5].

To evaluate and predict the service lifetime of PV modules in real-world operating conditions, mathematical approaches are usually utilized [2], [6], [7]. Physical and statistical methods have been commonly used and recently machine learning approaches are being applied. The basic concept of mathematical approaches is to extract the degradation rates from historical PV performance or climatic data and use the extracted degradation rates to extrapolate the performance until the PV module "lifetime". Indeed, it is also crucial to understand how the lifetime is defined in the PV performance context. Excluding catastrophic events (such as fire) it is unlikely that a PV module drops its power generation to zero. However, even though a PV module is still generating power, its power output might be too low to be economically viable to continue its operation. Therefore, for economic viability of PV projects, most PV module manufacturers guarantee a power reduction of less than 20%, referenced at standard test conditions (STC), modules tested under 25°C temperatures, 1000 W/m^2, irradiance, and air mass 1.5, within 25-30 years of operation. Therefore, in the manufacturers' context, the lifetime of a PV module is often defined as the time required for a PV module to lose its initial STC power by 20% (so-called degradation limit) [8].

For outdoor degradation evaluations, statistical methods are commonly used. Therefore, different statistical methods are available and are being proposed [9]–[11]. Although the methods are based on similar principals, that is, to determine the trends in the historical data, they differ in their accuracy. In this report, the commonly used statistical methods as well as the recently proposed methods are presented. The major drawback of statistical methods is the lack of a direct correlation of the evaluated degradation rates to the climatic variables and degradation processes. In this regard, physical models are utilized to capture these correlations. Different physical models have been proposed for different degradation mechanisms especially for indoor applications [9]. For outdoor degradation rate evaluation, little has been done in this direction with only a few authors that proposed physical models limited to the dominating stressors (temperature, UV irradiance, relative humidity, and temperature cycling) [6], [7]. Although these models can provide a representation of combined outdoor effects, more generalized models that considers all the influencing factors (including additional or specific stressors, e.g., corrosive salt mist) in addition to the so-called dominating factors are still needed. Such models will provide a good estimation of the degradation rates under different operating conditions. Additionally, most physical models are proposed based on the assumption that the degradation kinetics follow an Arrhenius temperature dependence. Due to the different degradation mechanisms, it is unlikely that all the mechanisms obey the Arrhenius temperature behaviour; therefore, an investigation of which degradation mechanisms follow the Arrhenius law and which ones do not can help to improve the accuracy of the degradation rate models.

For lifetime prediction, usually a linear approximation with a constant degradation rate is used. Although this can be a sufficient approximation depending on the performance degradation trend, it is not usually applicable and can lead to increased uncertainty in lifetime predictions. In this regard, different authors have recently investigated and proposed models for the non-linearity in performance degradations [12], [13]. Such studies will aid to improve the accuracy and reliability of service lifetime predictions [14].

2 TERMS AND DEFINITIONS

Since some relevant terminologies for the topic of the report have no standard definitions or are usually interchangeably used, in Table 1, the definitions of the different terms are presented as used in this report.

Table 1: Definitions of terms as used in this report.

Term	Definition
Acceleration	Increased rate of degradation in respect to a shorter time frame than i real-world conditions (definition for this report).
Acceleration Factor	Multiplier indicating the factor by which the degradation rate is increased. An acceleration factor is defined for a specific degradation mechanism in a specific material under a specific exposure condition. Otherwise acceleration factors tend to be crude approximations or inaccurate or incorrect.
Back sheet	Polymeric multi-layer foil; outermost sheet of the PV module on the rear-side. It is designed to protect the photovoltaic cells and electrical components from external stressors and to act as electric insulator. The back sheet typically consists of a multi-layer polymer laminate (or co-extrudate) that has high dielectric properties.
Climate	The average weather in a given area over a longer period of time. A description of a climate includes information on, e.g. the average temperature and humidity in different seasons, precipitation, wind, and sunshine/irradiation. A description of the (chance of) extremes is often included.
Climate Zone	Areas with distinct climates, can be classified using different climatic parameters. Climate classifications are the basis for detailed geozonal models of climate zones. The most popular classification scheme is the Köppen-Geiger climate classification scheme [15], but other classifications more specific to PV were developed (including the relevant correlation between climatic stressors and effects on PV).
Concentration	In chemistry: the amount of a substance in a defined volume or mass. As a ratio, the mass ratios (mass concentration) or the volume ratios (volume concentration) can be used.
Corrosion	The reaction of a material with its environment, which causes a measurable change in the material. Corrosion can impair the function of a component or system. An irreversible interfacial chemical reaction of a material with can result in consumption or in dissolution into the material.
Degradation / Ageing	The gradual process of change in characteristics with operational time of a material/component/system triggered by stress impact. Typically for PV this aging process causes a decrease in performance (power loss).
Degradation Rate	A parameter that quantifies the magnitude of a PV module power decay of its initial maximum output power.
Effects	Reactions, alterations, or changes of state, due to causes. Here typically due to the impact of stressors.

Encapsulation	Polymeric film embedding the solar cells and electrical circuits to prevent mechanical damage to the solar cells and to prevent water, water vapour or oxygen ingress to the electrical contacts.
Evaluations	The experimental measurements to be made at each exposure step in a study.
Exposure	The exposure conditions to be used in a study, include the specific stressors and stressor levels, and the times of each exposure step, between the experimental evaluations.
Homogeneous Material	Uniform materials; consisting of one substance in one defined state.
Homogeneous Load	Same mechanical load applied to all parts / sections of a material, component, or system.
Homogeneous Stressor Level	Same stressor level of a stressor applied to all parts / sections of a material, component, or system.
Hotspot	Localized heating of a PV module due to a) reverse biasing and junction breakdown of a solar cell, b) at a solder bond due to increase of contact resistance or fatigue, c) at contact points of separated parts of a cell.
Lifetime	Period of Usability of a Product.
Load	The stressor level for an applied mechanical stress as a load on a material / component / system.
Macroclimate	The general stressors (e.g., temperature, irradiance, humidity, rainfall) that a PV module is operating under which are often defined by climate zones (e.g., Köppen-Geiger). The sum of the general environmental and climatic stressors (e.g., temperature, irradiance, humidity, precipitation) at a location of interest; often given by the climate zone. For the report: describing the climatic conditions around the PV module.
Mass Transfer	Net movement of mass from one location, usually meaning stream, phase, fraction, or component, to another. Mass transfer occurs in many processes, such as absorption, evaporation, condensation, drying, precipitation, distillation or induced by concentration gradients of a given substance. For PV modules, especially moisture and oxygen ingress is of relevance [16].
Material Moisture	Water contained in a water absorbing material can be relative or an absolute value.
Microclimate	The local stressors that a PV module is operating under that are specific to its exact location (e.g., albedo, stress induced from mounting, variations in temperature, irradiance due to location in a PV field). The sum of the local stressors that an object, e.g. a PV module experiences during operation; is specific to its exact location and surrounding (e.g., albedo, stress induced from mounting, variations in temperature, irradiance due to location in a PV field) and design. The microclimate can be inhomogeneous even within a PV module (different humidity or cell temperature).

Performance Loss Rate	A parameter which assesses the performance evolution of a PV module or PV system based on a performance metric (e.g., electrical, or empirical metrics) [17].
Performance Ratio	A measure of the quality of a PV module, expressed as the ratio of the actual and theoretical PV module energy outputs [18].
Relative Humidity	The amount of water vapour present in air expressed as a percentage of the amount needed for saturation at the same temperature.
Reliability	Probability that a product, system, or service will perform its intended function adequately for a specified period of time or will operate in a defined environment without failure. PV Materials/Components/Systems, reliability means the probability that the material/component/system will operate adequately for a specific environment and time without failure. This is related to the specifics of service life and end of life definitions.
Reliability Model	A time dependent function that describes the evolution of PV modules power with increasing operation period.
Service Life	Period of use under operating conditions defined specifically for each module or installation. For PV modules, it can be often related to the expected business plan. **Life Cycle**: Description of all stages of a product; The life-cycle stages of photovoltaics involve (1) the production of raw materials, (2) their processing and purification, (3) the manufacture of modules and balance of system (BOS) components, (4) the installation and use of the systems, and (5) their decommissioning and disposal or recycling. **End of Life** (EoL); Depends on many factors such as technology, operational, and economical factors. In PV EoL is often related to warranty conditions (e.g., time required for a PV module to lose 20% of its initial STC power). For more details on the specifics see section 2.
Soiling	The deposition of airborne particles, including, but not limited to, mineral dust (silica, metal oxides, salts), pollen, and soot. Soiling also includes snow, ice, frost, various kinds of industry pollution, sulfuric acid particulates, bird droppings, falling leaves, agricultural feed dust, and the growth of algae, moss, fungi, lichen, or biofilms of bacteria. In PV, soiling is meant to be the accumulation of material on light-collecting surfaces in solar power systems [19].
Stress	Mechanical stress applied to a material / component / system from physical loads.
Stressor Level	Magnitude of a stressor applied to a material, component, module, or system. For example, if irradiance is the stressor, the level could be 0.5 suns. Stressor level x Time = stressor dose.
Stressor	Physical, chemical, mechanical, or biological stress which is acting on a material/component/system. Examples include temperature, irradiation (UV, VIs, NIR), water/moisture, electrical potential as well as mechanical stresses such as compressive or tensile impact.

Study Protocol	The complete definition of an experimental study, including definitions of the exposure conditions, the experimental evaluations used to characterize changes, the measurement plan for when the data of each evaluation will be acquired and analysed, and the results interpreted.
Thermal Shock	Thermal shock is caused by a type of rapid transient mechanical load. By definition it is a mechanical load caused by a rapid change of temperature.

2.1 Service Life Prediction

The methodology used to calculate the end-of-life of a product is called Service life prediction (SLP) [20], [21]. This methodology involves predicting the life of PV modules through the modelling of degradation as a function of impacting environmental and operational stressors [20]. Such calculations require adapted mathematical models which are able to include all relevant stressors and also specific parameters of the specific module type. So, the models can be rather complex and often require a lot of (experimental) work to supply all relevant data. Pickett [22] notes, "there is a fundamental difference between the SLP process and a standard test protocol. Evaluating and qualifying materials for commercial applications requires testing under standardized, agreed-upon conditions to generate pass/fail criteria. It is engineering. The problem comes in the question of how those test results correlate to the real world. SLP requires doing many experiments, constructing a model consistent with the data, and making the prediction with a range of uncertainty. It is science."

Service life prediction as it is applied in the present report is modelling the development of gradual degradation effects leading to a reduced functionality, in the case of PV modules, to a reduced maximum output power. Catastrophic failures resulting for extreme events like hailstorms, fire, human impacts etc cannot be included in such SLP models.

$P_{critical}$ is the minimum required functional property level that must be defined in quantifiable terms to implement SLP, see definition of end-of-life below. These failure criteria can be selected to examine different failure modes for different products. It is common to redefine the critical value defining failure several times over the course of SLP experiments as one receives more insight into the system under study [20]. Each specific failure mode will generate a SLP model that predicts the time-to-failure limited by that particular failure mode. When a single SLP model is able to predict several types of failure within an experiment, this is evidence that the different failure modes share the same degradation pathways.

2.2 Definition of End-of-Life

Service Life calculation requires a clearly described status of the product which defines the end-of-life. If a product reaches an unserviceable status the decision is clear but for PV-modules this is a very rare case and if it occurs, it is usually linked to extreme impacts like e.g. hailstorms or fire events. Such events are not included in the service life prediction approaches and models described in this report since they are not depending on intrinsic processes in the modules and not following gradual changes. An overview of potential module failures, influencing factors and effects can be found in a previous report of IEA PVPS Task 13 [23].

End-of-life is defined differently for PV modules, depending on the specific context or issue. The end-of-life is typically dependent on the use of the PV module and the specific conditions of the PV power plant. Current levelized costs of energy (LCOE) compared to replacing the modules or the operation and maintenance costs of modules are often influencing factors. The following chapters describe different terms and definitions related to the end of life of PV modules as well as influencing parameters.

The International Electrotechnical Commission (IEC) defines accelerated testing procedures by which to ensure a defined quality level of PV modules, summed up in so called “Type Approval Testing” standards such as the IEC 61215 series for terrestrial PV modules [24]. Unfortunately, these tests are linked in many people’s minds to specific service lifetimes or warranty times but is has to be clearly mentioned that this is not the case. The standards have been developed to identify specific weaknesses of modules and ensure a basic quality level

but do not address the issue of defined service lives. They especially do not differentiate between different climatic conditions where the modules will be operating in. These "Type Approval Tests" use four pass/fail criteria to determine if the module satisfies the requirements of a particular testing standard: First, the measured module power output (P_{max}) must not degrade by more than 8% of the initial power before testing. Additionally, there should be no open circuit or ground fault detected. There should be no evidence of major visual defects, and finally, the insulation test requirements are met [25]. It has to be mentioned that the test requirements have to be seen as minimum requirements and the tests are aimed to identify early faults (infant mortality) or product series defects, so all these simple pass/fail criteria are only defined to identify specific quality issues in these tests but cannot be interpreted as end-of-life conditions. So, neither the tests nor the pass/fail criteria can be used to perform service live prediction calculations and even more do not allow for a correlation of passing the standardized tests with specific service lives at a specific location.

2.2.1 End of Functional Life

A more general description of the end of functional life is required for PV modules in the field.

The functionality of products degrades over time. This degradation is described by mathematical models correlating influencing factors, in the case of PV modules typically environmental and operational stressors, with a reduction of a selected property, for PV modules the selected property is usually the module power. As described in section 2.1, the end of functional life is reached when the critical property has fallen below a certain value. Then the functional end of life is reached. From a purely technical viewpoint, the end of functional life of a PV module is only reached when the module does not deliver any electricity at all or electrical safety is not guaranteed anymore. This is from the practical viewpoint not reasonable and therefore often much higher levels of the critical parameter are chose, which can be influenced also by non-technical reasons (as warranty levels).

2.2.2 End of Economic Life

Depending on the economic situation of a specific PV system, the end-of-life can be reached due to changing contractual conditions (e.g., changing electricity prices) or if it comes economically attractive to replace PV modules by new ones with higher efficiency. In such cases, the end-of-life can be reached at all stages of degradation, but usually the degradation is influencing the decision since it influences performance and yield, see also description of end of functional life. For optimizing these decisions, using appropriate degradation models which can predict degradation is key.

3 CLIMATIC STRESSORS

3.1 Introduction to Climatic Stressors

Degradation of PV modules is controlled by the materials and components of the PV module, and the stressors (irradiance, temperature, humidity) the module is exposed to in the local climate zone. And these module and climate factors directly impact the service life of the PV modules. The term “Climatic Stressors” sums up all stressors which are arise from the local climate where the PV module is deployed.

Regarding service life and degradation estimation for technical products, one has to differentiate between macroclimatic stressors and microclimatic stressors. Macroclimatic stressors describe the macroscopic situation of the product, so more or less the conditions around the product, defined by the weather conditions etc. Microclimatic loads describe the specific situation on the very specific piece of material of interest. So microclimatic conditions describe the factors directly influencing degradation processes. Some of them are described by the same physical values as the macroclimate, e.g. temperature and humidity, others are additional, like e.g. mechanical tension within a product. There is usually a strong dependency of the microclimate on the macroclimate for PV modules since they operate in outdoor condition and so e.g. high ambient temperatures and irradiation levels (macroclimate) also lead to high temperatures of the module and high irradiation doses for the materials microclimate.

The chapter gives an overview on the different stressors, as well as on possibilities to determine and classify them and handle related uncertainties.

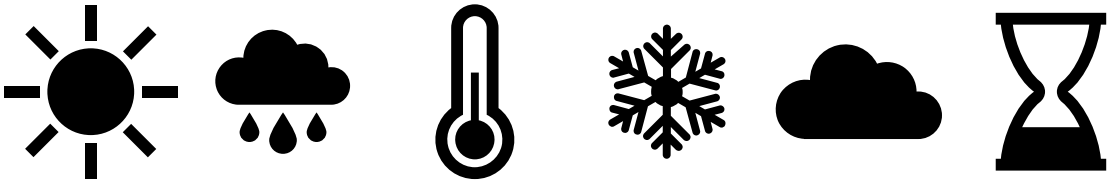

Figure 1: Schematic presentation of macroclimatic loads, e.g., irradiance, humidity, temperature, snow, short-term temperature changes triggered by clouds, sand.

3.2 Macroclimatic Loads

PV systems are operated under almost all kinds of extreme environmental conditions. For example, PV modules in deserts experience high levels of solar radiation which are associated with high module temperature differences between day and night. PV modules in alpine regions experience high mechanical loads from wind, ice, and heavy snow loads which place particularly high demands on the stability of the multi-material composite PV module. In every region, there is a very specific mix of climatic and environmental stressors. The influence of these stressors on the performance and reliability of PV systems is often difficult to predict. Synergistic effects between the stressors also occur such as moisture which can accelerate degradation reactions or open new reaction paths. In addition, the combination of mechanical loads and chemical stress can lead to drastic material degradation or failure.

3.2.1 Relevant Macroclimatic Stressors

The different factors of the ambient climatic conditions, the macroclimatic stressors, are impacting on the module conditions (microclimate) and influence the degradation processes in manifold ways. Some of the stressors can be directly linked to specific degradation processes, e. g. extreme snow loads to module breakage, others are linked to several or like in the case of temperature to more or less all processes.

The most important macroclimatic stressors are listed below, subdivided into (i) influence parameters determined by the climatic conditions and (ii) environmental influences on the materials/composites.

Table 2: Relevant Macroclimatic Stressors.

Stressors	Examples
Climate induced stressors	
Temperature	• Extreme values (often interrelated with high irradiance) • Influencing reaction rates of most chemical processes • Temperature cycles o short-term temperature changes triggered by clouds o day-night temperature differences o seasonal temperature fluctuations
Humidity	• Humidity (can induce chemical reactions - hydrolytic degradation) • Dew (can induce chemical reactions such as hydrolytic degradation) • High Surface Conductivity • Precipitation (often interrelated with mechanical impact or thermal shock) o rain o snow o ice o hail
Solar irradiation	• Ultraviolet (UV), Visible (can induce unwanted chemical reactions; C-C bond cleavage, photo-oxidative degradation) • IR (generates temperature increase and accelerates degradation reactions)

Environmental stressors	
soiling (mostly from natural local sources)	• bird droppings • aerosols, pollen • dust, sand
human pollution - pollutants generated by local sources (industry, heavy traffic, agriculture, …)	• chemical stressors o acidic air pollutants (e.g., NO_x, SO_x) o basic air pollutants (e.g., ammonia) o salt (e.g., road salt near the motorway) o oxygen
stress impact induced by the local geographical conditions	• near the coast o chemical stressor (e.g., salt) o mechanical stressor (e.g., high wind load) • in alpine regions o mechanical load (e.g., heavy snow load) • in regions prone to hail and thunderstorms o hail impact o lightning strike o storm-prone which manifest as mechanical and dynamical mechanical loads (e.g., storms, typhoon)

The time-dependent repeated application of combined climatic and environmental stresses can induce material degradation effects or fatigue, performance losses and induce failure modes. As some stressors can have a highly accelerating impact on degradation reactions and some impacts can act synergistically, the development of suitable accelerated ageing tests to simulate and predict various climatic and environmental conditions is a demanding task.

3.2.2 Classification of Macroclimatic Conditions

In order to generalize findings from differing PV sites, a classification system is needed that associates the similar climatic variables under a singular classification. For many scientific fields, the Köppen-Geiger classification is used to relate different geographic locations by similar climatic conditions. This system, first introduced in 1884 by Vladimir Köppen [26], was improved upon by Rudolf Geiger in 1961 [27]. The Köppen-Geiger classification divides the world into five main climatic groups, A, B, C, D, E (Tropical, Dry, Temperate, Continental, and Polar, respectively). These main climatic groups are based on the type of foliage that can grow in a specific region [26]. This climate classification is updated regularly to represent current climatic conditions [15].

Recently, groups have been designing specific classifications for certain applications. For example, the American Society of Heating, Refrigerating, and Air-Conditioning Engineers (ASHRAE) have developed their own climate zones. The ASHRAE system was designed around the usage of heating, ventilation, and air conditioning (HVAC) systems, relying on the number of ‘heating degree days’ or a measurement of how much heating would need to be applied to warm a space to room temperature [28]. Motivated by supplementing the com-

monly used Köppen-Geiger climate system, Ascencio-Vásquez et al. [29] have added irradiance based climatic conditions. The new system, named KGPV, only uses the main climatic classification (A - Tropical, B - Desert, C- Steppe, D – Temperate, E - Cold, F - Polar) and a category based on the average annual irradiance. The irradiance categories have been divided into 30th, 50th, 80th percentiles. Of the 24 climatic zone possibilities, 12 have been selected based on land coverage and population density. Photovoltaic degradation climate zone (PDCZ) is a new system based on the specific level of stressors that a module would be exposed to at a specific location [30]. PDCZ is specifically designed for use in the PV industry. The climatic classification consists of three categories: module temperature (T1-T8), mean specific humidity (H1-H5), and wind speed (W1-W5). The temperature category has been divided up into equal land area portions, whereas the humidity group has been binned for equal data distribution. To capture the performance and degradation of a PV site, a climate classification needs to be designated. Climatic categories elucidate the conditions modules operate under. A robust classification schema enables site owners/operators to cater their installations to the specific climate location. Using the KGPV classification system, Ascencio-Vásquez et al. [31], have mapped the amount of predicted degradation of modules for each climate zone. Alternatively, Karin et al. [30] have specifically selected the criterion for their climate classification to be stressors that affect the degradation of PV systems. A climatic classification combined with in-depth understanding of module degradation is critical to affirming manufacturing warranties and predicting module lifetime [32].

3.3 Conditions in Accelerated Testing

This section describes stressors and stress levels frequently applied for the testing of PV modules, and current research directions being pursued to increase the relevance of accelerated testing for PV. Accelerated stress testing involves applying stressors that PV modules experience in their field use conditions but at higher stress levels than the PV modules experience in the field. These include temperature (e.g., high temperature, low temperature, temperature cycling), solar irradiation, mechanical stress, humidity, impacts (e.g., hail, stones, projectiles), electrical discharge, acid, basic, and corrosive fluids. Indirect factors as a result of light include current, bias on the p-n junction, and system voltage. Tests should be applied to materials, components, mini-modules, and full-size modules. Stressors may be applied in single factor tests, steady state, multi-factor tests, sequential stress factor, and combined stress factor tests. A major challenge that accelerated testing has yet to address, is the fact that the response of a material to a five or ten time increase in the particular stress level for that stressor, may not be a linear function of the stress level. So, for example a material exposed to one sun irradiance vs. exposed to five suns irradiance, may not obey reciprocity, and may not degrade a factor of five times faster. This makes many, if not most, accelerated tests, while useful, not activating the same degradation mechanisms as real-world exposure conditions [33].

Most of the commonly applied stress tests originated in military and electronics test specifications which include the Commission of the European Communities (CEC), the European Solar Test Installation (ESTI), the Jet Propulsion Laboratory (JPL), and the IEC [8]. In the following sections tests and testing methods are described which are used in PV industries. Most tests are based on the type approval standard IEC 61215. These tests are also varied in several specific methods in different ways. Some of the methods mainly multiply the test durations or cycles of IEC 61215, grouped, and named as “extended IEC 61215 testing”. Other methods do not define specific test durations but apply the tests until a failure occurs. This approach is named “test to failure”. Both approaches can even be used to generate

rankings of samples, but it must be clearly mentioned that the results cannot be linked to expectable service life times of modules.

3.3.1 Damp Heat

Damp heat testing, otherwise known as high-temperature, high-humidity testing, examines the ability of the module to resist environmental factors such as corrosion of materials, water-vapour intrusion, hydrolysis, and delamination of encapsulant materials. The most common damp heat condition is 85°C and 85% relative humidity. The appropriate testing regime depends greatly on the PV module design and the mechanism to be accelerated. A conventional encapsulated c-Si cell using a polymeric backsheet experiences moisture ingress quickly in the field and in the damp heat chamber because typical backsheets are not moisture barriers. The relation between hours of damp heat testing with a 20-year module life at site-specific conditions and estimated 20 years exposure in Miami, Florida, is correlated with 144 h at 85°C, 85% relative humidity ion driven by the resistivity of polymeric encapsulants [34]. In contrast, in a glass–glass module with edge seal performing as a moisture barrier, it takes more than 3000 h at 85°C, 85% relative humidity condition to test for moisture ingress that would occur in 25 years in the Miami environment [35].

3.3.2 Temperature Cycling

The purpose of temperature cycling, or thermal cycling (TC) is to induce stress associated with diurnal and climatic temperature excursions. CEC Specification No. 201 [8], [36] defined a temperature cycling test alternating between -40°C to 85°C. The JPL Block V Buy included a test sequence with up to 200 thermal cycles [37]. Based on field results, 200 cycles of temperature cycling between -40°C and 85°C has been extrapolated to survive ten years in the field [38]. This type of failure is still observed in the field in hot climates [39]. In a modelling study for lead tin (PbSn) solder joints, the number of thermal cycles (-40°C to 85°C) required ranged 100 to 630 for various use environments for an equivalent 25-year exposure [40].

3.3.3 Humidity Freeze

Humidity Freeze is designed to evaluate delamination of encapsulant, junction box adhesion, and inadequate edge seal [41]. It generally reveals destructive effects caused by humidity penetration and subsequent expansion at below-zero temperatures. The current IEC 61215 qualification test requires at least 20 h at 85°C 85% relative humidity and 0.5 h freeze at -40°C, in ten repetitions [24].

3.3.4 Full Spectrum Light and UV Testing

Testing of PV modules has generally been unrepresentative and insufficient for outdoor lifetime prediction. Light produces various light-induced degradation (LID) effects, including those associated with bill of material (BoM) complexes, metallic impurities, and hydrogen. It also may contribute to delamination as a secondary effect caused by material degradation like embrittlement of encapsulants [41]. Correlation between the total UV exposure dose and module short circuit current (I_{sc}) for all exposures showed that UV radiation caused losses of 0.25%–0.6% per year [42]. Contributions to the degradation include degradation of passivation of the cells [43] and yellowing of the polymer [44]. UV light sources for the test include sunlight, Xenon arc lamps, metal-halide lamps, and fluorescent UV lamps in the UV-A and UV-B ranges. UV exposure at higher temperature accelerates the degradation in polymers as found in a study of PV module backsheets [45].

3.3.5 Mechanical Load

Mechanical loading, such as by static loading or cyclic dynamic mechanical loading can precipitate failure modes such as broken Interconnect, cell breakage, solder bond failures, glass breakage, and other structural failures. Load levels for static loading in IEC 61215 [24] qualification testing are 2,400 Pa, or optionally 5,400 Pa, for static loading, and per IEC 1000 Pa for cyclic dynamic mechanical loading in IEC TS 62782 [46]. It is frequently sought to alternate mechanical loading with environmental stress tests such as temperature cycling and humidity freeze cycles to grow cracks, precipitate delamination, and abrade the crack interfaces.

3.3.6 System Voltage

System voltage produces the class of phenomena called potential-induced degradation (PID) [47], these include PID-shunting, polarization, corrosion, and delamination abbreviated as PID-s, PID-p, PID-c, and PID-d, respectively. Shunting is most commonly understood to occur when cells are in negative potential with respect to the grounded module frame and exterior and Na+ ions of the glass front migrate into the cell causing a shunt at the junction and a loss of the cell fill factor (FF). Polarization occurs when charge collects on the passivating dielectric layers of the cell of polarity such that minority carriers are attracted to the surfaces and recombine, leading to loss of open circuit voltage and generation of photocurrent. Electrochemical corrosion usually happens over a longer term in crystalline silicon technologies, especially with respect to cell metallization interface with silicon, the metallization surface, and the anti-reflective coating. The nature of the degradation by the corrosion reactions and the pH resulting from the reactions depends on the polarity. System voltage also contributes to loss of adhesion and causes the formation of bubbles [48] .

3.3.7 Weathering Tests

Weathering tests typically involve application of temperature light and moisture. ASTM G155 “Standard Practice for Operating Xenon Arc Light Apparatus for Exposure of Non-Metallic Materials” and D7869 “Standard Practice for Xenon Arc Exposure Test with Enhanced Light and Water Exposure for Transportation Coatings” are standards with cyclically applied stress factors. Such cyclic tests, e.g., exposure in a xenon device with front-side water spray (3500 hours xenon 123 W/m^2 300 nm - 400 nm, 90°C BPT, 102 minutes UV dry, 18 minutes dark with water spray) have been used to manifest failures in backsheets [49]. Weathering Technical Standard IEC 62788-7-2 “Measurement procedures for materials used in photovoltaic modules - Part 7-2: Environmental exposures - Accelerated weathering tests of polymeric materials” specifies several steady state weathering conditions including factors of temperature, humidity UV exposures with Xenon source, also applied to evaluate backsheets and other polymeric materials [50]. A commonly applied IEC 62788-7-2 called A3 implements 65°C chamber air temperature with 20% relative humidity, 90°C black panel temperature, 0.8 W m^{-2} nm^{-1} at 340 nm.

3.3.8 Climate Specific Accelerated Ageing Tests

Based on the definition of the four climate profiles 1) dry and hot - arid, 2) moderate 3) humid and hot - tropical and 4) high irradiation - alpine, within the Austrian R&D project INFINITY (https://energieforschung.at/projekt/climate-sensitive-long-time-reliability-of-photovoltaics/) [51] a programme was worked out with 14 climate specific test conditions for accelerated ageing tests [52]. The big challenge in this respect was the adaption/advancement of existing standard procedures (e.g., PV module design qualification and type approval IEC 61215, PV

module safety requirements IEC 61730 [53], or salt mist corrosion testing IEC 61701 [54]), for PV modules/components testing in a way that reliable testing for certain climatic conditions optimized PV modules is possible [3], [38], [52]. The time-dependent repeated application of combined climatic and environmental stressors (e.g., temperature, temperature cycles, humidity, irradiation, mechanical load, salt mist) was used to induce performance loss, material degradation, and failures in test modules which resemble those effects occurring in real-world PV installations under comparable climatic and environmental conditions [55], [56]. The advanced analysis of the data and first approaches of advanced data treatment have already clearly shown that the electrical and material degradation of the test modules is dependent on (i) the type and combination, (ii) duration, and (iii) mode (sequential versus constant) of the stresses applied [57].The failures and performance losses observed in PV-plants installed in various climate zones worldwide [58], [59] were compared to the failure modes and degradation effects detected upon the climate specific accelerated ageing testing. The simulation of environmental stresses like heavy snow- and wind load and, enhanced frequency of temperature cycling resulting in cell cracks and cell connector breakage could be demonstrated. The accelerating effect of enhanced temperature, humidity, or additional irradiation on the degradation of power and especially the polymeric materials could be shown.

3.3.9 Combined Accelerated Stress Testing

While most of the above test methods have been optimized to replicate particular failure modes after they have been characterized in the field, here, the stressors of the natural environments are combined: humidity, temperature, light, rain, wind/snow loads, as well as voltage stress, into a single Combined-Accelerated Stress Test (C-AST) for PV modules [3]. This approach requires fewer modules and with fewer parallel tests and is designed to discover potential weaknesses that are not known a priori in new or changed module designs by applying the stressors of the natural environment at levels corresponding to their statistical tails in diurnal and seasonal sequences [60]. In addition to backsheet cracking, degradation modes were observed including solder/interconnect fatigue, various light-induced degradation modes, backsheet delamination, discoloration, corrosion, and cell cracking. The ability to simultaneously apply multiple stressors may allow many of the test sequences within the standardized design qualification procedure to be performed using a single test setup [3].

3.4 Microclimatic Loads for Modules

While the above described macroclimatic stressors which are measured in the (close) vicinity of the PV power plant and describe the local climate and environmental conditions, the temperature, humidity, and irradiance at the multilayer composite of a PV module can deviate strongly from the macroclimate. Thus, the term “microclimatic load” mainly describes the conditions (thermal impact, the humidity, and the radiative input) inside a PV-module (e.g., in the encapsulant, at the interface solar cell/polymer). These conditions are the relevant parameters for processes taking place in the module (e.g., chemical degradation reactions). Therefore, it is essential to be able to estimate the microclimatic conditions to estimate the reaction rates of degradation processes and so also degradation effects and service life.

3.4.1 Relevant Loads for Degradation Effects / Processes

Microclimatic loads are defined as a local (meaning in / at a specific piece of material of the module) / temporal specific climatic factor affecting the degradation of PV modules during their long-term operation. Microclimatic loads do not only depend on the macroclimatic factors, which are subjected by climate-classification schemes, such as Köppen-Geiger climate

classification [15], but also on operational conditions (e.g., electrical potential within the module). From this perspective, typical microclimatic loads related to degradation of PV modules are summarized in Table 3:

Table 3: Degradation Effects of Microclimatic Loads.

Climatic Factor	Microclimatic Loads	Degradation Effects
Temperature	Extreme High / Low Temperature	Physico-chemical property changes of polymeric materials (e.g., creep)
	Rapid temperature change	Thermo-mechanical fatigue in soldered portions
	Non-uniform temperature elevation	Hot Spot formation Bypass-diode failure
Irradiation	Non-uniform irradiation	Hot Spot formation
	(Shading)	Bypass-diode failure
	High content of UV radiation	Loss of encapsulant integrity
	Differences in albedo	Yellowing of polymeric materials
Dust / Soil	Non-uniform accumulation of dusts	Hot Spot formation
		Bypass-diode break
		PID risk increase
Humidity	Non-uniform penetration of moisture into PV module	Corrosion (interconnectors / gridlines)
Salt mist / Gas	Penetration of salts / gases into PV module	Acceleration of Corrosion Processes and PID
Wind / Snow	Non-uniform mechanical / thermal loads	Cell cracks / Frame brake / Demounting
Hail	Instantaneous mechanical impact	Cell cracks / Glass break

On the basis that PV modules are operated in places with an ambient temperature range of at least -40°C to +40°C, almost all of them have been designed and type-approved, in accordance with the international standards (IEC 61215 / 61730 series). This ambient temperature range is equivalent to the module temperature having a 98th percentile temperature of 70°C or less. However, when PV modules are mounted on a roof with only a small gap between modules and the roof under high-temperature conditions, the module temperature often exceeds 70°C in the 98th percentile temperature. Although the degradation caused by the temporal high-temperature is evaluated with the new test specification (IEC TS 63126: 2020 its effect in PV modules during long-term operation under the environments would be prudently considered in the modelling of service life prediction, while the temporal (and repeated) high-temperature modestly affects the physico-chemical properties of polymers in PV modules [61].

Furthermore, the module temperature is temporally changed by the shadow of moving clouds, as well as by the diurnal cycle with day and night. Indeed, by the shading, the module temperature can oscillate over 20K range within a short-term on a cloudy-hot day. The thermo-mechanical damage is consequently accumulated in the soldering bonds (in particular, the contacts between interconnector and busbar on the individual PV cells) [40], [62]. In a similar way thermo-mechanical damage leads to backsheet cracking (e.g., for Polyamide (PA)-backsheets [63]). This degradation effect has been included in a physical model for service life prediction [6], [9], as well as the evaluation procedure on this effect is published as IEC 62892:2019.

In addition, the diurnal shading with trees, buildings, and other obstacles for solar irradiation (including the non-uniform accumulation of dust / soil on PV modules) would induce not only the non-uniform temperature elevation within PV cell/module, but also the current mismatch of cells within the PV module. This spatial difference in temperature accelerated by the current mismatch could be a cause of the accumulation of thermo-mechanical damage in the soldering bonds, and the bypass-diode could eventually fail. Therefore, degradation due to shading should also be considered in estimating service life in certain situations. Another specific degradation can appear in locations having radiation spectrum with high UV content (e.g. high mountain). In those circumstances, the organic encapsulants have a heavier damage and it exists the risk of early loss of their properties giving rise to humidity ingress and further module degradation. The backsheet is impacted by differences in irradiance depending on differences in the albedo from ground covering (e.g., soil compared to vegetation) and the position of the backsheets in the field (e.g., top row compared to bottom row, edge of a row or the middle of a row) [64], [65].

Humidity works as a key stressor to degrade PV modules. Metal parts (especially in front metallization on the respective PV cells) are corroded by the moisture and the organic acids released from the encapsulant. Since the dynamic behaviour of moisture ingress mainly depends on the penetration kinetics from ambient moisture (from rear side through the inter-cell spaces) [66], [67], an inhomogeneous spatial distribution of moisture on each PV cell is observed [32]. Consequently, the non-uniform degradation within each PV cell is resulted by this behaviour of moisture ingress which is depending on some parameters (ambient temperature / humidity with diurnal cycling, water vapour transmission rate of backsheet, diffusion constant of water in encapsulant, width of inter-cell space, and others). In PV modules installed on a floating body on a water surface (e.g., lake or sea), the high-humidity atmosphere around them could continuously affect the degradation, for example, the leakage current between the frame and cells could be elevated in those of the floating PV system [68]. PV modules installed in coastal areas or on the roof of livestock barn could be excessively degraded by the corrosion facilitated with salt mist or ammonia gas, respectively, as the acceleration of potential-induced degradation (PID) has been reported under the salt-mist spraying on PV modules [69].

High-velocity wind due to a tropical cyclone and storm triggers the fracture of solar cells which would be a major cause of the hot-spot formation, by the cyclic loading of non-uniform mechanical pressure to PV modules installed in these regions [70]–[72]. Cell cracks can be caused by instantaneous hail impacts. Since the time of emergence and the intensity of these loads could not be easily predicted, the effects on the degradation of fielded PV modules is generally difficult to be included in a physics model on the degradation of PV modules operated in a field. However, newly proposed data-driven statistical and machine learning methods could provide a good solution to include these effects based on historical data.

3.4.2 Determination / Calculation of Microclimatic Loads

Usually SLP models (especially physics-based models) require microclimatic loads as inputs (e.g., module temperature instead of ambient temperature or humidity inside the PV module instead of ambient humidity). To provide the microclimatic data, several models are used to calculate microclimatic loads from macroclimatic conditions.

A. PV Module Temperature Models

Temperature is the macroclimatic impact factor, which has probably the biggest impact on degradation rates and Service Life of modules, since it is not only causing temperature driven processes, but it also acts as an acceleration factor for most degradation processes. The calculation of microclimatic temperature loads is therefore of highest importance for the estimation of degradation of modules. Several models have been developed to estimate microclimatic PV module temperature using ambient temperature, irradiance, and wind speed as input factors [73] [74]. Usually the specific module design and material properties are represented by PV module specific parameters.

Here are presented two commonly used models, one by Ross [75] (1) which is a function of ambient temperature and irradiance, and the other one by Faiman [76] (2), which takes the cooling effects due to wind into account:

- Ross model

$$T_{mod} = T_{amb} + k_{Ross} \times E_{POA} \quad (1)$$

- Faiman model

$$T_{mod} = T_{amb} + \frac{E_{POA}}{U_0 + U_1 \times ws} \quad (2)$$

where T_{mod} and T_{amb} $[^{\circ}C]$ are the PV module and ambient temperature, E_{POA} $[W/m^2]$ is the incident solar irradiance on the module, and ws $[m/s]$ is the wind speed. k_{Ross} is the Ross coefficient, which is related to the heat transfer properties of the materials [77]. U_0 $[W/(°C\ m^2)]$ and U_1 $[W\ s/(°C\ m^3)]$ are the coefficients describing the effect of the radiation on the module temperature and the cooling by the wind, [78] respectively.

B. Models for Humidity Ingress

Humidity is a very important parameter for the microclimatic conditions influencing degradation processes in PV modules. Heat transfer in PV modules is a fast process, usually faster than a change of the climatic conditions. The environmental conditions determining the module temperature can therefore usually be directly used as input in SLP models. However, moisture diffusion is a comparably slow process. The type of module, its layout, and materials used have a large impact on the speed of diffusion and possible moisture ingress pathways. For example, it can take several days for moisture to penetrate a backsheet, but several years to diffuse to the encapsulation in front of a crystalline silicon cell [79], [80]. The moisture content at different positions inside the module can thus vary strongly at any given time, as shown in Figure 2.

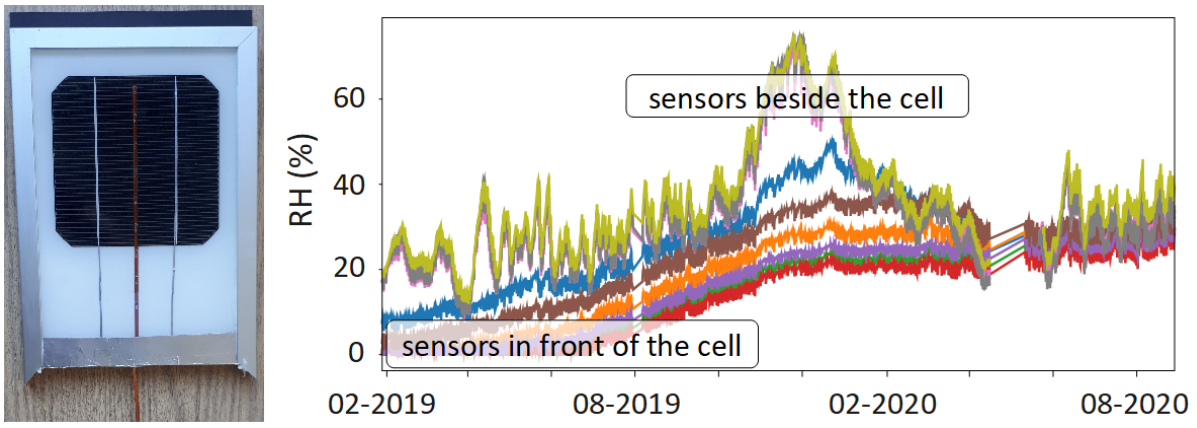

Figure 2: Moisture ingress measured with miniature RH sensors at various places in a 1-cell crystalline silicon mini-module mounted in Bolzano, Italy [80]. The module consists of an ethylene-vinyl acetate (EVA) encapsulant and a polyethylene terephthalate (PET) backsheet.

Simple analytical relations, equivalent to (3) and (4) for the temperature, are thus hard to find and specific to the type of module, the materials, the location of the installation and the position of the material within the module. SLP models therefore currently do not include all these factors and use e.g. an average moisture content inside the module, commonly linked directly to the relative humidity in the air. However, their accuracy could be increased in the future by correlating them to the spatially resolved moisture profile over time in the modules. This profile is usually calculated with finite element method (FEM) simulations. To combine the additional insights delivered by FEM simulations with SLP models the development of the moisture content at a selected position in a module over time can be calculated by FEM and used as input data set for SLP. Such data is relatively independent of short-term changes and therefore can be combined with e.g. temperature data with higher temporal resolution. Examples for such simulations to determinate the humidity content inside PV modules can be seen in Figure 3 and Figure 4. For both calculations the identical module design and material parameters have been used. In addition, measured ambient climatic data of two test sites, one on the island of Gran Canaria, Spain (Figure 3) with maritime climate and one in the Negev desert, Israel (Figure 4) with arid climate have been used. The humidity follows relatively fast the ambient conditions at the positions in the backsheet (named “Backsheet”) and in the interface between backsheet and encapsulation (named “Interface). In the encapsulation in the spacing between two cells (named “EVA centre”) also seasonal effects can be seen. For positions with longer diffusion way from the backsheet like in the encapsulation between cells and the glazing above the centre of the cell (named “EVA top”) or half way between the edges of the cell and the centre of the cell (named “EVA mid”) seasonal effects are negligible. The humidity levels within the modules, which are approached on the long term depending on materials and climatic conditions and can vary significantly or even be very similar, even in very different climates, as the examples in Figure 3 and Figure 4 show.

For service life prediction (SLP) modelling often humidity data is used representing long term average (for positions with high fluctuations) or long term stabilized (for positions with low fluctuations) values. The examples show that the microclimatic humidity conditions are far away from being homogeneous in a PV module and therefore working with only one value for SLP calculations leads to uncertainties, depending on the location of the different degradation processes in PV modules. This has especially to be considered if calculations shall address specific failure modes or specific materials or components.

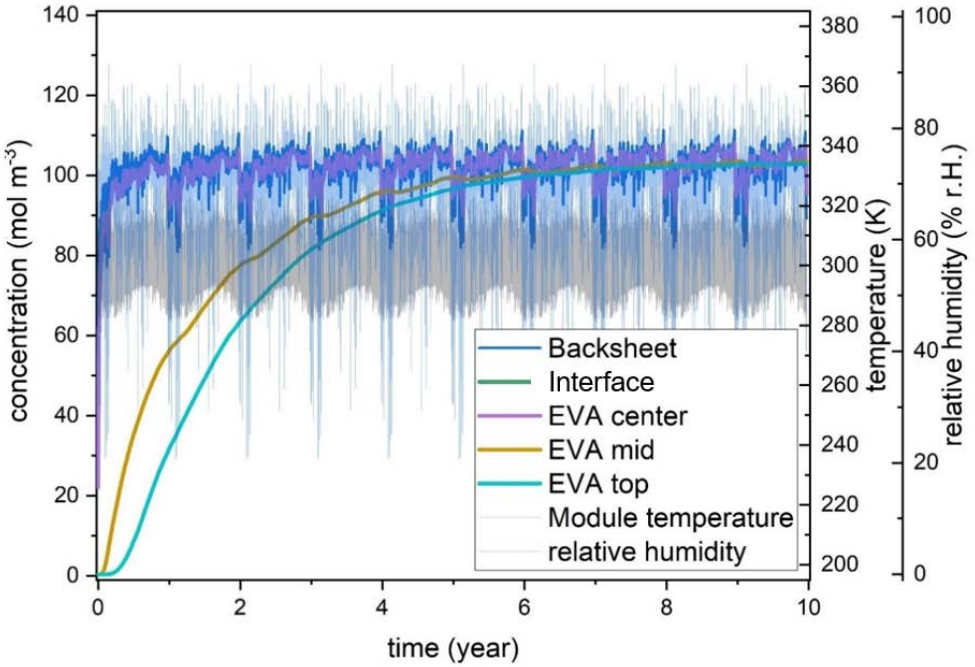

Figure 3: Development of humidity at different positions in a PV module over time using maritime ambient climatic data of a test site on Gran Canaria, Spain.

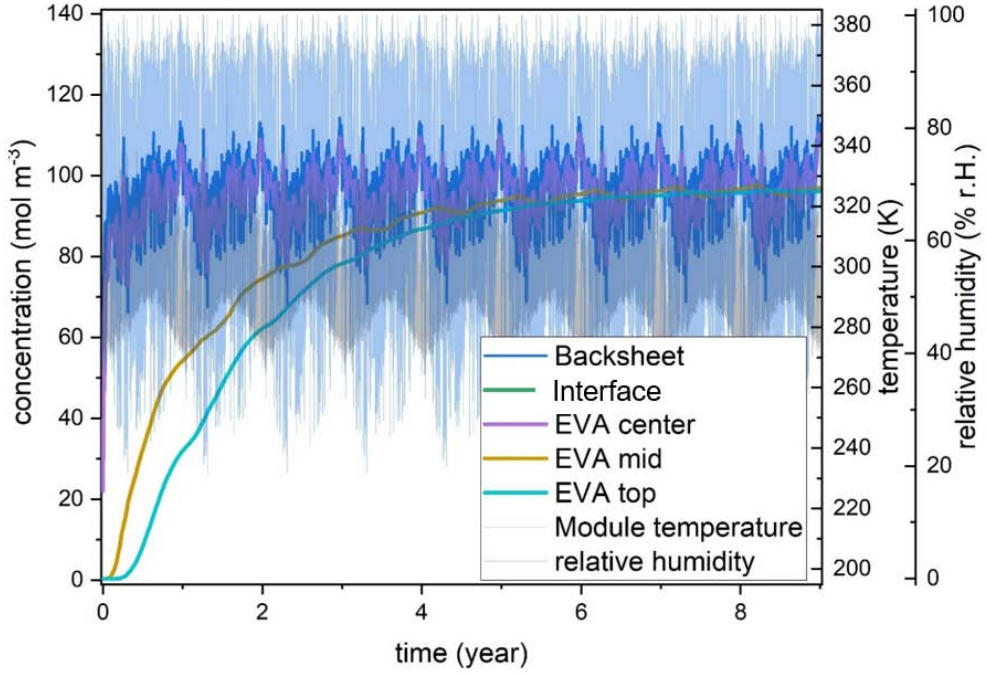

Figure 4: Development of humidity at different positions in a PV module over time using arid climatic data of a test site in Negev, Israel.

The governing equation for humidity diffusion is Ficks Second Law of Diffusion [66]. The change of the water concentration C [kg/m^3] over time is

$$\frac{\partial C}{\partial t} = D \times \Delta C \quad (3)$$

where D [m^2/s] is the diffusion coefficient. Such simulations have led to some non-intuitive results. For example, while initial sorption is much faster in a tropical climate, moderate and alpine climates can lead to a constantly higher moisture content in the front of crystalline silicon cells after several years of installation [79]

Deviations from Fickian behaviour have been reported in various encapsulants, for example thermoplastic polyolefins (TPO) or ionomers [81]. More complex models are better suited to describe these materials. An example is the dual-transport model presented in [82]. It solves equation (3) in FEM simulations and implements such deviations as an inhomogeneity in the material. The boundary conditions on each material interface can be derived from Henry's law, describing the equilibrium state on the boundary.

$$C = S \times p \quad (4)$$

Here, p [Pa] is the partial water vapour pressure and *S* [kg/m^{3}Pa] the solubility of water in the material. The temperature dependency of both *D* and *S* are described by an Arrhenius law, for example

$$D = D_0 \times exp\left(\frac{E_{A,D}}{k_B \times T}\right) \quad (5)$$

where D_0 [m^2/s] is the pre-exponential factor of *D* and $E_{A,D}$ [kJ/mol] is the activation energy. *D* and *S* can span many orders of magnitude in different encapsulants, backsheets and edge seals [35], [83]. Deviations from Henry-type sorption have been observed in polyvinyl butyral (PVB) [84], EVA and PET [85]. The Engaged Species Induced Clustering (ENSIC) model of Perrin and Favre [86], [87] can describe the absorption isotherms more accurately in these materials, using two fitting parameters k_1 and k_2.

$$C = \frac{exp[RH \times (k_1 - k_2)] - 1}{(k_1 - k_2)/k_2} \quad (6)$$

It results in a higher moisture content inside the module in a humid environment compared to the Henry sorption model.

3.4.3 Cross-Correlation of Accelerated Exposure and Real-World Operational Conditions

The exposure conditions used in indoor accelerated tests generally consist of simple controllable stressors. However, installed PV modules are subjected to multiple, complex environment stressors that vary in time, which make understanding PV module real-world degradation behaviours and failure complicated. Recently, studies have started to link the degradation observed in indoor accelerated exposure to degradation observed in outdoor exposure [6], [88], [89], [90]. Accelerated sequential indoor exposures are being used to evaluate PV module performance under synergistic stressors more similar to real-world PV modules [6]. This section focuses on module level studies to bridge the gap between accelerated indoor and multi-climate zone outdoor exposure conditions. Physics-based models and statistical models were used in these module level studies. An example of a physics-based modelling, Kaaya et al. [6] used multiple transformed Arrhenius equations to link indoor and outdoor

exposure by using the exposure conditions and module performance. In their study, three degradation mechanisms, hydrolysis, photo-degradation, and thermomechanical degradation, are assumed to be necessary for service lifetime prediction. The assumption was based on three indoor exposures: damp heat, damp heat with UV light and temperature cycling. Using indoor exposure data, the physics-based models of the three degradation mechanisms were calibrated, validated, and analysed as a first step. The second step was to derive a combined/total degradation rate model from the three specific degradation mechanisms rate models. The combined model was calibrated and validated using performance data of identical PV modules installed in three climatic zones, namely arid, maritime, and alpine. Severe degradation was predicted in arid due to higher temperatures in this zone that determines the reaction rates for other degradation mechanisms caused by other stressors such as hydrolysis by humidity and photo-degradation by UV dose. In correlation with indoor exposure, it was predicted that the hydrolysis mechanism has the lowest contribution to the total degradation rate compared to photo-degradation and thermomechanical mechanisms.

A statistical model uses module performance to answer the question of how similar and how fast the module degrades in different exposed conditions. This model is useful to get the degradation constant rate and determines module performance. A study by Liu et al. [89] uses stepwise I-V measurement for five brands of modules under two types of indoor accelerated test and eight modules installed in three climate zones. The performance of modules under different indoor and different climate zones outdoor exposures is modelled. In the next step, normalization is applied to get an optimal solution as cross correlation scale factor (CCSF). CCSF is calculated to be the sum of squared error by rescaling the time in the indoor model and the cross-correlation coefficient (CCC) for the overlapping time range of the outdoor model and scaled indoor model is determined. CCC is used to evaluate the similarity of the trend of module performance under different exposures, and CCSF indicates the ratio of degradation rate under different exposures. These are the two methods to correlate degradation in indoor and outdoor modules. Because different degradation mechanisms may cause similar change in overall performance, it is important to include more characterization results such as I-V features to obtain more cross-correlation coefficients. The result shows which indoor exposures induce more similar changes for each outdoor system. The results obtained from maximum power and I-V features analysis show good consistency. In particular, the modules installed in the Bwh (arid climate, desert climate, hot desert) Köppen-Geiger climatic zone correlate well with the two models.

4 MODELLING APPROACHES

There are two broad classes of empirical modelling approaches used in degradation studies: statistical models and mathematical (analytical or numerical) models incorporating equations for physical and chemical phenomena. Empirical modelling is the generic term for activities that create models by observation and experiment [91]. The distinction between statistical or physics\chemistry mathematical models is an important distinction because of the difference in perspective of these two approaches. Statistical models, often referred to as data-driven models and based in statistical inference, are empirical models that embody a set of statistical assumptions concerning the generation of the sample data (and similar data from a larger population), and in an idealized form, the data-generating process [92], [93]. Mathematical models, for example in the physical sciences, "start with most of the following elements: Governing equations for the physical or chemical processes being considered, supplementary sub-models with their defining equations and constitutive equations and associated assumptions and constraints such as Initial and boundary conditions and classical constraints and kinematic equations" [94]. These physical/chemical mathematical models can be based on closed form equations (an analytical model), or numerical approximations such as finite element or difference methods [95]. So statistical models and mathematical models are approaching degradation phenomena, modes, and mechanisms from opposite ends. The statistical models are closely tied to the measured data for the system, while the mathematical models are closely tied to the degradation mechanisms that the researcher believes are active in the system. By coupling both data-driven statistical modelling approaches and physical\chemical mathematical modelling approaches, we have the best opportunity to elucidate what is happening in the degrading system [9]. We can confirm the activation of mechanisms whose physics are well understood, and by comparing with the data-driven results, we can identify the gap between our mathematical model and the total sum of degradation mechanisms that are actually active in the system, enabling the identification of previously unidentified degradation phenomena [96].

4.1 Issues in Empirical Modelling: Bias versus Variance Trade-Off

Empirical modelling involves fitting models to data, and since data contains both noise and information, all modelling methods need to address issues of models that either overfit or underfit the data [97]. The case of overfitting corresponds to having a model (consider a statistical model with a polynomial functional form) with too many degrees of freedom, so that it fits not only the information present in the data, but it also fits the actual noise, the variance, present. Therefore, the fitted coefficients (the β_i) of this overfitting model, will be reporting the noise, in addition to extracting the information; the model has gone too far in fitting the data, it is fitting the variance in the data. An underfitting model is the opposite case, where the model has too few degrees of freedom and therefore is unable to extract all the information in the data. For example, fitting a simple straight line, to a phenomenon that is fundamentally exponential or quadratic in its nature, means that our "model", the straight line, has too much "bias" to extract the information from the data. This model can only be a straight line, so we are unable to extract the parabolic or exponential coefficients, and therefore are "underfitting" this model. This is a simple illustration of the bias versus variance trade-off that is faced by all empirical models, be they statistical or mathematical in nature. One of the main practices used in statistical data-driven modelling, is to initially split the experimental dataset into two parts, a training set, and a test set. With this, one is now able to fit many possible models, by "training" each model using the training dataset, and then the quality of the model fit, and the

bias versus variance trade-off, can be assessed using a learning curve, as shown in Figure 5. The trained models, with their fitted coefficients, are used to predict the y-axis response for all x data points in the test dataset, and the error (e.g. RMSE) is plotted for each model as a function of that model's degrees of freedom. The "best" model will have the minimum prediction error, when evaluated on the test dataset, since it will balance, or trade-off, the bias and variance present in the modelling of this dataset.

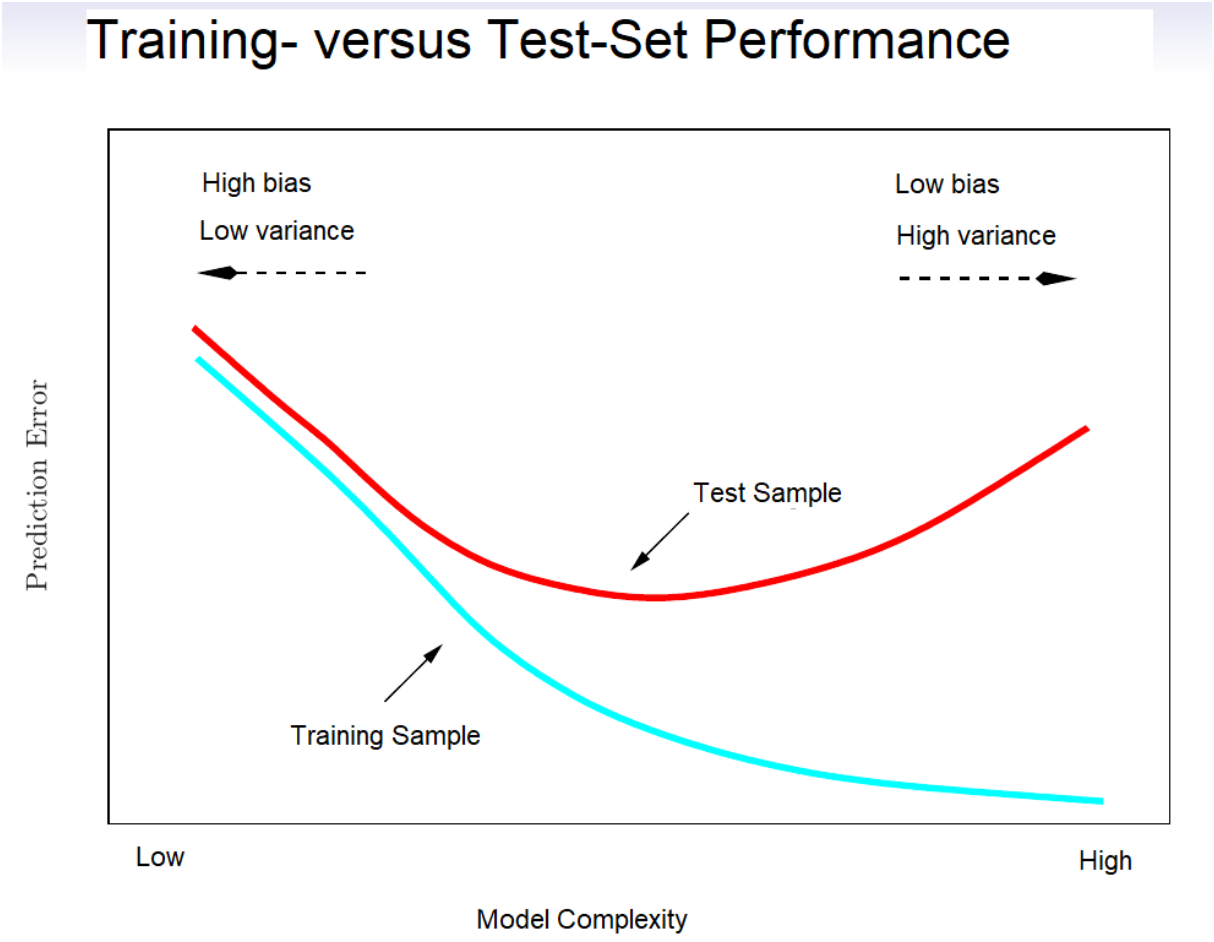

Figure 5: Performance of a model on the training dataset and the test dataset, as a function of model complexity, which is the number of degrees of freedom of the model, and the prediction error of the model. The learning curve for the test dataset, defines the optimal model, as being the model that minimizes the trade-off between variance and bias of the model [97].

As can be seen from the prior discussion, all empirical modelling can be considered as an attempt to use modelling to extract information from datasets, while leaving the noise behind in the data. In this sense, the resulting model, that optimally balances bias and variance, is the best tool for extracting the information we are interested in. Statistics has used hypothesis testing, and mathematical models use our chemical and physical understandings of phenomena to prescribe the functional forms used in models. Shannon's theory of Information Entropy, represents a third approach to model and variable selection, and this information theoretic approach has become very appealing in modern modelling approaches [98]–[101].

The third consideration in empirical modelling is the difference between predictive and inferential models. Inferential models are designed to infer the mechanisms that cause the re-

sponse; why does the system respond in this way. While a predictive model focuses on predicting the magnitude of the response. For inference, one wants a parsimonious model, defined as having a small number of degrees of freedom, and typically an additive model, in which the terms have coefficients that are associated with each term in the model. For accurate prediction, one can have a model that is very complex, and this many times will serve to produce more accurate predictions. To the user, knowing the desired utility of the model, helps define what characteristics, such as the number of degrees of freedom, the model should have.

4.2 Degradation Models of PV Module Materials, Components and Specific Degradation Modes

The current PV market has a need to address variations in climate-related and weather-related issues as well as to understand the underlying degradation mechanisms occurring in PV modules and module components, such as backsheets and solar cells, to improve the reliability and lifetime of modules. The topic of degradation of polymeric materials used in PV applications due to environmental weathering has been well researched. But there are still a significant number of areas with open questions which need future work to address.

Degradation of polyethylene terephthalate (PET), used as the core layer in many backsheets, has been studied under the stressors of temperature and humidity. The degradation of other polymeric materials under the stressors of UV irradiation, temperature, and humidity has also been studied, but the uncertainties are significant when the details of the particular polymer and the additives are not clear. Corrosion studies may be divided into those not involving the factor of voltage bias (e.g., acetic acid effects on the contacts between Si and Ag grid fingers) and those that involve leakage currents promoting charge migration, oxidation, or reduction at various components in the PV module. Solder bonds degrade by thermomechanical fatigue and depending on the alloy, formation of brittle intermetallic accelerated by temperature. Many degradation processes are not easily modelled considering multiple stressors (synergist effects) and sometimes a sequence of stressors leading to the degradation. Current understanding of these cases is presented.

It is useful to explore lifetime and degradation science (L&DS), which is based on the development of network modelling and structural equation models (netSEM), to gain insight into the mechanisms of degradation in modules [20], [96], [102]. Data-driven netSEM models, are statistical models which can be classified into two types: predictive and inferential. Predictive models make use of a stressor (S) and a response (R), represented by $<S|R>$ while inferential models take mechanistic (M) variables, or variables that track specific degradation mechanisms, into account (written as $<S|M|R>$). netSEM models are based on linear response theory [51] and utilize the bra-ket notation ($<S|M|R>$) [103] to easily represent the important stressors, mechanisms and responses. The modelling incorporates statistical tools and metrics such as Aikake Information Criterion (AIC) [104], Adjusted R-squared (Adj.R^2), Network Science [105], and Graph Theory [106] and appropriate functional forms and Markovian and multiple regression methods to compare and study the responses of PV components during accelerated and real-world exposure. Using the netSEM *R* package developed [107], this can be accomplished.

By using netSEM and L&DS, it is possible to discern the underlying degradation mechanisms under the influence of applied stressor conditions. In this methodology, relationships between stressors, mechanisms and responses can be mapped using statistical data analysis. Often, these results can be viewed in the form of a network degradation pathway model for materials, components, or full systems. Figure 6 shows the elements of PV L&DS.

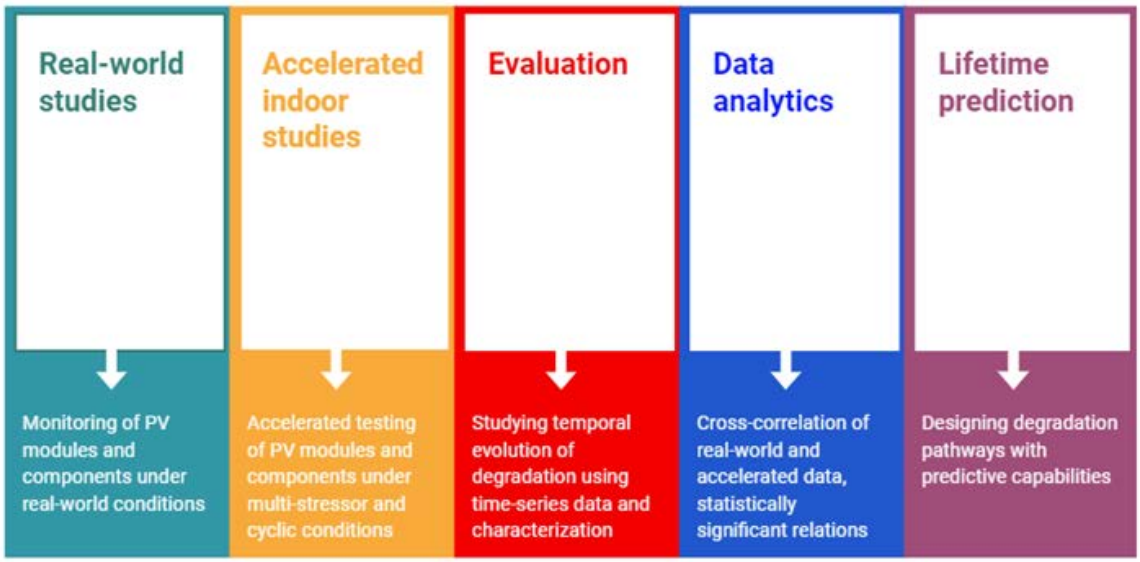

Figure 6: Different steps involved in PV lifetime and degradation science.

4.2.1 Predictive Model Example: PET Degradation

As an example of a predictive <Stressor|Response> *(<S|R>)* model we will consider PET degradation and predict the responses of yellowness index (*YI*) and haze. Using netSEM we can gain a better perspective of the active pathways and degradation mechanisms occurring in PET under exposure [20], [96].

Gok et al. [108], exposed three PET grades were analysed under four different exposures and performed an in-depth analysis of which quadratic and linear terms play a key role in modelling these degradation patterns with *<S|R>* models. Haze can be considered a response variable and so can be predicted using stressors. It has been observed that based on the exposure type, the trend varies. CyclicQUV (UV light with condensing humidity) has a dominant cubic trend while the rest of the exposures have a quadratic variation with very little haze formation. Figure 7 shows the results of this predictive modelling.

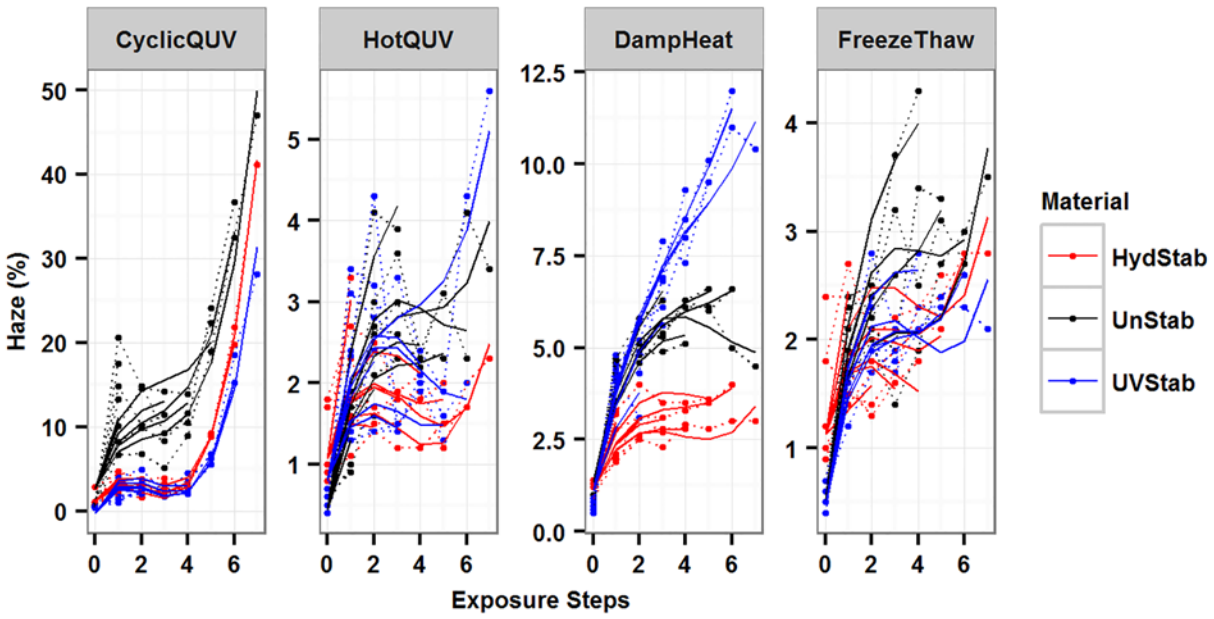

Figure 7: <*S*|*R*> models of the change in yellowness index (*YI*) for all material and exposure types as a function of exposure step. HydStab is hydrolytically stabilized PET; UnStab is unstabilized PET; UVStab is UV stabilized PET. All samples were evaluated stepwise over time every 168 hours (one week) for a total of 1176 hours for seven steps. Each exposure is plotted on a free scale.

4.2.2 Inferential Mechanistic Model Example: PET Degradation

In addition to studying how the response is impacted by the stressor using predictive <Stressor|Response> (<*S*|*R*>) models, in this example we will investigate how the mechanistic variables (M) are related to the stressor (*S*) and response (*R*) using inferential <*S*|*M*|*R*> models. <*S*|*M*|*R*> models connect these variables in a pairwise fashion using one of the seven model types: SL (simple linear), Quad (quadratic), SQuad (simple quadratic), Log (logarithmic), Exp (exponential), CP (change point) and nls (nonlinearizable exponential). Adjusted R-squared values are included between pairwise relationships to indicate the strength of the relationships.

As an example, <*S*|*M*|*R*> inferential models of PET degradation studied by Gok [11] provide quantitative insights into active degradation mechanisms and degradation pathways of three PET grades under four accelerated conditions. Figure 8 shows this inferential <*S*|*M*|*R*> model for PET films exposed to ASTM G154 Cycle 4 (cyclic exposure with UVA light at 1.55 W/m^2, 340 nm and 70°C with dark humidity at 50°C). In this study, yellowness index (*YI*) was chosen as the response variable, which is also a sensitive indicator of degradation in PET films. The mechanistic variables were chosen as UV-Vis optical absorption and FTIR features measured spectroscopically.

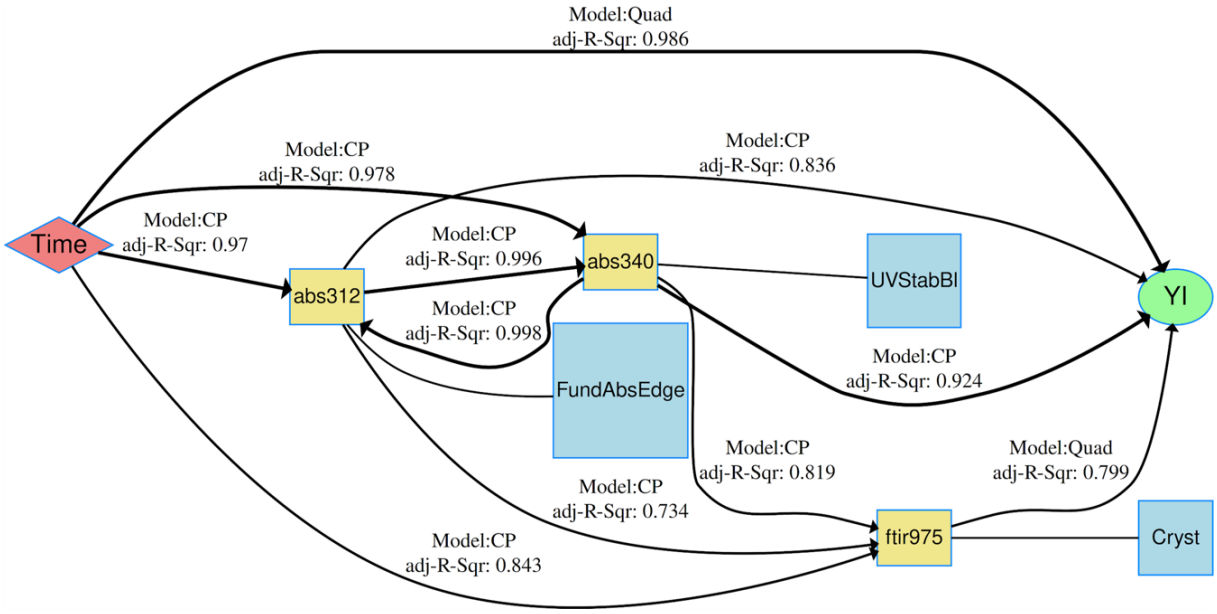

Figure 8: netSEM degradation pathway model of PET degradation with an explanation of mechanism in Table 4.

Figure 8 shows the PET degradation pathway under the ASTM G154-Cycle 4, with cyclic heat, humidity, and UV light (8 h of UVA light at 1.55 W/m^2 at 340 nm at 70˚C and 4 h of condensing humidity at 50˚C in dark). Time tracks the stressor (hours of exposure) <*S*| and yellowness index (*YI*) is the response |*R*>. The experimentally measured "tracking variables" for each mechanism are in yellow boxes, and the degradation mechanism they are correlated with are shown in blue boxes which are detailed in Table 4. These mechanisms are the fundamental absorption edge, the UV stabilizer peak, chain scission and crystallinity of the PET. For each pair-wise relationship in the network the functional form of the mathematical model (Model) that best fits the data is named and the adjusted R^2 values (adj-R^2 or adj-*R*-Sqr) for each of these model fits for the pair-wise relationship are given along the connection lines. The models are SL (simple linear), SQuad (simple quadratic), Quad (quadratic), Exp (exponential), Log (logarithmic), CP (change point), and nls (non-linear least squares regression).

Table 4: Explanation for degradation mechanisms for Figure 8 netSEM model.

Mechanistic variable		Description		Method	Represents
Yellow Box	**Meaning**	**Blue Box**	**Meaning**		
abs312	Absorption at 312 cm^{-1}	FundAbsEdge	Fundamental absorption edge	UV-Vis	Fundamental absorption edge shown by absorption at 312 cm^{-1}
abs340	Absorption at 340 cm^{-1}	UVStabBl	Bleaching of the UV stabilizer	UV-Vis	Bleaching of the UV stabilizer shown by absorption at 340 cm^{-1}
ftir975	Infrared signal at 975 cm^{-1}	Cryst	Change in crystallinity	FTIR	Infrared signal at 975 cm^{-1} indicating change in crystallinity

The formation of haze was also observed under cyclic heat and humidity along with UV-Vis light as illustrated in Figure 7. Age-induced crystallization can be tracked using IR absorptions at 975 cm^{-1}. Yellowing was found to be accelerated with a combination of humidity and UV light. Changes in haze correspond to variations in crystallization as evident from the <*S*|*M*|*R*> model and domain knowledge. Hence, one of the most important degradation pathways found in this study is the yellowing in UV exposure and haze formation in humidity [11].

4.2.3 Degradation Models of Polymers

Polymer weathering, or ageing, processes and their complex interactions result in polymer degradation and can be studied and described by measuring changes in a specified and defined physical or chemical property over time [109]. Relevant physical properties for polymer backsheets and encapsulants can be mechanical (tensile strength, elongation at break, modulus), thermomechanical (melting and crystallisation behaviour, thermal expansion coefficient) or optical (transmittance, reflectance, yellowing or colour index) [110]. Chemical properties include chemical interactions and the reactive behaviour which leads to further degradation such as the permeability of gases through the polymers [111], [112] and the degree of crosslinking of the encapsulant [113], [114]. Chemical changes of polymers induced by ageing can be monitored spectroscopically (FTIR peak ratios or carbonyl index, Raman, UV-VIS, NIR) and by thermal analysis [110], [112], [114]. Additional materials evaluations that have a relevant meaning for the performance and reliability of PV modules can also be monitored (see Figure 9). An overview over common polymer aging mechanisms and its effects are summarized in Table 5.

Table 5: Aging mechanisms of polymers [115].

Mechanism	Stressors	Additional accelerating factors	Effect
Thermo-oxidation	Temperature, Oxygen	Other oxidizing reactants (e.g. ozone, nitrogen oxide)	Embrittlement, discoloration, formation & outgassing of low molecular degradation products
Photo-oxidation	UV radiation, Oxygen	Temperature, oxidizing reactants	Embrittlement, fluorescence, dis-coloration, bleaching, formation & outgassing of low molecular degradation products
Hydrolysis	Humidity	Temperature, catalytic effective acids and bases	Embrittlement
Post-crystallization	Temperature	-	Shrinkage, warpage and crack formation
Relaxation	Temperature	-	Shrinkage, warpage and crack formation

Any change, an increase or decrease, of a defined property over time could in principle be simply fitted using existing mathematical functions such as linear, exponential, logarithmic, linear-linear change point etc. These mathematical functions can be used to make extrapolations to calculate when in time, a physical (or chemical) property reaches a certain value or threshold, in which the studied material, in this case a polymer, is not useful or it can be considered degraded. Of course, extrapolating results of a model beyond the range of variables and data used in fitting the model, can be inaccurate, so care is needed to validate the extrapolated predictions. Furthermore, whether there is a non-destructive or destructive evaluations, measurements or approaches, probabilistic models could also be derived such as the Weibull distribution [116].

Another classical and simple approach is the Arrhenius equation model (7). This model derived from chemical kinetics, which is limited to temperature driven processes, can also be used to model polymer ageing and degradation. If a property that is measured over time and at different temperatures (at least three), the resulting values can be plotted as the natural logarithm versus the inverse of the experimental temperature, and the mathematical linear fit of the defined ageing process can be obtained. Linearization of the fitted values can be used to determine the activation energy, E_a, and pre-exponential factor, A. This model has the main advantage of being easy to perform and determine experimentally, requires little computational power, and the possibility to interpolate or extrapolate a property value at a defined temperature [117]. A good application of the Arrhenius approach is the modelling of thermal and thermo-oxidative degradation mode for different polymers on thermal-gravimetric analysis (TGA) measurements [118], [119]. The Arrhenius approach is also very helpful to model transport phenomena processes involving polymers such as transmission rates, diffusion and solubility of water vapour, acetic acid, and oxygen [111]. Activations energies and pre-exponential factors are quite useful for polymer degradation simulations.

$$k(T) = A \times exp\left(\frac{-E_a}{R \times T}\right) \quad (7)$$

While it has been used in studies of the degradation of PV materials, there are many cases where its applicability is limited such as in glassy materials such as oxides and amorphous polymers [117], [120]–[122]. Due to several factors, often it is not possible to model weathering or ageing behaviour using the mentioned approaches. During the ageing processes some non-linearities or deviations in the measurements might appear, that could be attributed to experimental errors, outliers, hidden factors, and multiple processes occurring at the same time. A solution for this 'deviations' is the Aquilanti–Mundim [OG3] deformed Arrhenius model (8) [123]. This model has similar mathematical terms as the Arrhenius law, but with a deformation parameter, d, added to account for an observed deviation or non-linearity. Deviations from the Arrhenius law can be also denominated sub-Arrhenius and super-Arrhenius. There are also cases where more advanced forms of the Arrhenius equation are required for example where explicit temperature dependence of *A* the preexponential factor, or modification of *T* in the exponent is essential to model real physical phenomena, or where the preexponential incorporates other complex factors such as irradiance and humidity [124], [125].

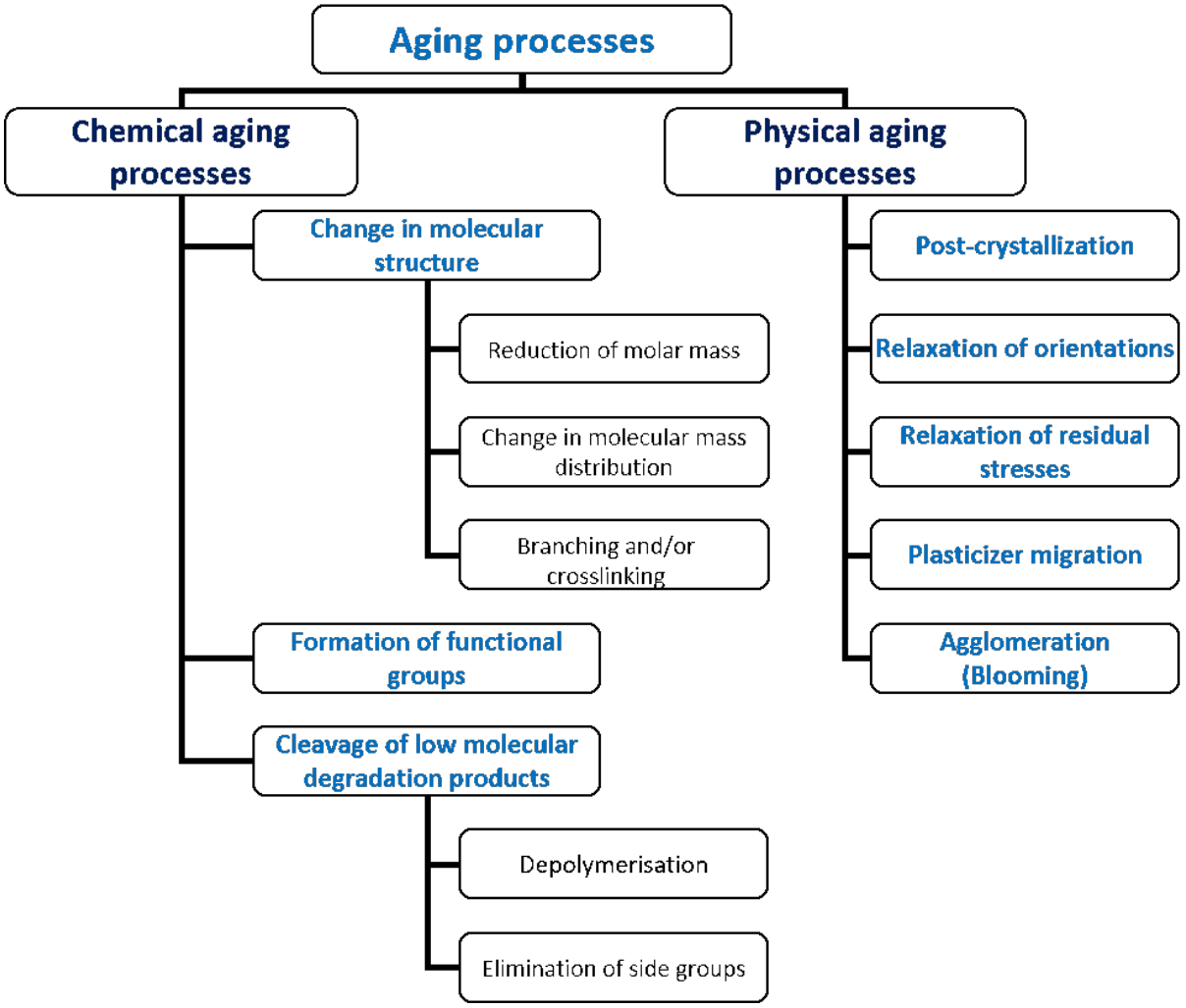

Figure 9: Aging processes of polymers [109].

$$k_d(T) = A \times (1 - dE_a/R \times T)^{1/d} \quad (8)$$

Current experimental research in the aging behaviour of polymeric backsheets and encapsulants involves more variables than just temperature. UV irradiation, moisture, and mechanical loads also have their share in polymer ageing and degradation. These external factors are sources of deviation and non-linearity. Other contributors of non-linearity or deviations are the polymers themselves. Polymers have characteristic time-temperature dependence of certain relaxation and transition processes such as creep behaviour and the glass transition temperature. Depending on the studied polymer, it is also possible that the experimental temperature of an ageing test can coincide with a transition temperature of the polymers used in backsheets and encapsulants causing difficulties in modelling the ageing behaviour. Additional polymer specific factors that could make ageing and degradation modelling difficult are: residual stresses, crystallinity degree, cross-linking degree, chemical resistance, molecular weight distributions, additives types and quantities, and material interactions [115]; Especially for backsheets, their multi-layer structure and the different compositions are a particular challenge (e.g. [110], [112], [126]).

Modelling polymer ageing and degradation in PV modules also requires the modelling of the microclimatic conditions like module temperature (based on solar irradiation), moisture and oxygen ingress processes into the module [116]. For this reason, new and more complex methods and numerical approaches are required, as e.g. described in chapter 3.4.2. Examples for these methods are finite element method (FEM) [127], deep and machine learning [128], multivariate data and correlation analysis [129] and principal component analysis (PCA) [130]. Multiscale models also include: Phase-field theory models, Monte-Carlo (MC) and kinetic Monte-Carlo simulations [131], [132] and molecular dynamics (MD) simulations [133], [134]. Using MD models to describe ageing processes would require an enormous computing capacity, although new approaches at the nano-scale are being studied [135].

PET hydrolysis, a typical degradation reaction for condensation polymers and critical for PV reliability, has been long studied using classical kinetic approaches. Launay et al. [136], studied the changes in properties such as molecular weight and crystallinity at neutral conditions, they found out that PET hydrolysis corresponds to a second order reaction. No auto-catalytic behaviour, random chain scission, and the production of ethylene glycol and terephthalic acid are enough to describe this degradation process [136]. This first kinetic approach cannot be applied for PET hydrolysis modelling in PV modules, because it was studied under stationary conditions, which are in contrast with the transient conditions of which PV modules are subjected. Also, from the chemical point of view, PET hydrolysis can proceed at neutral, basic, and acidic conditions, which is unknown for the PET in PV modules. A more PV-oriented kinetic modelling of PET hydrolysis study was done by Picket et. al. [137], in which the degradation rate is defined as the days to brittle failure. From this, an embrittlement kinetic is determined using an Arrhenius approach by measuring embrittlement at different temperatures and humidity levels to determine the activation and pre-exponential factors [137].

An example of modelling polymer degradation used in PV modules is the work of Gagliardi et. al. [127]. In their predictive modelling of the photo-oxidation of EVA, the degradation pathway is first described based on the known oxidation mechanism for polyolefins adapted for EVA. Each degradation step is written as a chemical reaction equation with its own temperature-dependent reaction rate coefficient. As degradation proceeds, small molecules react and other small molecules are being produced as degradation products, which simultaneously diffuse. These simultaneous processes are described as a reaction-diffusion (RD) system to describe the concentration of water and acetic acid. A key element of this work is

the discretization of the concentrations and temperature gradients as a finite element. Based on the concentration values of degradation from experimental photo-oxidation values, degradation products can be estimated for long periods of time, since temperature and relative humidity values from environmental data, can be used to calculate module temperature and water concentration in the PV module [127].

In principle, this modelling approach can be used for any polymer degradation process, in which the main degradation mechanism is identified, and a pathway is known, as well as the different degradation products. In general, for polymers oxygen and water concentrations are constant in any polymer degradation process. The difficulty of this approach is to first find the actual reaction rates coefficient, k(*T*), which are specific to each chemical equation and are temperature dependent, and even though they follow Arrhenius law, these require a known activation energy and pre-exponential factor. Another requirement to use this approach is to know the diffusion, solubility coefficients, which are also temperature dependent [20].

4.2.4 Empirical Models of Cracking

A. Cracking Overview

Cracking occurs as a result of thermomechanical stresses and the origin of cracks can begin from different stages such as preparation of wafers, module fabrication, transportation, and/or external environmental conditions. These cracks are seldom visible to the eye and can propagate, leading to considerable mechanical and electrical degradation.

To understand the different components that can be impacted by cracking, consider the glass-backsheet module architecture which has an asymmetrical stress state. Most commercial PV modules use glass-backsheet module architecture. The front side glass is usually about 3.2 mm. This non-symmetrical architecture causes the layer of solar cells to be in between the central layer and backsheet layer. Since the frame constrains the movement of the module, if the load was applied to the module in the scenario of wind, hail and so on, the module will tend to deform. When load is applied, the backside of the module is under tensile stress. This stress applies to both the cell layer and the backsheet. Silicon which is used in solar cells is very brittle with a low tensile strength. Cracks can propagate in a preferential manner based on the direction of loading and can be classified based on several criteria. The developed microcracks in the solar cell during installation or transportation is also easy to expand under tensile stress [138].

The backsheet film contains several layers of polymer that exhibit desirable elasticity and plasticity, which lower the risk of developing cracks under tensile stress. The mechanical properties of these elastic components degrade under long-term weathering. In addition, outdoor PV modules also face periodic temperature changes due to the daily and seasonal temperature changes in the outdoor environment and due to the operating temperature of the modules. The multilayer construction of backsheet materials leads to a discontinuity of coefficient of thermal expansion. The difference in thermal expansion coefficients cause mechanical stress under heating. The mechanical stress is concentrated at places with constrained deformation. The mechanisms of backsheet cracking is closely related to the chemical composition and process technologies of the backsheet. In addition, to wind and weight load, backsheet materials are subjected to other points of stress not due to external loading. Any internally raised area such as ribbon wiring or the edge of a cell can cause internal stress in the backsheet material [138].

B. Stochastic Weibull Models of Cell Cracking

To cut down the material costs involved in making commercial PV modules, the silicon wafer thickness is being reduced in current times. This leads to a higher propensity of crack formation under mechanical loading conditions. Progress is made by researchers to identify the components and factors that influence the initiation of cracks as well as their subsequent propagation which is outlined in the recent review article by Papargyri et al. [139].

Cracks in solar cells are generated at various stages of PV module fabrication starting from wafer production, soldering/lamination to transportation/installation as well as their exposure to various weather conditions and loads such as wind, rain, snow, etc. [140]. These processes generate micro cracks that are not visible to the eyes but can be seen from EL images. These micro cracks may lead to electrical disconnection of the affected cell region and higher series resistance along with reduced short-circuit current leading to power loss of the module [60]. The cracks formed from one or more of the stages lead to a higher probability of breaking and reduce the fracture strength of the PV module [141].

There are several classifications of cracks formulated on the basis of shape, size, direction, position, and criticality. The two most commonly observed crack shapes are line and star: line cracks are formed due to scratches and occur in the wafer production phase whereas star-shaped cracks originate due to point impacts in which line cracks tend to cross each other. Based on the size, cracks can be categorized into macrocracks and microcracks based on the width. A crack less than 30 μm wide is called a microcrack and anything higher than that is a macrocrack. There are several different directions in which cracks can form, including parallel and perpendicular to busbars, diagonal, +45°, -45° and multiple directions. Any crack that forms in the silicon solar cells can be expressed as a combination of these crack directions. Cracks based on cell position include facial and sub facial: facial cracks form on the surface on the solar cell whereas sub facial cracks propagate at the depth of the wafer even if they are initiated on or below the cell surface. Based on criticality or severity, there are three categories of cracks: A) type of cracks do not cause disconnections in cell regions, B) type of cracks cause some regions to crack and lead to partial isolation, and C) type of cracks result in complete isolation of the cell region and cause severe power loss [140], [142].

The most commonly used cell types are Al-BSF and PERC in the industry. Extensive studies have been done on cell cracking of Al-BSF cells and reported in the literature. It is known that the cell strength is dependent on loading direction [143]. Details about cell cracking and studies are discussed in a previous IEA PVPS report [23]. Typical crack patterns can be assigned to a cause: a repetitive crack from one PV string to the next which is oriented 180° can be attributed to production failure [144], dendritic cracks in PV modules can be associated with heavy mechanical loading or higher acceleration. There are specific cell cracking characteristics seen in encapsulated monocrystalline and multi-crystalline solar cells as reported by Sander et al [145]. It was observed that the loading parallel to busbar direction is much more critical in the case of multi-crystalline cells because of a lowered fracture stress and has a higher probability of cracking. An additional study by the authors also showed that cracks prefer to propagate from existing weak points formed during soldering or lamination. During the four-point bending tests, it was seen that monocrystalline Si mostly showed 45° cracks at the cell edges without pre-existing cracks. This is because cracks propagate along (100) oriented 45° to the cell edges. With pre-existing cracks, it was found that there was deviation from the 45° crack pattern. In multi-crystalline Si under perpendicular loading, dendritic cracks were seen to form pre-existing cracks during the module production phase. From the research done by Paggi et al. [146], the conclusion is that the elastic deformation is

an important factor for the electrical behaviour of the crack and cracks on the cell can recover electrical conductivity.

Studies are being conducted on PERC-based modules to inspect cracking characteristics. In a recent study of PERC modules under thermal cycling by Braid et al., it was concluded that bifacial PERC with localized contacts at the openings of the rear passivation layer are more prone to degradation due to cracking and corrosion. Most of the cracks that were formed were not correlated with power loss as cracks do not always lead to electrical isolation over large cell areas [147].

Mathematical (numerical) models of cell cracking have been advancing recently and are playing an important role in comparing the reliability of PERC and Al-BSF PV cells. Finite element, structural mechanics modelling of photovoltaic (PV) modules is becoming a more popular tool with which to design for, and evaluate, module reliability [148]. Combining Weibull analysis and weakest link theory one can calculate the unique probability of crystalline silicon PV cell fracture when measured as bare cells and when stressed in reduced- and full-sized modules [149]. Experimental results indicate that the characteristic cell strength is reduced by ~20% once packaged into the laminate of a one-cell module and loaded in four-point flexure (4PF). This experimental observation was shown consistent with a weakest link theory prediction that the strength limiting flaws reside on the surface of the cell's edge.

The predicted load-displacement response of the experimental bare cell loaded in 4PF is compared with the analytical solution according to Euler-Bernoulli beam theory. The numerical model is in excellent agreement with the experimental measurement and deviation from the analytical solution suggests that large deflections, such as required to achieve cell fracture, are beyond the small deflection assumption of beam theory. The analysis is ultimately extended to describe the equivalent loading of four-cell modules loaded by uniform pressure and 4PF and a uniformly loaded full-sized module in terms of the cell's probability of failure. A uniformly loaded full-sized module is not equivalent to smaller, representative modules. The smaller modules must be loaded to a much higher level than their parent full-sized modules to achieve an equivalent probability for cell fracture (Figure 10). The relatively low sensitivity of characteristic stress on Weibull effective region ratio for Weibull modulus values above 10, the equivalency relationships are anticipated to be consistent when modelling full-sized modules with a variety of mechanical constraints.

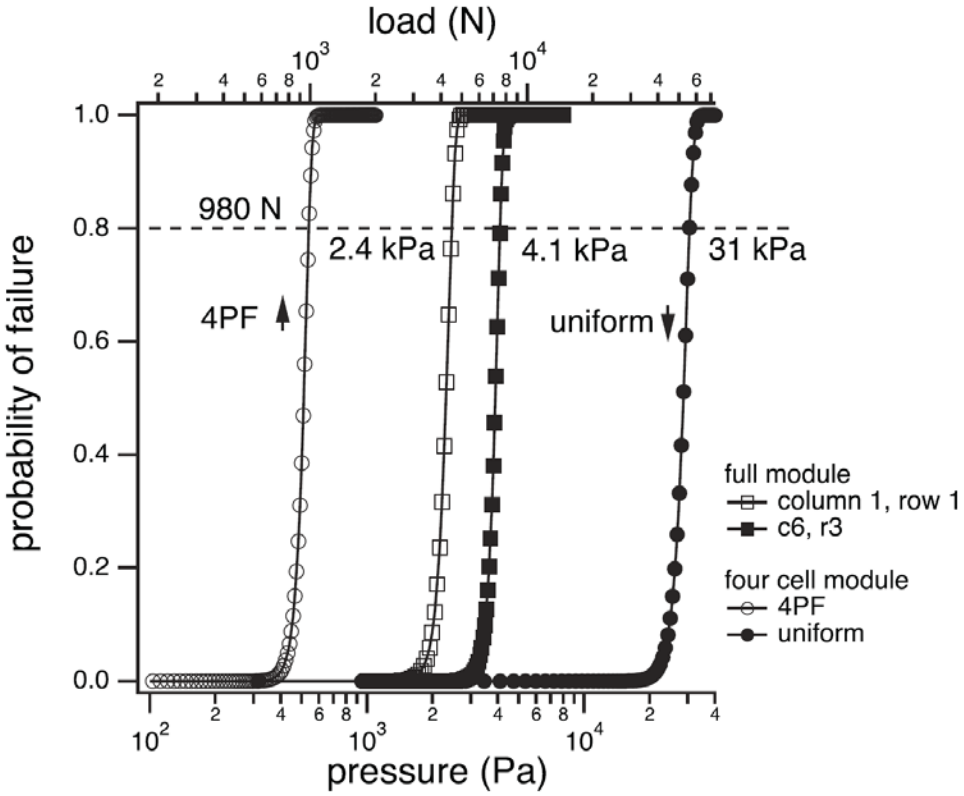

Figure 10: Calculated cell fracture probabilities for the cell within a four-cell module loaded uniformly and in 4PF and select cells within a uniformly loaded full-sized module. The two x-axes scales reconcile the application of pressure in uniform loading and force in 4PF. For illustrative purposes, each distribution is evaluated for 80% probability of cell fracture.

C. Models of Backsheet Cracking

Backsheets are critical to provide mechanical strength and electrical insulation to the module. As the material ages, degradation can lead to cracking and failure of the insulative properties posing a serious hazard. Currently much of the research in backsheet cracks has been related to determine the mechanisms and stressors behind the crack formation in different backsheet constructions and identifying crack types in real-world exposed modules [4], [63], [126], [150]–[152].

Mathematical modelling of backsheet cracking is complicated because of the multilayer nature of backsheets since backsheets can be coextruded or combined by adhesive layers. The degradation in the backsheet is generally nonuniform through the thickness and is initiated by multiple different types of mechanisms. Cracks initiate between cells on the sun-side layer in polyamide backsheets by the formation of acetic acid from EVA hydrolysis [63], [150]. Increases in the modulus of the backsheet is an indicator of future cracking by using the Derjaguim-Muller-Toporov (DMT) model [150]. Cracks under the busbars initiate from the air-side of the backsheet due to the stress induced at that point [63]. Owen-Bellini et al. showed that cracking in polyamide (PA or AAA) backsheets is a two-step process that starts with chemical degradation that then initiates microcracking and then a mechanical load to propagate the microcracks to form macrocracks. The authors performed finite element modelling that the localized stress concentrations are present regions in between cells and that

the stress driving the macrocracking is thermocycling [4]. Lyu et al. calculated the fracture energy of the brittle layer of polyamide backsheets using the Hsueh and Yanaka model (HY's model) to measure critical strains. The HY's model is based on the cracking of brittle film/ductile substrate systems where an effective substrate thickness is used which is proportional to the brittle layer thickness. The effective substrate is used to consider the perturbation of the existence of the brittle layer on the stress field of the substrate. The HY's model showed a good agreement with the measurements in terms of crack density vs. applied strain (Figure 11). This type of modelling informs the quantitative relationship between degradation and crack formation. Additionally, it helps with materials selection by identifying the backsheets that may crack under real-world exposure conditions [153].

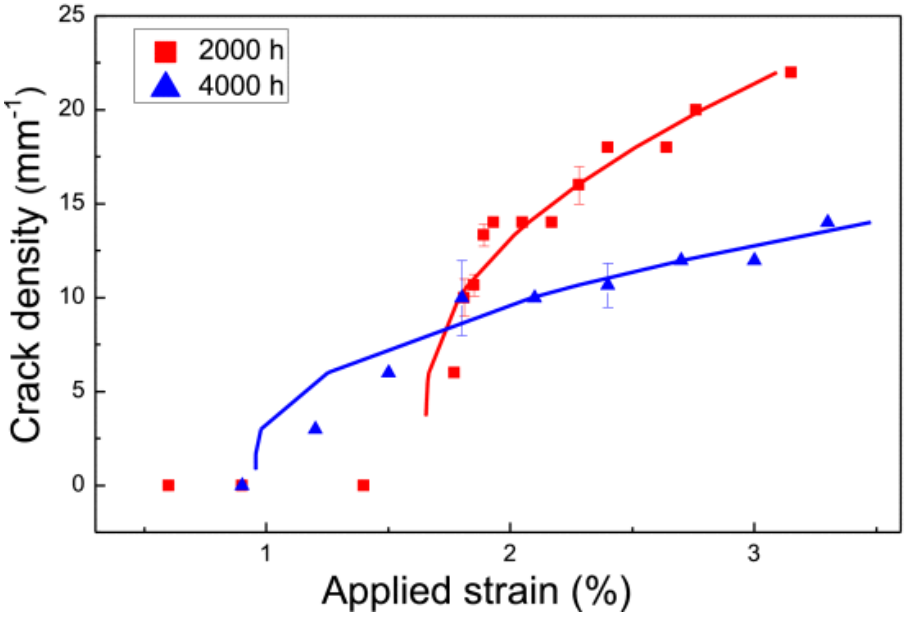

Figure 11: The Hsueh and Yanaka model results compared to the actual measurement of cracks per applied strain (%) for PA samples exposed to 2000 and 4000 hours of A3 condition in IEC 62788-7-2 [153].

Statistical modelling of backsheet cracking aides the identification of cracks is a time intensive process and can be automated using a combination of analytical and modelling techniques. The identification of different cracking mechanisms elucidates the different types of stress that the material experiences in the field. Likewise, Klinke et al. [154], developed a method of analysing profilometry scans of backsheet surfaces to identify and predict locations that cracking would occur (Figure 12). This method used a machine learning algorithm to identify the surface of the backsheet in the profilometry data and then identify outliers from that surface. The outliers are either cracks, bubbles, or delamination in the material. Then the crack width and depth are calculated for each crack that was identified. This method can quantify cracks over a large physical area, providing it with an advantage over techniques like X-ray computed tomography (XCT) and laser scanning confocal microscopy (LSCM). The method was also able to identify cracks before they were visually apparent in the material which could help with material selection by reducing the time needed in exposure to identify materials that had small microcracks. Zhang et al. used a fully convolutional deep neural network (F-CNN) to identify different types of cracking and delamination from images of backsheets with great precision and at a low computation time [155]. This technique used images of different types of cracked backsheets that had been exposed to accelerated and real-world exposure [157]. The images were labelled with different types of cracks and then

compared to the output of the F-CNN which had a 92.8% prediction accuracy. The comparison is seen in Figure 13. This type of imaging technique could be useful in field survey of PV modules to identify and quantify the types of backsheet cracking or degradation present in fielded PV modules [155].

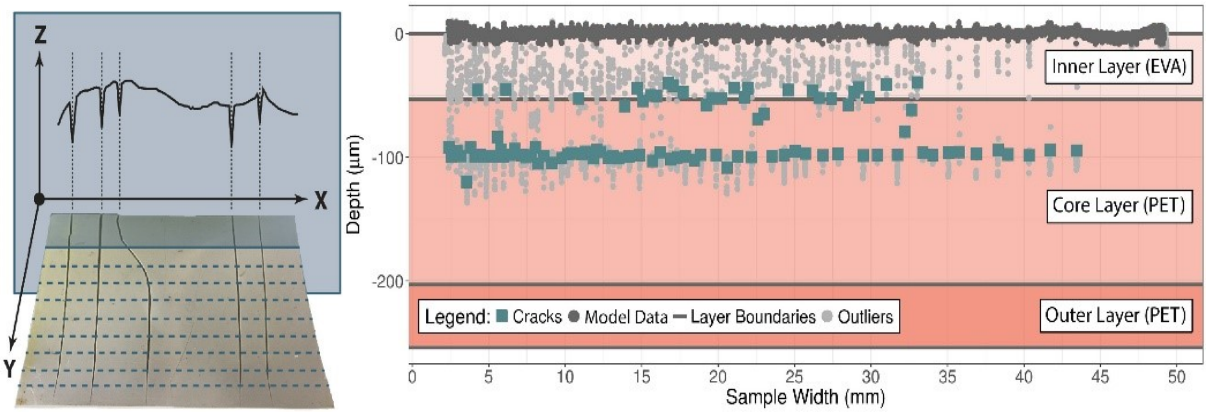

Figure 12: A diagram showing how the 3-D cracks are taken as 2-D optical profilometry data (left). The output for optical profiometry data after machine learning algorithm identifies the backsheet surface and the outliers representing cracks in the backsheet (right). The cracks only propagate into the core layer from the inner layer of backsheet (sun-side) [157].

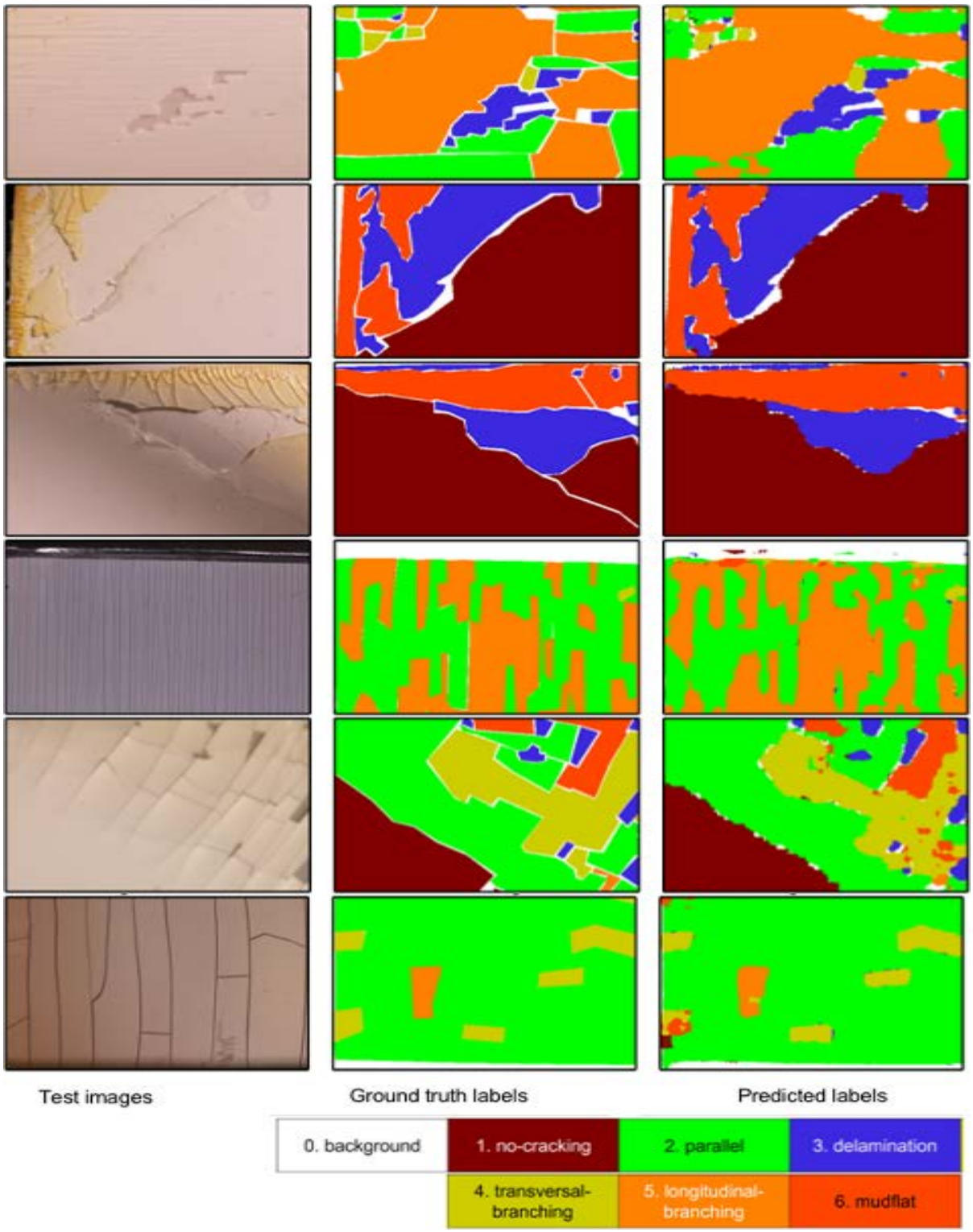

Figure 13: Six examples of crack inspection task performed on the test images (left column) using the trained F-CNN (right column). The middle column is the person labelled images. The different colours in the middle and right column images indicate different crack classes listed in the legend below [155].

4.3 Photovoltaic Performance Models

Physical models are developed based on the physical/chemical understanding and assumptions of specific degradation mechanisms. The models are developed to quantify the effect of climatic stressors on the electrical performance of PV modules. Generally, available physical models for PV degradation rates evaluations are still only heuristic models which do not include the influence of all intermediate degradation steps involved. In other words, the kinetics of a specific degradation mode are modelled by assuming one rate dominating process. For indoors applications several models are available [9]. For outdoor applications, a few authors [6], [7] have proposed physic-based models to quantify the effects of combined climatic stresses on PV performance degradation. Both models use UV irradiation, relative humidity, and temperature as stressors, which are assumed as the main climate degradation factors for PV modules. The formulations of the models are described below.

4.3.1 Degradation Model based on Bala et al. [7]

$$k(T, \Delta T, UV, RH) = \beta_0 \times exp\left(\frac{-\beta_1}{k_B \times T_{max}}\right) \times \left(\Delta T_{daily}\right)^{\beta_2} \times \left(UV_{daily}\right)^{\beta_3} \times \left(RH_{daily}\right)^{\beta_4} \quad (9)$$

where k [%/year] is the degradation rate, k_B (8.62 × 10^{-5} eV/K) is the Boltzmann constant, T_{max} [Kelvin] is the daily maximum temperature of the module, ΔT_{daily} is the daily cyclic temperature of the module, UV_{daily} [W/m^2] is the daily UV irradiance, RH_{daily}[%] the daily relative humidity, β_0[1/sec], β_1 [eV], β_2, β_3 and β_4 are the frequency factor, activation energy, parameters that measure the effects of cyclic temperature, UV radiation, and relative humidity, respectively.

The model was calibrated on degradation data of a mono-crystalline PV module. The calibrated model was applied to predict degradation rates of four different regions with different climatic classification as: hot and dry, cold, hot and humid, and semi-arid. The authors predicted strong degradation under hot and humid conditions.

4.3.2 Degradation Model based on Kaaya et al. [6]

In this approach, degradation rate models are proposed for specific degradation mechanisms/processes based on the applied climatic stresses. A combined/total degradation rate model was derived from the specific rate models as,

$$k_T = A_N \cdot \prod_{i=1}^{n} (1 + k_i) - 1 \quad (10)$$

where k_T[%/year] is the total degradation rate, A_N is the normalization constant of the physical quantities, n is the total number of degradation mechanisms and k_i is the degradation rate of the ith mechanism.

In their study, three degradation mechanism were assumed as: hydrolysis, photodegradation, and thermomechanical degradation. The total degradation rate based on these three mechanisms was expressed as:

$$k_T = A_N \cdot (1 + k_H)(1 + k_P)(1 + k_{Tm}) - 1 \quad (11)$$

Where k_H, k_P, and k_{Tm} are the degradation rates for hydrolysis, photodegradation, and thermomechanical degradation, respectively.

The degradation rates for each specific mechanism were evaluated as functions of climatic stresses as:

$$k_H(T, RH) = A_H \cdot exp\left(\frac{-E_{aH}}{k_B \cdot T}\right) \cdot RH^n \quad (12)$$

$$k_P(UV, T, RH) = A_P \cdot UV^y \cdot (1 + RH^n) \cdot exp\left(\frac{-E_{aP}}{k_B \cdot T}\right) \quad (13)$$

$$k_{Tm}(\Delta T, T_{max}) = A_T \cdot (\Delta T + 273)^x \cdot C_r \cdot exp\left(\frac{-E_{aT}}{k_B \cdot T_{max}}\right) \quad (14)$$

where, k_B (8.62 × 10^{-5} eV/K) is the Boltzmann constant, T [Kelvin] is the annual average module temperature, T_{max} [Kelvin] is the annual average maximum temperature of the module, ΔT is the annual average cyclic temperature of the module, UV [kWh/m^2] is the total annual UV dose, RH [%] is the annual average relative humidity, C_r [cycles/year] is the annual temperature cycling frequency A_H [1/year], A_P [1/kWh/m^2/year], and A_T [1/cycles] are the exponential coefficients for hydrolysis, photodegradation, and thermomechanical rates, respectively. E_{aH}, E_{aP}, and E_{aT} [eV] are the activation energies of power degradation due to hydrolysis, photodegradation, and thermomechanical mechanisms, respectively. n, y, and x are model parameters that measure the effect of RH, UV, and ΔT, respectively.

Using performance data of three identical mono-crystalline PV modules installed in three different regions: Negev in Israel, Gran Canaria in Spain and Zugspitze in Germany, the model was calibrated and validated. Figure 14 shows the annual distribution of relative humidity (A) and module temperature (B) in the three regions.

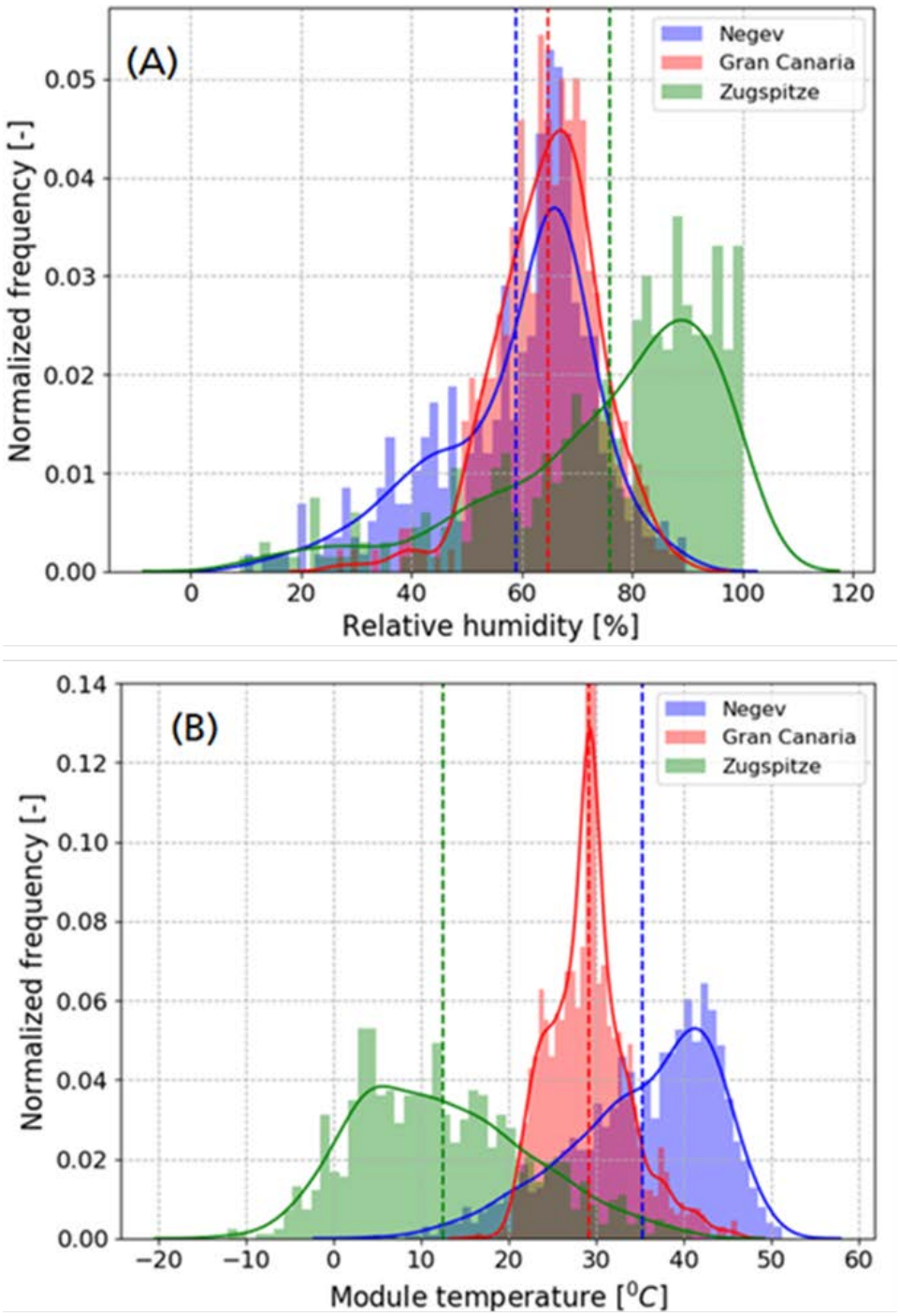

Figure 14: Annual distribution of relative humidity (A) and module temperatures (B) in Negev, Gran Canaria and Zugspitze. The dotted line shows the annual average values in all the locations. The data corresponds to the monitoring period of the year 2013.

Figure 15 shows the modelled power degradation prediction plotted with experimental data in the three locations. The classification of the regions as well as the predicted specific and total degradation rates are presented in Table 6.

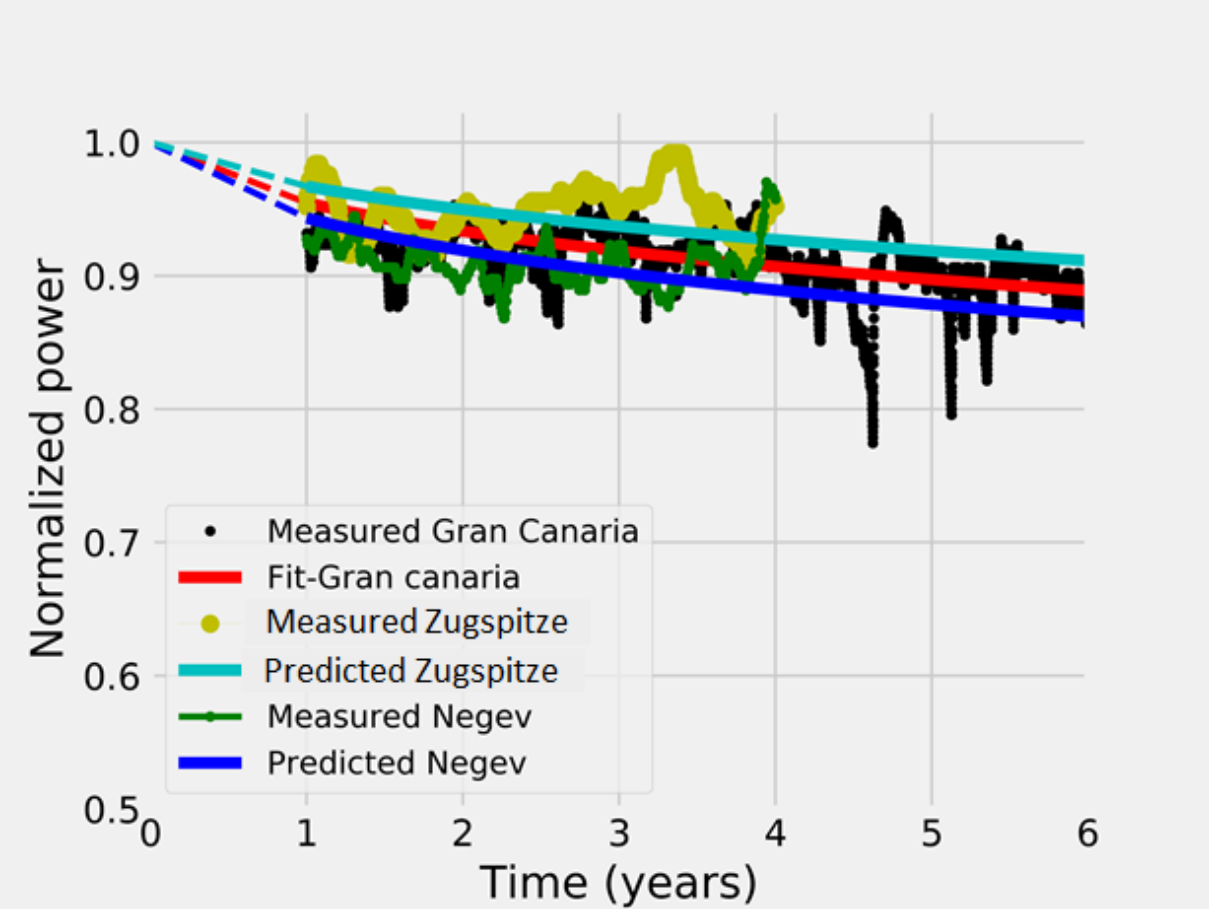

Figure 15: Normalized (with initial power before exposure) power degradation prediction in comparison with measured power degradation in the three locations [6].

Table 6: Climate classification as well as estimated degradation rates and failure time (20% loss in the initial power) in three regions [6].

Region	**Classification**	k_H **[%/year**	k_P **[%/year**	k_{Tm} **[%/year]**	k_T **[%/year]**	**Failure time** [years]
Negev	Arid	0.169	0.216	0.225	0.74	21.4
Gran Canaria	Maritime (Oceanic)	0.122	0.212	0.104	0.50	31.6
Zugspitze	Alpine (cold)	0.043	0.103	0.129	0.30	52.8

The authors predicted stronger degradation in Negev with hot and humid climatic conditions which is consistent with the predictions from the previous authors [7]. For specific degradation mechanisms, the model predicts lower impact due to hydrolysis in comparison with thermomechanical and photodegradation mechanisms. Indeed, very small degradation due to hydrolysis is predicted in Zugspitze despite the high levels of relative humidity. This could be explained by the low average module temperatures experienced in this region, hence slowing hydrolysis processes and the absolute water vapour concentration. In all cases, high rates are predicted in Negev. To extend the analysis, the authors applied the calibrated

model and the processed climatic data from ERA5 (Copernicus Climate Change Service ERA5) to evaluate and map the specific as well as the total degradation rates worldwide (see Figure 16) [31].

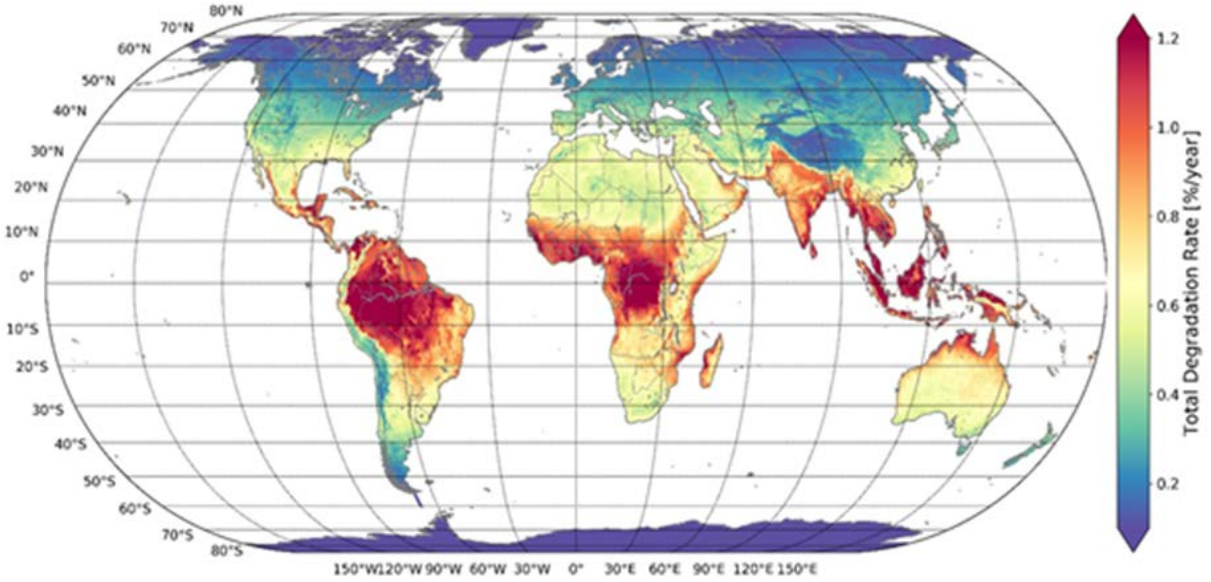

Figure 16: Total degradation rates based on a mono-crystalline silicon PV module [31].

From Figure 16 it is clear that strong degradation is predicted in AH regions (tropical with high irradiance) according to the newly developed KGPV zones [29]. Due to the very low relative humidity present in AK (tropical with very high irradiation), lower degradation rates were predicted in comparison to AH zones.

4.3.3 Photovoltaic Modules Service Prediction Models

PV modules SLP reliability models are defined as time dependent functions that describe the evolution of the performance of PV modules with increasing operation period. These functions are used to evaluate the long-term performance degradation from the calculated or extracted degradation rates. In most cases, the PV community applies a linear regression reliability model (15) to evaluate the long-term performance degradation. However, several authors have reported non-linearity in performance (power) degradation in fielded PV modules and systems. For example, Köntges et al. reported in [23] that the loss in power can take different shapes, for example: exponential-shaped, linear-shaped, and step and saturating power degradation loss over time. In [158], it is also reported that non-linearity of power loss is usually observed in the field depending on the PV module technology. Recently, Virtuani et al. [159] observed polynomial power degradation instead of a linear behaviour in several PV modules after 35 years of field exposure. To model these non-linear behaviours, the authors in [6] have proposed a non-linear power degradation reliability model (16) with a tuneable shape parameter (μ) to optimize different degradation shapes (see Figure 17 (A)) observed in the field. Moreover, in their recent publication [147], the authors demonstrated that evaluated energy yield of a PV module could highly depend on the degradation shape for the same evaluation time as shown in Figure 17 (B).

$$P(t) = P_0(1 - k \cdot t) \quad (15)$$

$$P(t) = P_0 \cdot exp\left(-\left(\frac{\theta}{k \cdot t}\right)^{\mu}\right) \quad (16)$$

$$t_f = \frac{0.2}{k} \quad (17)$$

$$t_f = \frac{\theta}{k \cdot (|ln(0.2)|)^{\mu^{-1}}} \quad (18)$$

Where $P(t)\ and\ P_0$ are the power at evaluation time and initial power respectively, k is the degradation rate [year^{-1}], (μ) is the shape parameter and θ parameters associated with the material. t_f in equation (17) and (18) is the failure time derived from the linear model (15) and non-linear model (16) respectively.

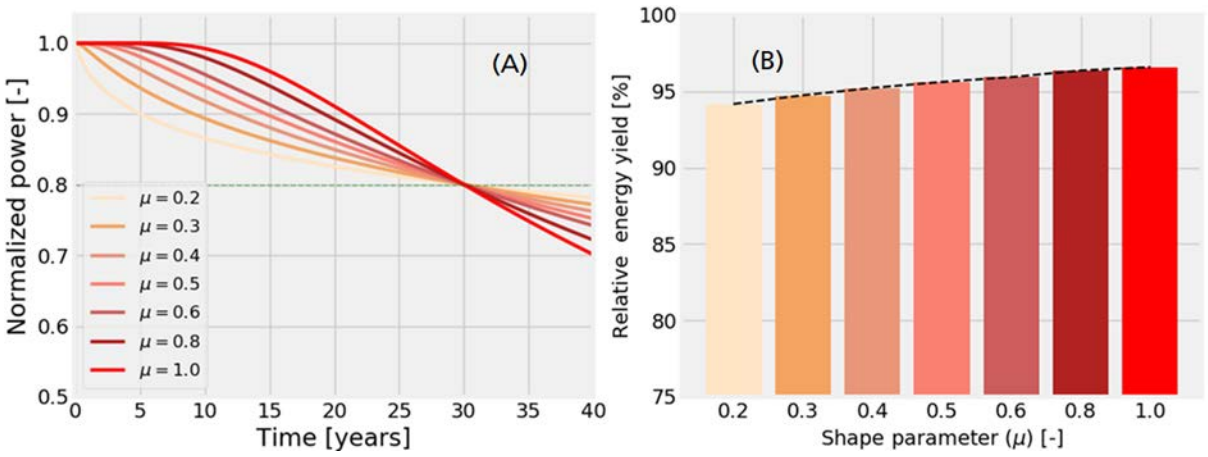

Figure 17: A, Optimization of power degradation shapes by altering the shape parameter μ. B, Relative energy yield corresponding to different values of μ [12].

For long-term performance degradation prediction, the degradation rate (k) can be evaluated from physics-based models described above or by fitting the model on the performance data after a given period of time. However, it should be noted that depending on the reliability model used in the calibration process, the evaluated or extracted degradation rates might differ for a given degradation dataset. For example, in Figure 18 (A) linear and non-linear models are calibrated on a PV module performance data after six years of field exposure. Using the linear model, a degradation rate of 1.1% per year corresponding to 18.2 years lifetime is evaluated. In comparison with the non-linear model, a degradation rate of 1.2% per year corresponding to 21.0 years lifetime is evaluated. From this example, despite a relatively higher degradation rate evaluated using a non-linear model in comparison with the linear model, a longer lifetime is predicted using a non-linear reliability model. This is because the failure time not only depends on the extracted degradation rate but also on other model parameters as shown in equation (18). These variations in degradation rates due to the different reliability models call for a change in degradation rates reporting and interpretation in the PV community. Indeed, to achieve a consistent interpretation of the reported degradation

rates, the best practice will be not only to report the degradation rates, as commonly done in the PV community but also the method used to extract them. Moreover, another concern is the use of a simple extrapolation after given years of field exposure to predict the long-term performance. A recent study has shown the pitfalls of this approach and proposed a new approach based on time dependent degradation rates for more reliable long-term predictions.

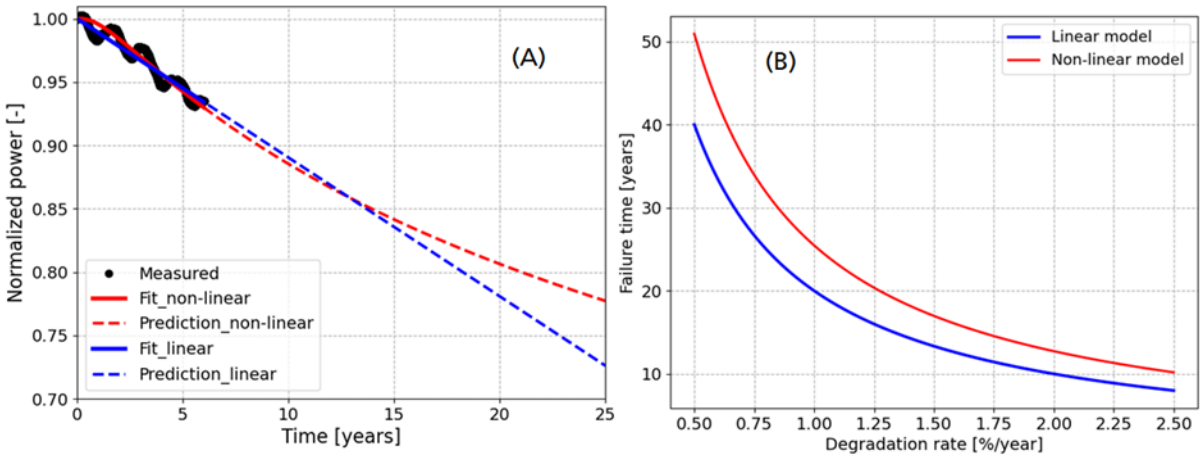

Figure 18: (A) Calibration of linear (blue) and non-linear (red) reliability models on outdoor measured PV module performance data (black) after six years of exposure. The dashed lines show the long-term performance degradation predictions. (B) Simulated change of failure time with degradation rates of the two reliability models.

4.3.4 Statistical Performance Loss Rate (PLR) Modelling Approaches

Statistical data-driven modelling approaches describe the performance of PV systems and PV modules over time. Traditionally, the performance decline is calculated by linearizing the performance trend of a PV system's performance data and commonly referred to as Performance Loss Rate (PLR). The PLR of PV systems is unknown and different approaches are used to provide a calculated PLR as close as possible to the true unknown value. In general, the calculation of PLR follows a uniform sequence, which includes input data quality check and data cleaning, data filtering, the selection of a performance metric and the application of a statistical model to determine the final PLR, reported in %/year. Although the sequence is similar, a variety of approaches has been developed and different methods are used depending on the analyst's preferences without knowing if these methods are close to the actual PLR of the PV system. In the recent Task 13 report "Assessment of Performance Loss Rate of PV Power Systems" [17], a large-scale benchmarking study has been conducted among leading research institutions and universities to answer the question, if a superior calculation approach exists today for the calculation of PLR across various PV systems. The study included next to several modelled PV system datasets also 19 real datasets of operating PV systems. 32 combinations of data filter – performance metrics – statistical models have been tested.

The study shows that today there is no superior uniform calculation procedure following a predetermined set of filters-metric-statistical model. Instead, it is suggested that a voting, or preference aggregation, method may represent an accurate approach for PLR evaluation. Averaging the results of calculated PLR using many filters, performance metrics and statistical modelling approaches does appear to provide consistent and robust PLR estimates. This multiple method approach may serve as an ensemble model in which inaccuracies of all the different approaches are minimized in the voted result. Furthermore, it is suggested to assign

a 95% confidence interval for each of the used approaches as uncertainty. Overlapping intervals indicate if methods are statistically similar. The average of an ensemble of similar approaches is assumed to be close to the actual unknown PLR. Like this it is possible to select calculation methods with overlapping confidence intervals, exclude outlying approaches, calculate the mean of these similar approaches and thereby provide a reliable PLR estimate. An example for this approach can be seen in Figure 19, where the PLR of a PV system has been calculated using 27 different filter-metric-model combinations and the mean of statistically similar approaches is used to calculate the PLR. The reported uncertainties are varying across the approaches due to different uncertainty calculation approaches, an issue discussed in the report [17]. That is why the shown cloud of confidence intervals is just estimated in this example.

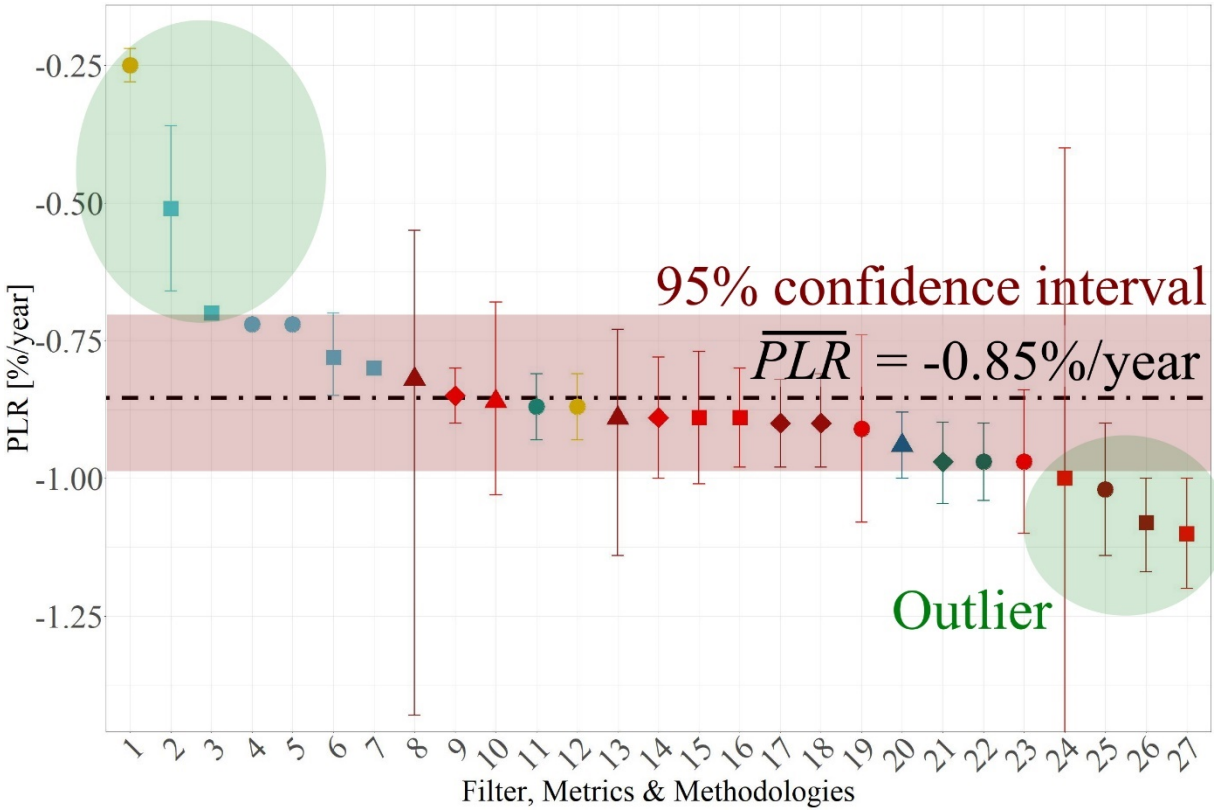

Figure 19: Ensemble Approach for PLR estimation, combination of filter, metrics and statistical methods along x-axis, PLR along y-axis together with suggest confidence interval and outlying approaches.

Statistical modelling approaches are usually assuming a linear, constant performance degradation over time. This representation is important for possible warranty claims, a basic health check of the plant and can be used to intercompare similar systems in the field. Nevertheless, as discussed in this report, the time dependent performance evolution of PV systems is very complex and highly nonlinear.

A novel approach to calculate multi-step performance losses (MS-PL) is presented [160], which provides a more detailed picture of the PV system performance. Here, the non-linear performance trend of a PV systems time series is divided into linear segments by automatically detected breakpoints. Breakpoints divide the performance timeseries into subsets of varying performance behaviour. Like this, the performance can be assessed in greater detail compared to a linear evaluation. The algorithm provides a trade-off between an easily under-

standable and at the same time fairly precise PLR rating. Multiple sublinear PLR with the according time period are returned.

The dataset preparation is similar as for linear PLR calculations. After an input data quality check, tailored filters are applied on raw PV power and high-quality irradiance time series. Consequently, these data are transformed and aggregated to a monthly temperature corrected PR time series. Seasonal and trend decomposition [161] is applied to separate a nonlinear performance trend from the time series by data decomposition of trend, seasonality and a reminder. Finally, an adapted version of $R^2{}_{adjusted}$, a parameter used in multivariate regression to determine the optimal number of predictors for a model to find the optimal number of breakpoints based on the nonlinear trend. Thereby, different multi-step performance loss models with a varying number of breakpoints are tested and a maximized adapted $R^2{}_{adjusted}$, yields the best model which presents an optimum between performance evaluation simplicity and detail. The exact location of the breakpoints on the time axis together with the fitted linear trend-lines is. The function returns a table with an optimized number of linear performance loss values together with the corresponding breakpoint dates (see Table 7). The algorithm has been applied to an operating multi-crystalline PV system, installed in Bolzano, Italy. The results are presented in Figure 20 and Table 7:

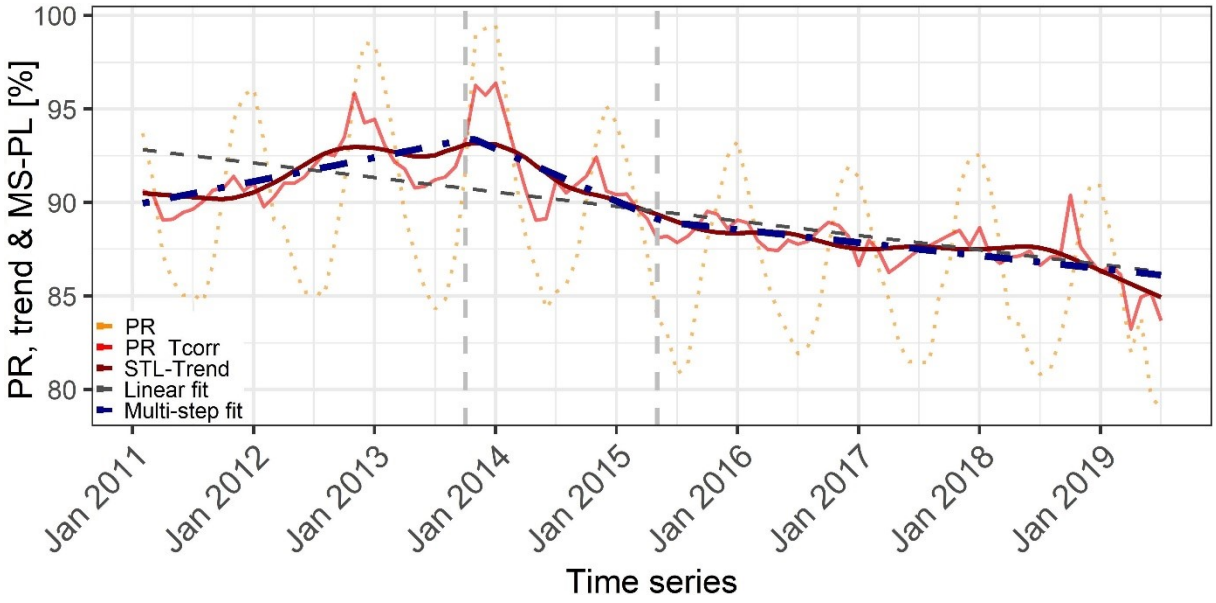

Figure 20: Multi-step performance fit for multi-crystalline PV system in operation for eight years: PR (orange - dotted), temperature corrected PR (red - straight), trend-line of temperature corrected PR (dark-red - straight), Linear fit (grey - dashed), multi-step fit (darkblue - dotdashed) and vertical breakpoints (light-grey - dashed).

Table 7: Optimized number of linear performance loss values together with the corresponding breakpoint dates.

Optimized	$PL[\%/year]$	Breakpoint
PLR_{lin}	-1.01	February 2011 – February 2019
PLR_1	0.76	January 2014
PLR_2	-2.94	August 2015
PLR_3	-0.97	
RMSE	0.33	

In the table, next to the overall PLR as well as the individual performance loss values and corresponding breakpoints, the RMSE between the non-linear performance trend and the modelled fit is listed. In order to present a more accurate uncertainty estimation, it is suggested to add the residuals back to the non-linear performance trend before calculating the RMSE. It is visible that the system experiences an initial performance gain for the first three years of $PLR_1 = 0.76\,\%/a$, followed by a strong decrease for one and a half years and finally settles at a constant performance loss value of $PLR_3 = -0.97\,\%/a$, which is very close to the over linear PLR estimation of $PLR = -1.01\,\%/a$. The initial gain has also been observed for other systems installed under the same conditions and in the vicinity.

It is suspected that the initial gain is based on a combination of PV technology behaviour and favourable weather conditions. In the summer of 2013 and winter of 2013 to 2014 high temperature corrected PR values were recorded before a measurable reduction in performance was detected. As efficiency of crystalline systems decreases under low irradiance conditions due to higher related resistance losses, high average irradiance conditions under constant temperature yields high efficiency values and therefore an increase in performance [162], [163]. These high-performance values can be connected to a very sunny July, in which the highest monthly yield was recorded, and a mild and sunny following winter where the PR reaches very high values of almost 100%.

The presented algorithm goes a step beyond the usually presented linear PLR and thereby allows studying performance affecting events over the course of the systems lifetime and, especially, close to breakpoint dates. The MS-PL algorithm can be used in combination with individual degradation models presented in section 4.2 and section 4.3 and on-site characterization methods to divide the overall performance behaviour into its root causes. Thereby, we could gain a greater understanding of climate stressor dependent performance in the field and better estimate the lifetime of PV modules and systems installed under various conditions.

4.3.5 Variations and Uncertainties in PV Modules Degradation Rates and Lifetime Prediction

In addition to a sensitivity analysis of degradation rates in different climates, the estimated degradation rates using physical models should be close to realistic values in order to be used for service lifetime predictions. However, due to the many environmental stressors and factors influencing associated with physical degradation models, the accuracy of the estimated degradation rates is affected. In [14], the different sources of variations and uncertainties associated with physical models where explored. The authors categorized the sources of variations and uncertainties into two major categorises:

- Variations and uncertainties due to simplification of reliability and degradation rate models. They showed that the variations can be as high as 65.5%
- Variations and uncertainties due to estimation of micro-climate variables from macro-climate variables (e.g., module temperature from ambient conditions, UV from global irradiation).

The authors showed that estimation of module temperatures has the highest uncertainty compared to other climatic variables (relative humidity and UV). The uncertainties where dependent on location and on the model used to estimate the module temperature, for example, in Figure 21, the benchmark of the module temperature estimated according to Faiman and Ross models are presented using monthly box plots. In Table 8, the uncertainties and variations of different temperature ranges are presented. The minimum and maximum temperatures are evaluated as the 5th and 95th percentiles of the annual temperature distribution respectively. Finally, in Figure 22, the variations in degradation rate and failure time estimations using measured and modelled PV module temperatures are shown.

According to the authors, the Faiman model that considers the effect of wind speed could improve the prediction accuracy since it showed better prediction in comparison to the Ross model.

The highest discrepancies between measured and modelled temperatures are visible in extreme temperature ranges (e.g., in minimum and maximum temperatures ranges)**.**

A correlation of uncertainty in module temperature estimation to the uncertainty in degradation rate /failure time estimation is highly location dependent**.** That is, in locations with lower operating temperatures higher uncertainty in module temperatures estimations show less impact on the degradation rate accuracy in comparison with locations with higher operating temperatures. The authors linked this observation to the Arrhenius temperature dependence nature of the degradation rate models.

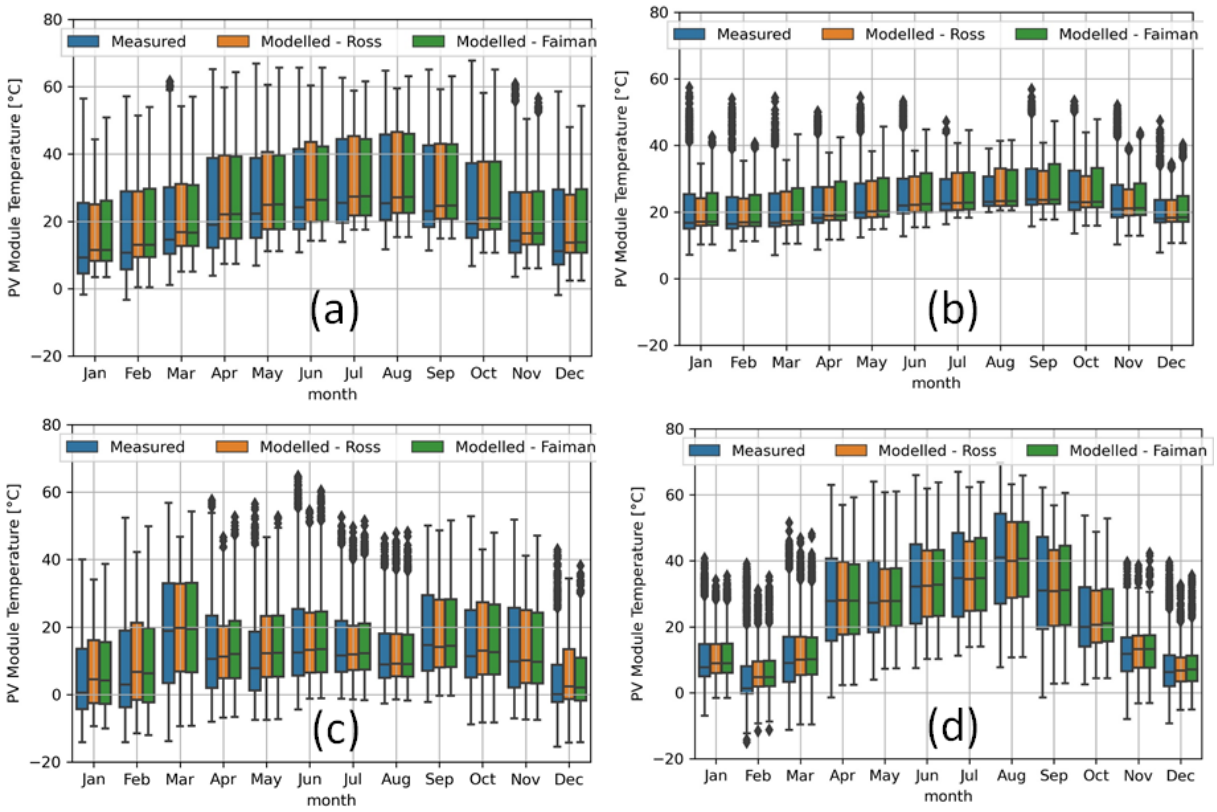

Figure 21: Monthly box plots of measured and modelled PV module temperature in the four locations:(a) Negev, Israel; (b) Gran Canaria, Spain; (c) Zugspitze, Germany; (d) Ljubljana, Slovenia. The plots correspond to the year 2014 for Negev, Gran Canaria and Zugspitze and 2018 for Ljubljana [14].

Table 8: NRMSE of module temperature estimation (T_{mod}) and the relative differences of measured and modelled annual; average module (T_{avg}), minimum (T_{min}) and maximum (T_{max}) temperatures in different locations using Faiman and Ross models.

Location	NRMSE and relative difference of module temperature estimation							
	Faiman model				Ross Model			
	T_{mod}	T_{avg}	T_{min}	T_{max}	T_{mod}	T_{avg}	T_{min}	T_{max}
Negev	12.8%	0.8%	14.8%	2.5%	14.3%	0.8%	13.0%	3.5%
Gran Canaria	15.9%	8.1%	11.0%	4.8%	17.0%	3.9%	10.4%	5.3%
Zugspitze	37.6%	2.5%	37.3%	4.0%	40.8%	1.3%	49.0%	9.2%
Ljubljana	13.5%	7.2%	77.3%	3.0%	14.7%	7.2%	76.2%	3.9%

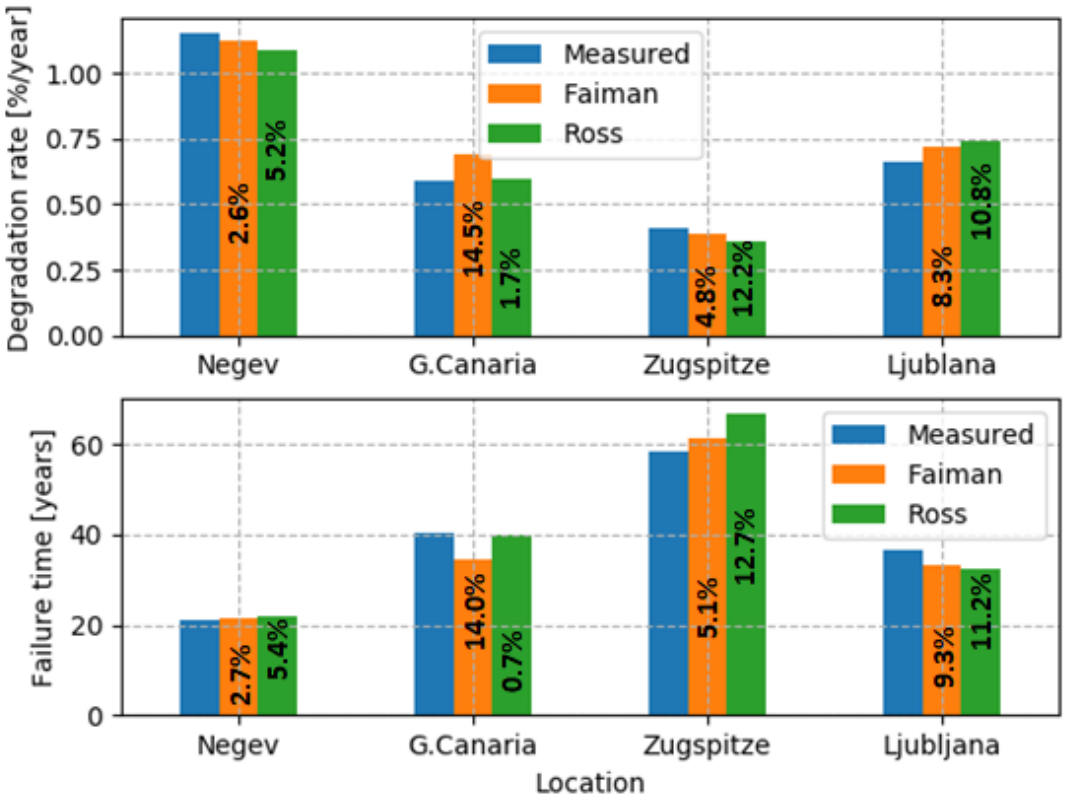

Figure 22: Variations in degradation rates and failure times using measured and modelled PV module temperatures. The percentages are the relative differences compared to degradation rates evaluated using measured PV module temperatures [14]. Failure time defined as a 20% loss of the initial power.

5 CONCLUSION

Service lifetime prediction of PV modules and components is of interest to all PV stakeholders. For example, reliable service lifetime predictions aid: PV module and components manufacturers to provide more realistic warranties, PV project investors to make good financial decisions, and consumers to increase their trust in PV energy. More reliable service lifetime prediction of PV modules and components is still quite a challenge. This report provides the state-of-the-art of the different methods used for PV modules service lifetime prediction.

The report presents the following essential aspects: main climatic stressors, degradation models and mechanisms, degradation pathway models, degradation rates, and reliability models. Different physical and statistical methods used for degradation rate estimation as well as service lifetime prediction are presented. According to the studies in this report, the following key observations establish the current state-of-the-art of service lifetime prediction:

The main degradation stressors are well understood; however, the corresponding induced, or activated, degradation mechanisms are difficult to generalize. The reason for this is because new PV materials are being proposed frequently and usually react differently to the different stressors (e.g., have different degradation kinetics). The degradation mechanisms activated are a function of the specific materials exposed.

Degradation pathway network models are proposed for specific degradation models using the network structural equation modelling (netSEM) analysis. netSEM analysis is a useful and robust approach to map stressors, mechanisms, and responses. It can help to understand the complex interactions between variables and includes metrics that highlight statistically significant relationships. This in-depth insight into the mechanisms of degradation in PV modules can help to develop more reliable degradation kinetics models and hence pave the way to improve reliability and lifetime prediction of PV modules.

Several physical models are proposed to evaluate the degradation rates of specific degradation modes/mechanisms for indoor applications. However, few developments are available for models that combine different degradation mechanisms for outdoor applications. A few models which are available are based on basic assumptions for example, considering few (so-called main stressors) and neglecting others. These assumptions limit the application of the available models in locations where the neglected factors have a significant impact. Moreover, the models also assume the kinetics of degradation to be influenced by a single dominant degradation mechanism. This means that the models neglect the degradation pathways. More complex models that consider the relevant degradation pathways could help to generate a clear correlation of the observed performance degradation with the active degradation mechanics.

Although traditional statistical methods such as: classical seasonal decomposition (CSD), autoregressive integrated moving average (ARIMA), and seasonal-trend decomposition using LOESS (STL), are applicable for PV applications to evaluate the performance loss rate of operational PV modules and PV systems. These models are generally used in different fields for time series data and not developed specifically for PV applications. New statistical methods such as Yearly Degradation Score (YDS) and Multi-step Performance Losses (MS-PL) are proposed specifically for PV applications. Such PV specific degradation methods could help to capture PV performance dependent factors that cannot be achieved using the traditional time series methods. Additionally, new approaches to identify degradation mechanisms signatures from fielded PV data are being proposed. These new developments could be the

solution to correlate the extracted degradation rates from statistical models to the degradation mechanism which has been the major drawback of time series methods.

For service lifetime prediction, linear performance degradation with a constant degradation rate is an approximation or assumption that is still widely used in the PV community. However, this assumption does not usually apply – as demonstrated in recent research. Therefore, using this approximation may result in high uncertainty in lifetime yield predictions. The positive news is that this issue is attracting interest from different researchers to evaluate and propose models for non-linear degradation rates and performance degradation. Such improvements are promising to improve the accuracy and reliability of service lifetime predictions. Additionally, the inconsistencies in degradation rates by different methods and analysts is also a challenging aspect for reliable lifetime predictions. In addition, there is no existing standardized procedure for degradation rates estimation and reporting. Such a standardized procedure is necessary to have more consistent and reusable degradation rates.

REFERENCES

[1] "D. Moser, S. Lindig, M. Richter, J. Ascencio Vásquez, I. Horvath, B. Müller, M. Green, J. Vedde, M. Herz, B. Herteleer, K.A. Weiß, and B. Stridh, Uncertainties in Yield Assessments and PV LCOE, Report IEA-PVPS T13-18: ISBN 978-3-907281-06-2, 2020.," *IEA-PVPS*. [Online]. Available: https://iea-pvps.org/key-topics/uncertainties-yield-assessments/. [Accessed: 19-Mar-2021].

[2] K. A. Weiss, G. Oreski, E. klimm, B. jäckel, I. Kaaya, S. Herceg, and S. Pinto Bautista, *Photovoltaic Modules – Reliability and Sustainability*, 2nd ed. DeGruyer, ISBN 978-3-11-068554-1, 2021.

[3] M. Owen-Bellini, P. Hacke, S. Spataru, D. Miller, and M. Kempe, "Combined-Accelerated Stress Testing for Advanced Reliability Assessment of Photovoltaic Modules," in *35th European Photovoltaic Solar Energy Conference and Exhibition*, 2018.

[4] M. Owen-Bellini, S. L. Moffitt, A. Sinha, A. M. Maes, J. J. Meert, T. Karin, C. Takacs, D. R. Jenket, J. Y. Hartley, D. C. Miller, P. Hacke, and L. T. Schelhas, "Towards validation of combined-accelerated stress testing through failure analysis of polyamide-based photovoltaic backsheets," *Scientific Reports*, vol. 11, no. 1, pp. 1–13, Jan. 2021.

[5] P. L. Hacke, M. Owen-Bellini, M. D. Kempe, D. C. Miller, T. Tanahashi, K. Sakurai, W. J. Gambogi, J. T. Trout, T. C. Felder, K. R. Choudhury, N. H. Philips, M. Koehl, K.-A. Weiss, S. Spataru, C. Monokroussos, and G. Mathiak, "Chapter 11: Combined and Sequential Accelerated Stress Testing for Derisking Photovoltaic Modules," Amsterdam, The Netherlands: Elsevier, NREL/CH-5K00-72451, May 2019.

[6] I. Kaaya, M. Köhl, A.-P. Mehilli, S. de C. Mariano, and K. A. Weiss, "Modeling Outdoor Service Lifetime Prediction of PV Modules: Effects of Combined Climatic Stressors on PV Module Power Degradation," *IEEE Journal of Photovoltaics*, vol. 9, no. Nr.4, pp. 1105–1112, 2019.

[7] A. Bala Subramaniyan, R. Pan, J. Kuitche, and G. TamizhMani, "Quantification of Environmental Effects on PV Module Degradation: A Physics-Based Data-Driven Modeling Method," *IEEE Journal of Photovoltaics*, vol. 8, no. 5, pp. 1289–1296, Sep. 2018.

[8] C. R. Osterwald and T. J. McMahon, "History of accelerated and qualification testing of terrestrial photovoltaic modules: A literature review," *Progress in Photovoltaics: Research and Applications*, vol. 17, no. 1, pp. 11–33, 2009.

[9] S. Lindig, I. Kaaya, K.-A. Weiß, M. Topic, and D. Moser, "Review of statistical and analytical degradation models for photovoltaic modules and systems as well as related improvements," *IEEE Journal of Photovoltaics*, vol. 8, no. Nr.6, pp. 1773–1786, 2018.

[10] A. Phinikarides, N. Kindyni, G. Makrides, and G. E. Georghiou, "Review of photovoltaic degradation rate methodologies," *Renewable and Sustainable Energy Reviews*, vol. 40, pp. 143–152, Dec. 2014.

[11] A. Gok, C. Fagerholm, R. French, and L. Bruckman, "Temporal evolution and pathway models of poly(ethylene-terephthalate) degradation under multi-factor accelerated weathering exposures," *PloS one*, vol. 14, no. 2, p. e0212258, Feb. 2019.

[12] I. Kaaya, S. Lindig, K.-A. Weiss, A. Virtuani, M. S. de C. Ortin, and D. Moser, "Photovoltaic lifetime forecast model based on degradation patterns," *Progress in Photovoltaics: Research and Applications*, vol. 28, no. 10, pp. 979–992, 2020.

[13] M. Theristis, A. Livera, C. B. Jones, G. Makrides, G. E. Georghiou, and J. S. Stein, "Nonlinear Photovoltaic Degradation Rates: Modeling and Comparison Against Conventional Methods," *IEEE Journal of Photovoltaics*, vol. 10, no. 4, pp. 1112–1118, Jul. 2020.

[14] I. Kaaya, J. Ascencio-Vásquez, K. A. Weiss, and M. Topič, "Assessment of uncertainties and variations in PV modules degradation rates and lifetime predictions using physical models," *Solar Energy*, vol. 218, pp. 354–367, Apr. 2021.

[15] M. Kottek, J. Grieser, C. Beck, B. Rudolf, and F. Rubel, "World Map of the Köppen-Geiger climate classification updated," *Meteorologische Zeitschrift*, pp. 259–263, Jul. 2006.

[16] "Mass transfer," *Wikipedia*. 30-Nov-2020.

[17] "R.H. French, D. Moser, S. Lindig, M. Herz, B. Müller, M. Richter, I. Horvath, B. Müller, M. van Ise-ghem, W. van Sark, J.S Stein, F. Baumgartner, L. Bruckman, and J. Ascencio Vásquez,D.Bertani, G.Maugeri, A.J.Curran,K.Rath, J.Liu, A.Khalilnejad,M.Meftah, D.Jordan, C.Deline, G.Makrides, G.Georghiou,

A.Livera, B.Meyers, G.Plessis,M.heristis, W.Luo, Assessment of Performance Loss Rate of PV Power Systems, Report IEA-PVPS T13-22: 978-3-907281-10-9, 2020."

[18] J., "Bonilla Castro, M. Schweiger, D. Moser, T. Tanahashi, B.H. King, G. Friesen, L. Haitao, R.H. French, B. Müller, C. Reise, G. Eder, W. van Sark, Y. Sangpongsanon, F. Valencia, J.S. Stein, J. Ascencio Vásquez, C. Ulbrich, M.A. Sevillano Bendezú, A. Gracia Amillo, E. Dunlop, N. Taylor, R. Valckenborg, M.R. Vogt, J. Blakesley, and D.E. Guzman Razo, Climatic Rating of Photovoltaic Mod-ules: Different Technologies for Various Operating Conditions, Report IEA-PVPS T13-20: ISBN 978-3-907281-08-6, 2021."

[19] "Soiling (solar energy)," *Wikipedia*. 29-Jan-2021.

[20] H. E. Yang, R. French, and L. Bruckman, *Durability and Reliability of Polymers and Other Materials in Photovoltaic Modules*. William Andrew, 2019.

[21] C. C. White, K. M. White, and P. E. James, *Service Life Prediction of Polymers and Plastics Exposed to Outdoor Weathering - 1st Edition*, 1st ed. Elsevier, 2018.

[22] C. C. White, K. M. White, and J. Pickett, "Service Life Prediction -Why is this so hard?," vol. 1, pp. 1–16, Nov. 2017.

[23] M. Köntges, S. Kurtz, C. E. Packard, U. Jahn, K. A. Berger, K. Kato, T. Friesen, H. Liu, M. Van Iseghem, J. Wohlgemuth, D. Miller, M. Kempe, P. Hacke, F. Reil, N. Bogdanski, W. Herrmann, C. Buerhop-Lutz, G. Razongles, and G. Friesen, "Review of Failures of Photovoltaic Modules," IEA International Energy Agency-ISBN 978-3-906042-16-9, Report, 2014.

[24] "IEC 61215-1:2021 - Terrestrial photovoltaic (PV) modules - Design qualification and type approval - Part 1: Test requirements," *iTeh Standards Store*. [Online]. Available: https://standards.iteh.ai/catalog/standards/iec/1452c391-ebde-4588-9a4a-afd9b73b1330/iec-61215-1-2021. [Accessed: 15-Apr-2021].

[25] E. Dunlop, D. Halton, and H. A. Ossenbrink, "20 years of life and more: where is the end of life of a PV module?," *Conference Record of the Thirty-first IEEE Photovoltaic Specialists Conference, 2005.*, 2005.

[26] W. Köppen, "The thermal zones of the Earth according to the duration of hot, moderate and cold periods and to the impact of heat on the organic world," *Meteorologische Zeitschrift*, pp. 351–360, Jun. 2011.

[27] R. Geiger, "Das Klima der bodennahen Luftschicht," *Anzeiger für Schädlingskunde*, vol. 34, no. 10, pp. 159–159, Oct. 1961.

[28] M. C. Baechler, J. L. Williamson, T. L. Gilbride, P. C. Cole, M. G. Hefty, and P. M. Love, "Building America Best Practices Series: Volume 7.1: Guide to Determining Climate Regions by County," *UNT Digital Library*, 30-Aug-2010. [Online]. Available: https://digital.library.unt.edu/ark:/67531/metadc827424/. [Accessed: 17-Sep-2020].

[29] J. Ascencio-Vásquez, K. Brecl, and M. Topič, "Methodology of Köppen-Geiger-Photovoltaic climate classification and implications to worldwide mapping of PV system performance," *Solar Energy*, vol. 191, pp. 672–685, Oct. 2019.

[30] T. Karin, C. Jones, and A. Jain, "Photovoltaic Degradation Climate Zones," in *IEEE 46th Photovoltaic Specialists Conference (PVSC)*, 2019, pp. 0687–0694.

[31] J. Ascencio-Vásquez, I. Kaaya, K. Brecl, K.-A. Weiss, and M. Topič, "Global Climate Data Processing and Mapping of Degradation Mechanisms and Degradation Rates of PV Modules," *Energies*, vol. 12, no. 24, p. 4749, Jan. 2019.

[32] W. Raymond, X. Arthur, F. Roger, and B. Laura, "Evaluation and Augmentation of Köppen-Geiger Climate Zone Based off of Real-World Satellite Weather Data," in *47th IEEE Photovoltaic Specialists Conference (PVSC),* 2020.

[33] A. Gok, D. A. Gordon, D. M. Burns, S. P. Fowler, R. H. French, and L. S. Bruckman, "Reciprocity and spectral effects of the degradation of poly(ethylene-terephthalate) under accelerated weathering exposures," *Journal of Applied Polymer Science*, vol. 136, no. 22, p. 47589, 2019.

[34] D. Otth and R. G. Ross, "Assessing photovoltaic module degradation and lifetime from long term environmental tests," 1983.

[35] M. D. Kempe, D. Panchagade, M. O. Reese, and A. A. Dameron, "Modeling moisture ingress through polyisobutylene-based edge-seals," *Progress in Photovoltaics: Research and Applications*, vol. 23, no. 5, pp. 570–581, 2015.

[36] K. H. Krebs and E. Rossi-Gianoli, "Photovoltaic Testing in the European Communities," in *Photovoltaic Solar Energy Conference*, Springer, Dordrecht, 1981, pp. 287–292.

[37] D. Moore, *Cyclic Pressure-load Developmental Testing of Solar Panels: Low-cost Silicon Solar Array Project*. Jet Propulsion Laboratory, California Institute of Technology, 1977.

[38] J. Miller, Z. Xia, J. Shaner, D. Amin, D. Cunningham, and J. H. Wohlgemuth, "Using Accelerated Tests and Field Data to Predict Module Reliability and Lifetime," *23rd European Photovoltaic Solar Energy Conference and Exhibition, 1-5 September 2008, Valencia, Spain*, pp. 2663–2669, Nov. 2008.

[39] A. Sinha, V. S. P. Buddha, E. J. Schneller, K. O. Davis, and G. Tamizhmani, "Solder Bond Degradation of Fielded PV Modules: Climate Dependence of Intermetallic Compound Growth," in *2019 IEEE 46th Photovoltaic Specialists Conference, PVSC 2019*, 2019, pp. 1393–1397.

[40] N. Bosco, T. Silverman, and S. Kurtz, "The Influence of PV Module Materials and Design on Solder Joint Thermal Fatigue Durability," *IEEE Journal of Photovoltaics*, vol. 6, no. 6, pp. 1407–1412, 2016.

[41] J. Wohlgemuth and S. Kurtz, "Reliability testing beyond Qualification as a key component in photovoltaic's progress toward grid parity," *2011 International Reliability Physics Symposium*, 2011.

[42] C. R. Osterwald, J. P. Benner, J. Pruett, A. Anderberg, S. Rummel, and L. Ottoson, "Degradation in weathered crystalline-silicon PV modules apparently caused by UV radiation," *3rd World Conference on-Photovoltaic Energy Conversion, 2003. Proceedings of*, 2003.

[43] R. Witteck, B. Veith-Wolf, H. Schulte-Huxel, A. Morlier, M. R. Vogt, M. Köntges, and R. Brendel, "UV-induced degradation of PERC solar modules with UV-transparent encapsulation materials," *Progress in Photovoltaics: Research and Applications*, vol. 25, no. 6, pp. 409–416, 2017.

[44] J. F. Pern, W. A. Czanderna, A. . Emery, and R. . Dhere, "Weathering degradation of EVA encapsulant and the effect of its yellowing on solar cell efficiency.," *Conference Record of the IEEE Photovoltaic Specialists Conference*, vol. 22nd, no. Vol 1, pp. 557–561, 1991.

[45] M. Koehl, P. Hacke, H.-S. Wu, and A. Zielnik, "Round-robin weathering test of various polymeric backsheets for PV modules with different ultraviolet irradiation and sample temperatures," *Progress in Photovoltaics: Research and Applications*, vol. 28, no. 8, pp. 808–815, 2020.

[46] "IEC TS 62782 : Photovoltaic (PV) modules – Cyclic (dynamic) mechanical load testing." [Online]. Available: https://global.ihs.com/doc_detail.cfm?document_name=IEC%20TS%2062782&item_s_key=00672456. [Accessed: 15-Apr-2021].

[47] M. Köntges, G. Oreski, U. Jahn, M. Herz, P. Hacke, and K.-A. Weiß, "Assessment of photovoltaic module failures in the field : International Energy Agency Photovoltaic Power Systems Programme : IEA PVPS Task 13, Subtask 3 : report IEA-PVPS T13-09:2017, ISBN 978-3-906042-54-1," International Energy Agency, 2017.

[48] P. L. Hacke, M. D. Kempe, J. Wohlgemuth, J. Li, and Y.-C. Shen, "Potential-Induced Degradation-Delamination Mode in Crystalline Silicon Modules: Preprint," National Renewable Energy Lab. (NREL), Golden, CO (United States), NREL/CP-5J00-67256, Mar. 2018.

[49] W. J. Gambogi, T. C. Felder, S. W. Macmaster, K. Roy-Choudhury, B.-L. Yu, K. M. Stika, H. Hu, N. Phillips, and T. J. Trout, "Sequential Stress Testing to Predict Photovoltaic Module Durability," *2018 IEEE 7th World Conference on Photovoltaic Energy Conversion (WCPEC) (A Joint Conference of 45th IEEE PVSC, 28th PVSEC & 34th EU PVSEC)*, 2018.

[50] T. C. Felder, W. J. Gambogi, N. Phillips, S. W. MacMaster, B.-L. Yu, and T. J. Trout, "Comparison of higher irradiance and black panel temperature UV backsheet exposures to field performance," in *Reliability of Photovoltaic Cells, Modules, Components, and Systems X*, 2017, vol. 10370, p. 1037002.

[51] www.ait.ac.at, "INFINITY - AIT Austrian Institute Of Technology," *ait.ac.at*, 26-May-2020. [Online]. Available: https://www.ait.ac.at/en/research-topics/photovoltaics/projects/infinity/. [Accessed: 26-May-2020].

[52] G. C. Eder, Y. Voronko, S. Dimitriadis, K. Knöbl, G. Újvári, K. A. Berger, M. Halwachs, L. Neumaier, and C. Hirschl, "Climate specific accelerated ageing tests and evaluation of ageing induced electrical, physical, and chemical changes," *Progress in Photovoltaics: Research and Applications*, vol. 27, no. 11, pp. 934–949, 2019.

[53] "IEC 61730-1:2016 - IEC-Normen - VDE VERLAG." [Online]. Available: https://www.vde-verlag.de/iec-normen/223810/iec-61730-1-2016.html. [Accessed: 16-Apr-2021].

[54] "IEC 61701:2020 - IEC-Normen - VDE VERLAG." [Online]. Available: https://www.vde-verlag.de/iec-normen/248812/iec-61701-2020.html. [Accessed: 16-Apr-2021].

[55] W. Gambogi, S. MacMaster, B.-L. Yu, T. Felder, H. Hu, K. R. Choudhury, T. J. Trout, and D. P. Solutions, "Sequential testing that better predicts field performance," in *Atlas-NIST Workshop*, 2017.

[56] G. . Ede, Y. Voronko, P. Grillberger, K. . Berger, G. Újvári, and K. Knöbl, “Development of climate specific accelerated ageing tests for Photovoltaic modules,” in *European Weathering Symposium EWS “Natural and Artificial Ageing of Polymers*, Basel, 2019, vol. 19.

[57] G. C. Eder, Y. Voronko, K. Knöbl, S. Dimitriadis, G. Újvári, K. A. Berger, and L. Neumaier, “Climate specific accelerated ageing tests,” in *2019 IEEE 46th Photovoltaic Specialists Conference (PVSC)*, 2019, pp. 2398–2405.

[58] M. Halwachs, L. Neumaier, N. Vollert, L. Maul, S. Dimitriadis, Y. Voronko, G. Eder, A. Omazic, W. Muehleisen, C. Hirschl, M. Schwark, K. Berger, and R. Ebner, “Statistical evaluation of PV system performance and failure data among different climate zones,” *Renewable Energy*, vol. 139, Mar. 2019.

[59] D. C. Jordan, T. J. Silverman, J. H. Wohlgemuth, S. R. Kurtz, and K. T. VanSant, “Photovoltaic failure and degradation modes,” *Progress in Photovoltaics: Research and Applications*, vol. 25, no. 4, pp. 318–326, 2017.

[60] S. Spataru, P. Hacke, and M. Owen-Bellini, “Combined-Accelerated Stress Testing System for Photovoltaic Modules,” in *Proceedings of the 2018 IEEE 7th World Conference on Photovoltaic Energy Conversion*, 2018, pp. 3943–3948.

[61] M. D. Kempe, D. C. Miller, J. H. Wohlgemuth, S. R. Kurtz, J. M. Moseley, Q. A. Shah, G. Tamizhmani, K. Sakurai, M. Inoue, T. Doi, A. Masuda, S. L. Samuels, and C. E. Vanderpan, “Field testing of thermoplastic encapsulants in high-temperature installations,” *Energy Science & Engineering*, vol. 3, no. 6, pp. 565–580, 2015.

[62] N. Bosco, T. J. Silverman, and S. Kurtz, “Climate specific thermomechanical fatigue of flat plate photovoltaic module solder joints,” *Microelectronics Reliability*, vol. 62, pp. 124–129, Jul. 2016.

[63] G. C. Eder, Y. Voronko, G. Oreski, W. Mühleisen, M. Knausz, A. Omazic, A. Rainer, C. Hirschl, C. Hirschl, and H. Sonnleitner, “Error analysis of aged modules with cracked polyamide backsheets,” *Solar Energy Materials and Solar Cells*, Dec. 2019.

[64] Y. Wang, W. Huang, A. Fairbrother, L. S. Fridman, A. Curran, N. R. Wheeler, S. Napoli, A. W. Hauser, S. Julien, X. Gu, G. O’brien, K. Wan, L. Ji, M. Kempe, K. P. Boyce, R. French, and L. Bruckman, “Generalized Spatio-Temporal Model of Backsheet Degradation From Field Surveys of Photovoltaic Modules,” *IEEE-JPV*, vol. 9, no. 5, pp. 1374–1381, 2019.

[65] A. Fairbrother, M. Boyd, Y. Lyu, J. Avenet, P. Illich, M. Kempe, B. Dougherty, L. Bruckman, and X. Gu, “Differential degradation patterns of photovoltaic backsheets at the array level,” *Solar Energy*, vol. 163, pp. 62–69, 2018.

[66] M. D. Kempe, “Modeling of rates of moisture ingress into photovoltaic modules,” *Solar Energy Materials and Solar Cells*, vol. 90, no. 16, pp. 2720–2738, Oct. 2006.

[67] P. Hülsmann and K.-A. Weiss, “Simulation of water ingress into PV-modules: IEC-testing versus outdoor exposure,” *Solar Energy*, vol. 115, pp. 347–353, May 2015.

[68] M. Jankovec, F. Galliano, E. Annigoni, H. Y. Li, F. Sculati-Meillaud, L.-E. Perret-Aebi, C. Ballif, and M. Topič, “In-situ monitoring of moisture ingress in PV modules using digital humidity sensors,” *IEEE journal of photovoltaics*, vol. 6, no. 5, pp. 1152–1159, 2016.

[69] S. Suzuki, N. Nishiyama, S. Yoshino, T. Ujiro, S. Watanabe, T. Doi, A. Masuda, and T. Tanahashi, “Acceleration of potential-induced degradation by salt-mist preconditioning in crystalline silicon photovoltaic modules,” *Jpn. J. Appl. Phys.*, vol. 54, no. 8S1, p. 08KG08, Jul. 2015.

[70] S.-T. Hsu, W.-Y. Lin, and S.-J. Wu, “Environmental Factors for Non-uniform Dynamic Mechanical Load Test due to Wind Actions on Photovoltaic Modules,” *Energy Procedia*, vol. 150, pp. 50–57, Sep. 2018.

[71] C. Buerhop, S. Wirsching, A. Bemm, T. Pickel, P. Hohmann, M. Nieß, C. Vodermayer, A. Huber, B. Glück, J. Mergheim, C. Camus, J. Hauch, and C. J. Brabec, “Evolution of cell cracks in PV-modules under field and laboratory conditions,” *Progress in Photovoltaics: Research and Applications*, vol. 26, no. 4, pp. 261–272, 2018.

[72] C. Camus, P. Offermann, M. Weissmann, C. Buerhop, J. Hauch, and C. J. Brabec, “Site-specific assessment of mechanical loads on photovoltaic modules from meteorological reanalysis data,” *Solar Energy*, vol. 188, pp. 1134–1145, 2019.

[73] P. M. Segado, J. Carretero, and M. Sidrach-de-Cardona, “Models to predict the operating temperature of different photovoltaic modules in outdoor conditions,” *Progress in Photovoltaics: Research and Applications*, vol. 23, no. 10, pp. 1267–1282, 2015.

[74] M. Koehl, M. Heck, S. Wiesmeier, and J. Wirth, “Modeling of the nominal operating cell temperature based on outdoor weathering,” *Solar Energy Materials and Solar Cells*, vol. 95, no. 7, pp. 1638–1646, Jul. 2011.
[75] R. Ross, “Interface design considerations for terrestrial solar cell modules,” in *12th Photovoltaic Specialists Conference*, New York, 1976, pp. 801–806.
[76] D. Faiman, “Assessing the outdoor operating temperature of photovoltaic modules,” *Progress in Photovoltaics: Research and Applications*, vol. 16, no. 4, pp. 307–315, 2008.
[77] E. Skoplaki and J. A. Palyvos, “Operating temperature of photovoltaic modules: A survey of pertinent correlations,” *Renewable Energy*, vol. 34, no. 1, pp. 23–29, Jan. 2009.
[78] M. Koehl, M. Heck, and S. Wiesmeier, “Categorization of weathering stresses for photovoltaic modules,” *Energy Science & Engineering*, vol. 6, no. 2, pp. 93–111, 2018.
[79] P. Hülsmann, M. Heck, and M. Köhl, “Simulation of Water Vapor Ingress into PV-Modules under Different Climatic Conditions,” *Journal of Materials*, 27-Feb-2013. [Online]. Available: https://www.hindawi.com/journals/jma/2013/102691/. [Accessed: 23-Oct-2020].
[80] S. Mitterhofer, J. Slapšak, M. Jankovec, M. Topic, A. Astigarraga, D. Moser, W. Luo, Y. Sheng Khoo, G. Oviedo Hernandez, P. V. Chiantore, J. Rabanal-Arabach, E. Fuentealba, P. Ferrada, and M. Trigo-Gonzalez, “Measurement and simulation of moisture ingress in PV modules in various climates,” presented at the 37th EUPVSEC, Online, 2020.
[81] M. D. Kempe, A. A. Dameron, and M. O. Reese, “Evaluation of moisture ingress from the perimeter of photovoltaic modules,” *Progress in Photovoltaics: Research and Applications*, vol. 22, no. 11, pp. 1159–1171, 2014.
[82] S. Mitterhofer, C. Barretta, L. F. Castillon, G. Oreski, M. Topič, and M. Jankovec, “A Dual-Transport Model of Moisture Diffusion in PV Encapsulants for Finite-Element Simulations,” *IEEE-JPVc*, vol. 10, no. 1, pp. 94–102, 2020.
[83] P. Hülsmann, K.-A. Weiß, and M. Köhl, “Temperature-dependent water vapour and oxygen permeation through different polymeric materials used in photovoltaic-modules,” *Progress in Photovoltaics: Research and Applications*, vol. 22, no. 4, pp. 415–421, 2014.
[84] R. Meitzner and S.-H. Schulze, “Method for determination of parameters for moisture simulations in photovoltaic modules and laminated glass,” *Solar energy materials and solar cells*, vol. 144, pp. 23–28, 2016.
[85] N. Kyranaki, “Corrosion in crystalline silicon photovoltaic modules and the influence on performance,” PhD thesis, Loughborough University, 2020.
[86] L. Perrin, Q. T. Nguyen, D. Sacco, and P. Lochon, “Experimental Studies and Modelling of Sorption and Diffusion of Water and Alcohols in Cellulose Acetate,” *Polymer International*, vol. 42, no. 1, pp. 9–16, 1997.
[87] E. Favre, R. Clément, Q. T. Nguyen, P. Schaetzel, and J. Néel, “Sorption of organic solvents into dense silicone membranes. Part 2.—Development of a new approach based on a clustering hypothesis for associated solvents,” *J. Chem. Soc., Faraday Trans.*, vol. 89, no. 24, pp. 4347–4353, Jan. 1993.
[88] X. Gu, D. Stanley, W. E. Byrd, B. Dickens, I. Vaca-Trigo, W. Q. Meeker, T. Nguyen, J. W. Chin, and J. W. Martin, “Linking Accelerated Laboratory Test with Outdoor Performance Results for a Model Epoxy Coating System,” in *Service Life Prediction of Polymeric Materials*, Boston, MA, 2009, pp. 3–28.
[89] J. Liu, A. J. Curran, J. S. Fada, X. Ma, W. Huang, C. B. Jones, E. Schnabel, M. Kohl, J. L. Braid, and R. H. French, “Cross-correlation Analysis of the Indoor Accelerated and Real World Exposed Photovoltaic Systems Across Multiple Climate Zones,” *2018 IEEE 7th World Conference on Photovoltaic Energy Conversion (WCPEC) (A Joint Conference of 45th IEEE PVSC, 28th PVSEC & 34th EU PVSEC)*, 2018.
[90] D. A. Gordon, W.-H. Huang, D. M. Burns, R. H. French, and L. S. Bruckman, “Multivariate multiple regression models of poly(ethylene-terephthalate) film degradation under outdoor and multi-stressor accelerated weathering exposures,” *PLOS ONE*, vol. 13, no. 12, p. e0209016, Dec. 2018.
[91] “Empirical modelling,” *Wikipedia*. 19-Sep-2020.
[92] “Statistical model,” *Wikipedia*. 19-Mar-2021.
[93] D. R. Cox, “Principles of Statistical Inference,” *Cambridge Core*, Aug-2006. [Online]. Available: https://www.cambridge.org/core/books/principles-of-statistical-inference/BCD3734047D403DF5352EA58F41D3181. [Accessed: 22-Mar-2021].
[94] “Mathematical model,” *Wikipedia*. 15-Feb-2021.

[95] A. R. Estabragh, M. R. S. Pereshkafti, and A. A. Javadi, “Comparison Between Analytical and Numerical Methods in Evaluating the Pollution Transport in Porous Media,” *Geotech Geol Eng*, vol. 31, no. 1, pp. 93–101, Feb. 2013.

[96] L. Bruckman, N. R. Wheeler, J. Ma, E. Wang, C. Wang, I. Chou, J. Sun, and R. H. French, “Statistical and Domain Analytics Applied to PV Module Lifetime and Degradation Science,” *IEEE Access*, 2013.

[97] G. James, D. Witten, T. Hastie, and R. Tibshirani, *An Introduction to Statistical Learning: with Applications in R*. New York: Springer-Verlag, 2013.

[98] C. E. Shannon, “A Mathematical Theory of Communication,” *Bell System Technical Journal*, vol. 27, no. 3, pp. 379–423, 1948.

[99] H. Akaike, “Information Theory and an Extension of the Maximum Likelihood Principle,” in *Selected Papers of Hirotugu Akaike*, Springer, New York, NY, 1998, pp. 199–213.

[100] P. A. Stephens, S. W. Buskirk, G. D. Hayward, and C. Martínez Del Rio, “Information theory and hypothesis testing: a call for pluralism,” *Journal of Applied Ecology*, vol. 42, no. 1, pp. 4–12, Feb. 2005.

[101] P. M. Lukacs, W. L. Thompson, W. L. Kendall, W. R. Gould, P. F. Doherty Jr, K. P. Burnham, and D. R. Anderson, “Concerns regarding a call for pluralism of information theory and hypothesis testing,” *Journal of Applied Ecology*, vol. 44, no. 2, pp. 456–460, Apr. 2007.

[102] R. H. French, R. Podgornik, T. J. Peshek, L. S. Bruckman, Y. Xu, N. R. Wheeler, A. Gok, Y. Hu, M. A. Hossain, D. A. Gordon, P. Zhao, J. Sun, and G.-Q. Zhang, “Degradation science: Mesoscopic evolution and temporal analytics of photovoltaic energy materials,” *Current Opinion in Solid State and Materials Science*, vol. 19, no. 4, Jan. 2015.

[103] P. a. M. Dirac, “A new notation for quantum mechanics,” *Mathematical Proceedings of the Cambridge Philosophical Society*, vol. 35, no. 3, pp. 416–418, Jul. 1939.

[104] H. Akaike, “A New Look at the Statistical Model Identification,” in *Selected Papers of Hirotugu Akaike*, Springer, New York, NY, 1974, pp. 215–222.

[105] M. Coskun and M. Koyutürk, “Link prediction in large networks by comparing the global view of nodes in the network,” in *2015 IEEE International Conference on Data Mining Workshop (ICDMW)*, 2015, pp. 485–492.

[106] J. Zhou, G. Cui, Z. Zhang, C. Yang, Z. Liu, L. Wang, C. Li, and M. Sun, “Graph Neural Networks: A Review of Methods and Applications,” *arXiv.org*, Dec. 2018.

[107] W.-H. Huang, N. Wheeler, A. Klinke, Y. Xu, W. Du, A. K. Verma, A. Gok, D. Gordon, Y. Wang, J. Liu, A. Curran, J. Fada, X. Ma, J. Braid, J. Carter, L. Bruckman, and R. French, *netSEM: Network Structural Equation Modeling*. 2018.

[108] A. Gok, D. K. Ngendahimana, C. L. Fagerholm, R. H. French, J. Sun, and L. S. Bruckman, “Predictive models of poly(ethylene-terephthalate) film degradation under multi-factor accelerated weathering exposures,” *PLOS ONE*, vol. 12, no. 5, p. e0177614, Dec. 2017.

[109] “Training School,” *PEARL PV*, 21-Sep-2020. .

[110] Y. Voronko, G. C. Eder, M. Knausz, G. Oreski, T. Koch, and K. A. Berger, “Correlation of the loss in photovoltaic module performance with the ageing behaviour of the backsheets used,” *Progress in Photovoltaics: Research and Applications*, vol. 23, no. 11, pp. 1501–1515, 2015.

[111] G. Oreski, A. Mihaljevic, Y. Voronko, and G. C. Eder, “Acetic acid permeation through photovoltaic backsheets: Influence of the composition on the permeation rate,” *Polymer Testing*, vol. 60, pp. 374–380, Jul. 2017.

[112] M. Knausz, G. Oreski, G. C. Eder, Y. Voronko, B. Duscher, T. Koch, G. Pinter, and K. A. Berger, “Degradation of photovoltaic backsheets: Comparison of the aging induced changes on module and component level,” *Journal of Applied Polymer Science*, vol. 132, no. 24, 2015.

[113] B. S. Chernev, C. Hirschl, and G. C. Eder, “Non-Destructive Determination of Ethylene Vinyl Acetate Cross-Linking in Photovoltaic (PV) Modules by Raman Spectroscopy,” *Appl. Spectrosc., AS*, vol. 67, no. 11, pp. 1296–1301, Nov. 2013.

[114] C. Hirschl, M. Biebl–Rydlo, M. DeBiasio, W. Mühleisen, L. Neumaier, W. Scherf, G. Oreski, G. Eder, B. Chernev, W. Schwab, and M. Kraft, “Determining the degree of crosslinking of ethylene vinyl acetate photovoltaic module encapsulants—A comparative study,” *Solar Energy Materials and Solar Cells*, vol. 116, pp. 203–218, Sep. 2013.

[115] G. Ehrenstein and S. Pongratz, *Resistance and Stability of Polymers*. Hanser Publishers, ISBN 978-1-56990-456-5, 2013.

[116] W. Weibull, “A Statistical Distribution Function of Wide Applicability,” *Journal of Applied Mechanics*, vol. 8, pp. 293–297, 1951.
[117] O. Haillant, D. Dumbleton, and A. Zielnik, “An Arrhenius approach to estimating organic photovoltaic module weathering acceleration factors,” *Solar Energy Materials and Solar Cells*, vol. 95, no. 7, pp. 1889–1895, Jul. 2011.
[118] J. H. Chan and S. T. Balke, “The thermal degradation kinetics of polypropylene: Part I. Molecular weight distribution,” *Polymer Degradation and Stability*, vol. 57, no. 2, pp. 113–125, Aug. 1997.
[119] J. D. Peterson, S. Vyazovkin, and C. A. Wight, “Kinetics of the Thermal and Thermo-Oxidative Degradation of Polystyrene, Polyethylene and Poly(propylene),” *Macromolecular Chemistry and Physics*, vol. 202, no. 6, pp. 775–784, 2001.
[120] M. Koehl, T.-J. Trout, T. Felder, K. Choudhury, S. Padlewski, and A. Borne, “Analysis of UV Degradation of PV Backsheets Using Arrhenius Formalism to Extract Intrinsic Material Characteristics and Model Lifetime Performance,” in *33rd European Photovoltaic Solar Energy Conference and Exhibition*, 2017, pp. 1349–1353.
[121] H. S. Blanks, “Arrhenius and the temperature dependence of non-constant failure rate,” *Quality and Reliability Engineering International*, vol. 6, no. 4, pp. 259–265, 1990.
[122] V. Saux, P. L. Gac, Y. Marco, and S. Calloch, “Limits in the validity of Arrhenius predictions for field ageing of a silica filled polychloroprene in a marine environment,” *Polymer Degradation and Stability*, vol. 99, pp. 254–261, 2014.
[123] N. J. Luiggi Agreda, “Aquilanti–Mundim deformed Arrhenius model in solid-state reactions,” *J Therm Anal Calorim*, vol. 126, no. 3, pp. 1175–1184, Dec. 2016.
[124] M. A. Bohn, “The Connection Between the Parameters of WLF Equation and of Arrhenius Equation,” *Propellants, Explosives, Pyrotechnics*, vol. 44, no. 6, pp. 696–705, 2019.
[125] B. X. J. Yu, R. Lv, J.-N. Jaubert, G. Xing, J. Dupuis, E. Sandré, C. Dugué, and G. Goaer, “Failure modes of polyolefin encapsulated double glass modules and corresponding degradation modeling — Part 1 optical durability,” in *47th IEEE Photovoltaic Specialists Conference (PVSC),* 2020, pp. 1002–1007.
[126] Y. Lyu, A. Fairbrother, M. Gong, J. Kim, X. Gu, M. Kempe, S. Julien, K. Wan, S. Napoli, A. W. Hauser, G. O’brien, Y. Wang, R. French, L. Bruckman, L. Ji, and K. P. Boyce, “Impact of environmental variables on the degradation of photovoltaic components and perspectives for the reliability assessment methodology,” *Solar Energy*, vol. 199, pp. 425–436, 2020.
[127] M. Gagliardi, P. Lenarda, and M. Paggi, “A reaction-diffusion formulation to simulate EVA polymer degradation in environmental and accelerated ageing conditions,” *Solar Energy Materials and Solar Cells*, vol. C, no. 164, pp. 93–106, 2017.
[128] W. Nash, T. Drummond, and N. Birbilis, “A review of deep learning in the study of materials degradation,” *npj Materials Degradation*, vol. 2, no. 1, pp. 1–12, Nov. 2018.
[129] E. Smidt, M. Schwanninger, J. Tintner, and K. Boehm, “Ageing and Deterioration of Materials in the Environment – Application of Multivariate Data Analysis, Multivariate Analysis in Management, Engineering and the Sciences, Leandro Valim de Freitas and Ana Paula Barbosa Rodrigues de Freitas, IntechOpen, DOI: 10.5772/53984 [Titel anhand dieser DOI in Citavi-Projekt übernehmen] . Available from: https://www.intechopen.com/books/multivariate-analysis-in-management-engineering-and-the-sciences/ageing-and-deterioration-of-materials-in-the-environment-application-of-multivariate-data-analysis,” 2013.
[130] H. Song, P. Xu, Z. Wu, Y. Xia, and M. Yun, “Annual Degradation Rates of Crystalline Silicon Photovoltaic Modules in Different Climatic Zones in China,” in *35th European Photovoltaic Solar Energy Conference and Exhibition*, 2018, pp. 1189–1191.
[131] E. V. Bystritskaya, O. N. Karpukhin, and A. V. Kutsenova, “Monte Carlo Simulation of Linear Polymer Thermal Depolymerization under Isothermal and Dynamic Modes,” *International Journal of Polymer Science*, 08-Jun-2011. [Online]. Available: https://www.hindawi.com/journals/ijps/2011/849370/. [Accessed: 21-Sep-2020].
[132] K. Binder, “1.17 - Monte Carlo Simulations in Polymer Science,” in *Polymer Science: A Comprehensive Reference*, K. Matyjaszewski and M. Möller, Eds. Amsterdam: Elsevier, 2012, pp. 461–474.
[133] H. Makki, K. N. S. Adema, E. A. J. F. Peters, J. Laven, L. G. J. van der Ven, R. A. T. M. van Benthem, and G. de With, “Multi-scale simulation of degradation of polymer coatings: Thermo-mechanical simulations,” *Polymer Degradation and Stability*, vol. 123, pp. 1–12, Jan. 2016.

[134] M. R. Nyden and J. W. Gilman, “Molecular dynamics simulations of the thermal degradation of nano-confined polypropylene,” *Computational and Theoretical Polymer Science*, vol. 7, no. 3, pp. 191–198, Jan. 1997.

[135] A. Morshedifard, S. Masoumi, and M. J. A. Qomi, “Nanoscale origins of creep in calcium silicate hydrates,” *Nature Communications*, 2018.

[136] A. Launay, F. Thominette, and J. Verdu, “Hydrolysis of poly(ethylene terephthalate): a kinetic study,” *Polymer Degradation and Stability*, vol. 46, no. 3, pp. 319–324, Jan. 1994.

[137] J. E. Pickett and D. J. Coyle, “Hydrolysis kinetics of condensation polymers under humidity aging conditions,” *Polymer Degradation and Stability*, vol. 98, no. 7, pp. 1311–1320, Jul. 2013.

[138] A. Omazic, G. Oreski, M. Halwachs, G. C. Eder, C. Hirschl, L. Neumaier, G. Pinter, and M. Erceg, “Relation between degradation of polymeric components in crystalline silicon PV module and climatic conditions: A literature review,” *Solar Energy Materials and Solar Cells*, vol. 192, pp. 123–133, Apr. 2019.

[139] L. Papargyri, M. Theristis, B. Kubicek, T. Krametz, C. Mayr, P. Papanastasiou, and G. E. Georghiou, “Modelling and experimental investigations of microcracks in crystalline silicon photovoltaics: A review,” *Renewable Energy*, vol. 145, pp. 2387–2408, Jan. 2020.

[140] X. Gou, X. Li, S. Wang, H. Zhuang, X. Huang, and L. Jiang, “The Effect of Microcrack Length in Silicon Cells on the Potential Induced Degradation Behavior,” *International Journal of Photoenergy*, 18-Feb-2018. [Online]. Available: https://www.hindawi.com/journals/ijp/2018/4381579/. [Accessed: 22-Sep-2020].

[141] M. Köntges, M. Siebert, A. Morlier, R. Illing, N. Bessing, and F. Wegert, “Impact of transportation on silicon wafer-based photovoltaic modules,” *Progress in Photovoltaics: Research and Applications*, vol. 24, no. 8, pp. 1085–1095, 2016.

[142] M. Köntges, I. Kunze, S. Kajari-Schröder, X. Breitenmoser, and B. Bjørneklett, “The risk of power loss in crystalline silicon based photovoltaic modules due to micro-cracks,” *Solar Energy Materials and Solar Cells*, vol. 95, no. 4, pp. 1131–1137, 2011.

[143] F. Kaule, W. Wang, and S. Schoenfelder, “Modeling and testing the mechanical strength of solar cells,” *Solar Energy Materials and Solar Cells*, vol. 120, pp. 441–447, Jan. 2014.

[144] U. Jahn, I. Kunze, S. Kajari-Schröder, and M. Köntges, “Crack Statistic of Crystalline Silicon Photovoltaic Modules,” *26th European Photovoltaic Solar Energy Conference and Exhibition*, pp. 3290–3294, Oct. 2011.

[145] M. Sander, S. Dietrich, M. Pander, M. Ebert, and J. Bagdahn, “Systematic investigation of cracks in encapsulated solar cells after mechanical loading,” *Solar Energy Materials and Solar Cells*, vol. 111, pp. 82–89, Apr. 2013.

[146] M. Paggi, I. Berardone, A. Infuso, and M. Corrado, “Fatigue degradation and electric recovery in Silicon solar cells embedded in photovoltaic modules,” *Scientific Reports*, vol. 4, no. 1, p. 4506, Mar. 2014.

[147] J. L. Braid, A. J. Curran, J. Sun, E. J. Schneller, J. S. Fada, J. Liu, M. Wang, A. J. Longacre, J. Dai, B. D. Huey, K. O. Davis, J.-N. Jaubert, L. S. Bruckman, and R. H. French, “EL and I-V Correlation for Degradation of PERC vs. Al-BSF Commercial Modules in Accelerated Exposures,” in *2018 IEEE 7th World Conference on Photovoltaic Energy Conversion (WCPEC) (A Joint Conference of 45th IEEE PVSC, 28th PVSEC 34th EU PVSEC)*, 2018, pp. 1261–1266.

[148] N. Bosco, M. Springer, and X. He, “Viscoelastic Material Characterization and Modeling of Photovoltaic Module Packaging Materials for Direct Finite-Element Method Input,” *IEEE-JPV*, vol. 10, no. 5, pp. 1424–1440, 2020.

[149] N. Bosco, M. Springer, J. Liu, S. Nalin Venkat, and R. H. French, “Employing Weibull Analysis and Weakest Link Theory to Resolve Crystalline Silicon PV Cell Strength Between Bare Cells and Reduced- and Full-Sized Modules,” *IEEE journal of photovoltaics*, vol. 11, no. 3, pp. 731–741, 2021.

[150] Y. Lyu, A. Fairbrother, M. Gong, J. H. Kim, A. Hauser, G. O’Brien, and X. Gu, “Drivers for the cracking of multilayer polyamide-based backsheets in field photovoltaic modules: In-depth degradation mapping analysis,” *Progress in Photovoltaics: Research and Applications*, vol. 28, no. 7, pp. 704–716, 2020.

[151] R. Wieser, Y. Wang, A. Fairbrother, S. Napoli, S. Julien, A. W. Hauser, L. Ji, K. Wan, G. S. O’Brien, R. H. French, M. D. Kempe, X. Gu, K. P. Boyce, and L. S. Bruckman, “Characterization of Real-World and Accelerated Exposed PV Module Backsheet Degradation,” Piscataway, NJ: Institute of Electrical and Electronics Engineers (IEEE), NREL/CP-5K00-78482, Oct. 2020.

[152] T. Jared, C. K. Roy, G. William, F. Thomas, G.-I. Lucie, H. Hongjie, T. T. John, K. Rahul, J. Xia, and H. Yushi, “Survey of Material Degradation in Globally Fielded PV Modules,” *IEEE Conference Proceedings*, vol. 2019, no. PVSC, pp. 874–879, 2019.

[153] Y. Lyu, J. H. Kim, A. Fairbrother, and X. Gu, “Degradation and Cracking Behavior of Polyamide-Based Backsheet Subjected to Sequential Fragmentation Test,” *IEEE journal of photovoltaics*, vol. 8, no. 6, pp. 1748–1753, 2018.

[154] A. G. Klinke, A. Gok, S. I. Ifeanyi, and L. S. Bruckman, “An Automated Algorithm for Quantifying Cracks in Photovoltaic Backsheets Under Accelerated and Real-World Exposures,” in *2018 IEEE 7th World Conference on Photovoltaic Energy Conversion (WCPEC) (A Joint Conference of 45th IEEE PVSC, 28th PVSEC 34th EU PVSEC)*, 2018, pp. 1295–1300.

[155] B. Zhang, J. Grant, L. S. Bruckman, O. Wodo, and R. Rai, “Degradation Mechanism Detection in Photovoltaic Backsheets by Fully Convolutional Neural Network,” *Scientific Reports*, vol. 9, no. 1, pp. 1–13, Nov. 2019.

[156] S. Zhang, Y. Zhang, and J. Zhu, “Residual life prediction based on dynamic weighted Markov model and particle filtering,” *J Intell Manuf*, vol. 29, no. 4, pp. 753–761, Apr. 2018.

[157] A. G. Klinke, A. Gok, S. I. Ifeanyi, and L. Bruckman, “A non-destructive method for crack quantification in photovoltaic backsheets under accelerated and real-world exposures,” *Polymer Degradation and Stability*, vol. 153, pp. 244–254, 2018.

[158] D. C. Jordan, T. J. Silverman, B. Sekulic, and S. R. Kurtz, “PV degradation curves: non-linearities and failure modes,” *Progress in Photovoltaics: Research and Applications*, vol. 25, no. 7, pp. 583–591, 2017.

[159] A. Virtuani, M. Caccivio, E. Annigoni, G. Friesen, D. Chianese, C. Ballif, and T. Sample, “35 years of photovoltaics: Analysis of the TISO-10-kW solar plant, lessons learnt in safety and performance—Part 1,” *Progress in Photovoltaics: Research and Applications*, vol. 27, no. 4, pp. 328–339, 2019.

[160] S. Lindig, D. Moser, B. Mueller, and K. Keifer, “Application of Dynamic Multi-Step Performance Loss Algorithm,” in *47th IEEE Photovoltaic Specialists Conference (PVSC),* Calgary, AB, Canada, 2021.

[161] R. B. Cleveland, W. S. Cleveland, J. E. McRae, and I. Terpenning, “STL: A seasonal-trend decomposition,” *Journal of official statistics*, vol. 6, no. 1, pp. 3–73, 1990.

[162] F. Mavromatakis, F. Vignola, and B. Marion, “Low irradiance losses of photovoltaic modules,” *Solar Energy*, vol. 157, no. C, Sep. 2017.

[163] I. D. L. Parra, M. Muñoz, E. Lorenzo, M. García, J. Marcos, and F. Martinez-Moreno, “PV performance modelling: A review in the light of quality assurance for large PV plants,” *undefined*, 2017. [Online]. Available: /paper/PV-performance-modelling%3A-A-review-in-the-light-of-Parra-Mu%C3%B1oz/23743bbaac4e4c7f02c3e549f98825c637562587. [Accessed: 22-Mar-2021].

ISBN 978-3-907281-05-5